

**IMPACT OF SO<sub>x</sub> AND NO<sub>x</sub> DEPOSITION ON THE  
LEACHING BEHAVIOUR OF SOILS AND WATER QUALITY  
IN THE SOUTH AFRICAN HIGHVELD**

**C Mabhaudhi**

Submitted in fulfilment of the requirements for the degree of  
Master of Science in Hydrology

Centre for Water Resources Research  
University of KwaZulu-Natal  
Pietermaritzburg

2014

## ABSTRACT

Atmospheric emissions of sulphur and nitrogen oxides lead to the formation of acid rain, which, when deposited, can result in soil and water acidification. Cases of soil and water acidification have been reported in temperate climates, such as Europe, the United States and Asia. However, in semi-arid grassland areas, such as South Africa, where seasonal wetting and drying climatic cycles are experienced, the impacts of atmospheric deposition are expected to differ from those in temperate climatic zones. Hence, the purpose of this study was to determine the impacts of atmospheric deposition on soils and water in the semi-arid grassland areas of the South African Eastern Highlands. This was done by investigating the leaching characteristics and susceptibility to acidification, of soils exposed to atmospheric deposition in the Sandspruit Catchment, and to determine the influence of deposition on catchment water quality.

Soil samples were collected from a farm located within the Sandspruit Catchment, in the Vaal River basin, from two hillslope transects (WS and WM) at the crest and toe slope positions. Soils from the four sampling positions were subjected to aerated and non-aerated column leach tests, using distilled water (pH 7.05) and a simulated acid rain solution (pH 4.35). Leachate from each column was collected as fractions of pore volume aliquots and measurements for EC, pH and redox potential were conducted immediately after collection. Further analysis was conducted for base cations, metals and anions and the data presented as breakthrough curves.

Comparing the leaching characteristics of the two hillslope soils, both WS crest and toe soils result in leachate with higher EC values, indicating that there are more base cations and anions in WS soil column leachates than WM soil column leachates. The pH for WS soil column leachates remained in the alkaline to slightly acidic range, whilst that for WM soil columns was mostly in the slightly acidic range. This indicates that even after the addition of an acidic solution, the soil had the capacity to neutralise some of the acidity through CEC and exchangeable bases. Hence, the two invading liquids, at pH 4.35 and 7.05 resulted in similar leachate pH values ranging from 6.05 to 8.0. The level of aeration within the columns also determined the leaching characteristics of WS and WM soils. WS soil column leachates had lower redox potential values (below 0 mV), indicating reducing conditions, hence had a

higher concentration of Mn in solution. On the other hand, the WM soil had higher redox potential values (greater than 150 mV), indicating oxidising conditions, hence the Mn concentrations in these columns was below detection limits.

Surface water samples were obtained from the farm catchment and sampling was extended to the quaternary scale, comprising tributaries downstream of the research site that feed into the Sandspruit River. The samples were taken on a seasonal basis between 2011 and 2012. The pH and EC of the samples was measured upon collection and further analysed for sulphate, nitrate and base cations. The results showed that atmospheric deposition had not resulted in surface water acidification, as the pH of the water was in the alkaline zone (greater than pH 7). However, there was some evidence of sulphur loading to concentrations greater than those from an atmospheric input of 2.84 mg/L. The sulphate concentration in the surface water was greater than 10 mg/L across all sampling positions with the Sandspruit Catchment.

The results of the column leach tests, together with catchment scale monitoring, show that leaching is a complex process that is influenced by the leaching solution, the chemical and physical characteristics of soil, as well as the hydraulic processes during leaching. The soil leaching behaviour differs with different slope positions and the effect of leaching on surface water quality is a summation of these different processes at each catchment position, as evidenced by the same chemical characteristics of the WM soil column leachates and water samples from the borehole (close to the windmill), and the WS soil column leachates and the spring (close to the weather station).

## DECLARATION

I .....declare that

- (i) The research reported in this document, except where otherwise indicated, is my original work.
- (ii) This thesis has not been submitted for any degree or examination at any other university.
- (iii) This thesis does not contain other persons' data, pictures, graphs or other information, unless specifically acknowledged as being sourced from other persons.
- (iv) This thesis does not contain other persons' writing, unless specifically acknowledged as being sourced from other researchers. Where other written sources have been quoted, then:
  - (a) their words have been re-written, but the general information attributed to them has been referenced;
  - (b) where their exact words have been used, their writing has been placed inside quotation marks and referenced.
- (v) Where I have reproduced a publication of which I am author, co-author or editor, I have indicated, in detail, which part of the publication was actually written by myself alone and have fully referenced such publications.
- (vi) This thesis does not contain text, graphics or tables copied and pasted from the internet, unless specifically acknowledged, and the source being detailed in the thesis and references sections.

Signed: .....

Supervisor: Prof. S. Lorentz .....

## ACKNOWLEDGEMENTS

I would like to thank the following people and organisations for making this research project a success.

Firstly, I would like to thank my supervisor, Professor Simon Lorentz for his input and guidance throughout the research process. I would like to also thank my co-supervisor, Ms Jenny Blight for her input and suggestions.

I would like to thank the technical staff in the Centre for Water Resources Research, namely, Mr Cobus Pretorius and Simphiwe Mfeka for their much valued support in the field and laboratory. Special thanks also go to the Department of Soil Science staff, mainly Rajiv Singh for assistance with some of the laboratory work, and to the Department of Chemistry staff, namely, Bheki Dhlamini, for his valued assistance with the ICP analysis. Many thanks go to Mrs Rees for her assistance in editing this document.

My sincere gratitude also extends to ESKOM and the Water Research Commission for the financial support provided for this research.

Special mention goes to my colleagues in the Centre for Water Resources Research for your friendship and moral support during the duration of my research. Yes, we survived the research process and came out stronger than before.

I would like to also thank my friends and family for their love, support and prayers.

Last but not least, I would like to thank my husband, Tafadzwa, for his love and support and for believing in me.

## TABLE OF CONTENTS

ABSTRACT.....	i
DECLARATION .....	iii
ACKNOWLEDGEMENTS.....	iv
TABLE OF CONTENTS.....	v
LIST OF TABLES.....	viii
LIST OF FIGURES .....	x
1. INTRODUCTION.....	1
2. LITERATURE REVIEW .....	7
2.1 Atmospheric Deposition.....	7
2.1.1 Sources of atmospheric emissions .....	8
2.1.2 Formation of acid rain.....	11
2.2 Soil Chemical and Physical Parameters .....	12
2.3 Biogeochemical Nutrient Cycles.....	16
2.3.1 Sulphur cycle .....	16
2.3.2 Nitrogen cycle.....	18
2.4 Soil Buffering Mechanisms in Response to Atmospheric Deposition.....	21
2.5 Impacts of Atmospheric Deposition.....	22
2.5.1 Impacts on soils.....	23
2.5.2 Impacts on surface water .....	26
2.6 Leach Tests.....	28
2.6.1 Column leach tests .....	29
2.7 Conclusion.....	35
3. METHODOLOGY .....	36
3.1 Introduction .....	36
3.2 Site Description.....	36

3.3	Soil Sampling .....	37
3.4	Soil Characterisation .....	39
3.5	Column Leach Tests.....	40
3.6	Catchment Water Sampling and Analysis.....	45
4.	THE LEACHING BEHAVIOUR OF SANDSPRUIT CATCHMENT SOILS EXPOSED TO SIMULATED ACID RAIN AND DISTILLED WATER .....	48
4.1	Introduction .....	48
4.2	Soil Characterisation .....	48
4.3	Leach Column Results Expressed as Concentration .....	52
4.3.1	Electrical conductivity .....	53
4.3.2	pH and redox potential.....	55
4.3.3	Chloride breakthrough curve .....	61
4.3.4	Base cations .....	65
4.3.5	Aluminium, manganese and iron .....	76
4.3.6	Sulphur.....	85
4.3.7	Nitrate and ammonium .....	90
4.4	Leach Column Results Expressed as Cumulative Mass.....	96
4.4.1	Base cations cumulative mass.....	96
4.4.2	Sulphur and nitrate cumulative mass .....	96
4.5	Conclusion.....	101
5.	THE IMPACT OF SO <sub>x</sub> AND NO <sub>x</sub> DEPOSITION ON SURFACE WATER QUALITY IN THE SANDSPRUIT CATCHMENT .....	104
5.1	Introduction .....	104
5.2	Surface Water Quality Monitoring.....	104
5.2.1	pH and redox potential.....	104
5.2.2	Electrical conductivity, sulphate and nitrate .....	110
5.2.3	Base Cations.....	112
5.3	Conclusion.....	115

6.	GENERAL DISCUSSION, CONCLUSIONS AND RECOMENDATIONS .....	116
6.1	General Discussion.....	116
6.2	Conclusions .....	117
6.3	Recommendations .....	118
7.	REFERENCES .....	120
8.	APPENDICES .....	127
8.1	Appendix 1 .....	127
8.2	Appendix 2 .....	128
8.3	Appendix 3 .....	129
8.4	Appendix 4 .....	130
8.5	Appendix 5 .....	131
8.6	Appendix 6 .....	132
8.7	Appendix 7 .....	133
8.8	Appendix 8 .....	134
8.9	Appendix 9 .....	135
8.10	Appendix 10.....	136
8.11	Appendix 11 .....	137
8.12	Appendix 12 .....	138
8.13	Appendix 13 .....	139
8.14	Appendix 14.....	140
8.15	Appendix 15 .....	141
8.16	Appendix 16.....	142
8.17	Appendix 17.....	143
8.18	Appendix 18.....	144
8.19	Appendix 19.....	145



## LIST OF TABLES

Table 2.1	Base saturation as an indicator of leaching status (Hazeth and Murphy, 2007)	13
Table 2.2	Soil condition at various redox potential ranges (Macías and Arbestain, 2010)	14
Table 3.1	Soil physical parameters used to pack and run leach columns .....	41
Table 3.2	Leaching liquid and level of aeration applied to both set of columns (weather station and windmill soils). Each setup consisted of 8 columns as indicated in the right hand column .....	44
Table 3.3	Rainwater chemistry for Amersfoort, Mpumalanga, and the simulated rainwater used in the column leach experiments .....	45
Table 4.1	Soil physical and chemical characteristics determined in a 1:2.5 extract. All soil samples were obtained from the 0-100mm depth .....	50
Table 4.2	Soil exchangeable bases and effective cation exchange capacity determined by extraction with 0.1M BaCl <sub>2</sub> solution.....	50
Table 4.3	Water soluble cations and anions from saturated paste extract .....	51
Table 4.4	Breakthrough sample pH, EC and redox potential values for all leach columns .. .....	55
Table 4.5	Chloride BTC shape, BTC, maximum and tail (after 2.5 pore volumes) concentration for WM soil columns .....	64
Table 4.6	Calcium BTC shape, BTC, maximum and tail (after 2.5 pore volumes) concentration for WS and WM soil columns.....	67
Table 4.7	Magnesium BTC shape, BTC, maximum and tail (after 2.5 pore volumes) concentration for WS and WM soil columns.....	69
Table 4.8	Sodium BTC shape, BTC, maximum and tail (after 2.5 pore volumes) concentration for WS and WM soil columns.....	72
Table 4.9	Potassium BTC shape, BTC, maximum and tail (after 2.5 pore volumes) concentration for WS and WM soil columns.....	74
Table 4.10	Aluminium BTC shape, BTC, maximum and tail (after 2.5 pore volumes) concentration for WS and WM soil columns.....	80
Table 4.11	Manganese BTC shape, BTC, maximum and tail (after 2.5 pore volumes) concentration for WS and WM soil columns.....	82

Table 4.12	Iron BTC shape, BTC, maximum and tail (after 2.5 pore volumes) concentration for WS and WM soil columns.....	84
Table 4.13	Sulphur BTC shape, BTC, maximum and tail (after 2.5 pore volumes) concentration for WS and WM soil columns.....	89
Table 4.14	Nitrate BTC shape, BTC, maximum and tail (after 2.5 pore volumes) concentration for WS and WM soil columns.....	93
Table 4.15	Ammonium BTC shape, BTC, maximum and tail (after 2.5 pore volumes) concentration for WS and WM soil columns.....	95
Table 4.16	Mass leached (mg/kg soil) of Mg and Ca up to 2.00 pore volumes .....	98
Table 4.17	Mass leached (mg/kg soil) of Na and K up to 2.00 pore volumes.....	99
Table 4.18	Mass leached (mg/kg soil) of S and Nitrate after 2.00 pore volumes.....	100

## LIST OF FIGURES

Figure 1.1	Map showing areas in South Africa where acidic critical loads have been exceeded (adapted from Josipovic, <i>et al.</i> , 2011). 1 meq m <sup>-2</sup> yr <sup>-1</sup> is equal to 1 mmol <sub>c</sub> m <sup>-2</sup> yr <sup>-1</sup> .....	3
Figure 2.1	Dry and wet deposition (Csaba and Csaba, 2011) .....	8
Figure 2.2	Contribution to atmospheric deposition of S and N by source in Mpumalanga, South Africa (adapted from Scorgie and Kornelius, 2009) .....	10
Figure 2.3	pH and redox potential (Eh) diagram showing the reduction sequence of Mn (top) and S (bottom) in water at different pH and redox conditions (Husson, 2013) .....	15
Figure 2.4	Sulphur cycle (adapted from Johnson, 1984; Reuss and Johnson, 1986) .....	17
Figure 2.5	Nitrogen cycle (adapted from Söderlund and Svensson, 1976; Gundersen and Bashik, 1994; Bernhard, 2010) .....	19
Figure 2.6	Impacts on soil N system associated with NH <sub>4</sub> NO <sub>3</sub> (top left), (NH <sub>4</sub> ) <sub>2</sub> SO <sub>4</sub> (top right) and HNO <sub>3</sub> (bottom left) (adapted from Reuss and Johnson, 1986) .....	20
Figure 2.7	Typical Breakthrough curves for column leach tests (adapted from Nielsen and Biggar, 1962) .....	31
Figure 2.8	Inverted breakthrough curves for contaminated soil (adapted Rao, 1974) .....	32
Figure 2.9	Breakthrough curve for S and Mn for Sabie Midslope (0-100mm) leached with distilled water (Lorentz <i>et al.</i> , 2010) .....	34
Figure 3.1	Location of the Sandspruit Experimental Catchment (Lorentz, et al., 2010) ....	37
Figure 3.2	Map of the Sandspruit Research Catchment showing, soil sampling positions in relation to the weather station, windmill and spring .....	38
Figure 3.3	Soil sampling using an auger (left) and soil cores (right) .....	39
Figure 3.4	Components used in packing aerated and non-aerated columns .....	42
Figure 3.5	Leach column set-up showing direction flow of leaching liquid in the column and leachate collection positions .....	43
Figure 3.6	Eight columns mounted on the wall bracket, with 4 aerated columns (top) and 4 non-aerated columns (bottom) .....	43
Figure 3.7	Map indicating the location of surface water sampling positions in the Sandspruit Catchment .....	47

Figure 4.1	Typical BTCs used to group WS and WM column leach test results. Curves 1, 2, 3 are illustrated on the top graph, Curve 4 on the bottom left and Curve 5 on the bottom right.....	53
Figure 4.2	Leachate EC breakthrough curves for WS (left: crest above, toe below) and WM (right: crest above, toe below) soil columns.....	56
Figure 4.3	Leachate pH breakthrough curves for WS (left: crest above, toe below) and WM (right: crest above, toe below) soil columns.....	59
Figure 4.4	Leachate redox potential breakthrough curves for WS (left: crest above, toe below) and WM (right: crest above, toe below) soil columns.....	60
Figure 4.5	pH and redox potential diagrams for WS (left: crest above, toe below) and WM (right: crest above, toe below) leachate samples .....	62
Figure 4.6	Chloride breakthrough curves for WM soil columns as concentration (left: crest above, toe below) and as relative concentration (right: crest above and toe below) .....	63
Figure 4.7	Calcium breakthrough curves for WS (left: crest above, toe below) and WM (right: crest above, toe below) soil columns .....	66
Figure 4.8	Magnesium breakthrough curves for WS (left: crest above, toe below) and WM (right: crest above, toe below) soil columns .....	68
Figure 4.9	Sodium breakthrough curves for WS (left: crest above, toe below) and WM (right: crest above, toe below) soil columns .....	71
Figure 4.10	Potassium breakthrough curves for WS (left: crest above, toe below) and WM (right: crest above, toe below) soil columns .....	73
Figure 4.11	Aluminium breakthrough curves for WS (left: crest above, toe below) and WM (right: crest above, toe below) soil columns. The Al concentration for WS crest soil column leachates (left top) were all below detection limits.....	79
Figure 4.12	Manganese breakthrough curves for WS (left: crest above, toe below) and WM (right: crest above, toe below) soil columns .....	81
Figure 4.13	Iron breakthrough curves for WS (left: crest above, toe below) and WM (right: crest above, toe below) soil columns .....	83
Figure 4.14	Sulphur breakthrough curves for WS (left: crest above, toe below) and WM (right: crest above, toe below) soil columns .....	88
Figure 4.15	Nitrate breakthrough curves for WS (left: crest above, toe below) and WM (right: crest above, toe below) soil columns .....	92

Figure 4.16	Ammonium breakthrough curves for WS (left: crest above, toe below) and WM (right: crest above, toe below) soil columns .....	94
Figure 5.1	pH and redox potential variation at Sites, 1: Wessel borehole (top), 2: Wessel Spring (middle) and 3: Wessel Catchment Outlet at the Research Catchment.....	106
Figure 5.2	pH and redox potential variation at Sites 4: Sandspruit Kloof u/s of Junction (top), 5: Sandspruit Drift (middle) and 6: Sandspruit Bridge near Wessel Farm (bottom) in the Sandspruit Catchment .....	107
Figure 5.3	pH and redox potential variation at Sites 7: Sandspruit Bridge on N11 (top), 8: Steel Bridge on N23 (middle) and 9: Bridge near Perdokop (bottom) in the Sandspruit Catchment .....	108
Figure 5.4	pH and redox potential variation at Sites 10: Sandspruit Junction off S446 Bridge (top), 11: Klip u/s of Junction (middle) and 12: Klip d/s of Junction (bottom) of the Sandspruit River .....	109
Figure 5.5	Map of the Sandspruit Catchment with the measured winter and summer EC and sulphate values for all the 12 sampling positions.....	111
Figure 5.6	Map of the Sandspruit Catchment with the measured winter and summer Ca, Mg, Na and K values for all the 12 sampling positions.....	114
Figure 8.1	Chloride BTC curve as relative concentration for WM (crest: top and toe: bottom) soil columns.....	127
Figure 8.2	Calcium BTC curve as relative concentration for WS (left, crest: top and toe: bottom) and WM (right, crest: top and toe: bottom) soil columns .....	128
Figure 8.3	Magnesium BTC curve as relative concentration for WS (left, crest: top and toe: bottom) and WM (right, crest: top and toe: bottom) soil columns .....	129
Figure 8.4	Sodium BTC curve as relative concentration for WS (left, crest: top and toe: bottom) and WM (right, crest: top and toe: bottom) soil columns .....	130
Figure 8.5	Potassium BTC curve as relative concentration for WS (left, crest: top and toe: bottom) and WM (right, crest: top and toe: bottom) soil columns .....	131
Figure 8.6	Aluminium BTC curve as relative concentration for WS (left, crest: top and toe: bottom) and WM (right, crest: top and toe: bottom) soil columns .....	132
Figure 8.7	Manganese BTC curve as relative concentration for WS (left, crest: top and toe: bottom) and WM (right, crest: top and toe: bottom) soil columns .....	133
Figure 8.8	Iron BTC curve as relative concentration for WS (left, crest: top and toe: bottom) and WM (right, crest: top and toe: bottom) soil columns .....	134

Figure 8.9	Sulphur BTC curve as relative concentration for WS (left, crest: top and toe: bottom) and WM (right, crest: top and toe: bottom) soil columns .....	135
Figure 8.10	Nitrate BTC curve as relative concentration for WS (left, crest: top and toe: bottom) and WM (right, crest: top and toe: bottom) soil columns .....	136
Figure 8.11	Ammonium BTC curve as relative concentration for WS (left, crest: top and toe: bottom) and WM (right, crest: top and toe: bottom) soil columns .....	137
Figure 8.12	EC and sulphate variation at Sites, 1: Wessel borehole (top), 2: Wessel Spring (middle) and 3: Wessel Catchment Outlet (bottom) at the Research Catchment .. .....	138
Figure 8.13	EC and sulphate variation at Sites 4: Sandspruit Kloof u/s of Junction (top), 5: Sandspruit Drift (middle) and 6: Sandspruit Bridge near Wessel Farm (bottom) in the Sandspruit Catchment .....	139
Figure 8.14	EC and sulphate variation at Sites 7: Sandspruit Bridge on N11 (top), 8: Steel Bridge on N23 (middle) and 9: Bridge near Perdokop (bottom) in the Sandspruit Catchment .....	140
Figure 8.15	EC and sulphate variation at Sites 10: Sandspruit Junction off S446 Bridge (top), 11: Klip u/s of Junction (middle) and 12: Klip d/s of Junction (bottom) of the Sandspruit River.....	141
Figure 8.16	Ca, Mg, K and Na variation at Sites, 1: Wessel borehole (top), 2: Wessel Spring (middle) and 3: Wessel Catchment Outlet at the Research Catchment .....	142
Figure 8.17	Ca, Mg, K and Na variation Sites 4: Sandspruit Kloof u/s of Junction (top), 5: Sandspruit Drift (middle) and 6: Sandspruit Bridge near Wessel Farm (bottom) in the Sandspruit Catchment .....	143
Figure 8.18	Ca, Mg, K and Na at Sites 7: Sandspruit Bridge on N11 (top), 8: Steel Bridge on N23 (middle) and 9: Bridge near Perdokop (bottom) in the Sandspruit Catchment .....	144
Figure 8.19	Ca, Mg, K and Na variation at Sites 10: Sandspruit Junction off S446 Bridge (top) and 11: Klip u/s of Junction (bottom) of the Sandspruit River .....	145

# 1. INTRODUCTION

The increase in industrialisation has led to the deterioration of air quality. The main pollutants have been identified as emissions from industry, motor vehicles, households and agricultural activities. The emissions include sulphur, (S) nitrogen (N) and carbon (C) particulates, as well as lead and volatile organic compounds (Wamukonya *et al.*, 2006). The emissions lead to diffuse non-point source pollution, as their impacts are not limited to the source, but are prevalent over vast areas (Carpenter *et al.*, 1998). The problems caused by these emissions are evident in parts of the world with high electricity consumption and high levels of industrialisation. Such places include developed countries such as the United States of America, Europe and Asia. These developed countries have experienced problems associated with atmospheric emissions from industrial activities and therefore measures have been implemented to reduce emissions from coal fired power stations. Developing countries, such as those in Africa, Asia and South America, still lag behind in industrialisation, but others, such as South Africa, show rapid industrial growth, resulting in an increased demand for electricity.

For instance, increased demand for electricity in South Africa means more use of coal and increased atmospheric emissions from coal power stations. Coal is widely used due to its abundance in the region and its lower cost compared, to development of renewable energy sources (Wamukonya *et al.*, 2006). As highlighted by Jeffrey (2006) highlighted that coal burning provides 75% of South Africa's primary energy and that 95% of the country's electricity generation is coal-fired thermal generation. This use of coal contributes to the atmospheric deposition of S, N and C oxides, which can lead to detrimental environmental impacts, such as those observed in the USA, Europe and Asia.

The detrimental impacts of atmospheric deposition arise mostly when acid rain is formed. The formation of acid rain occurs when oxides of S, N and C from atmospheric emissions interact with sunlight and water vapour to form sulphuric acid ( $H_2SO_4$ ), nitric acid ( $HNO_3$ ) and carbonic acid ( $H_2CO_3$ ), derived from oxides of S, N and C, respectively (Likens *et al.*, 2005; Warby, 2007). Some of the impacts of atmospheric deposition observed in temperate climates are summarised below:

- (a) Water quality degradation results in the decline of aquatic species and populations (Moldan and Cerny, 1994; Warby, 2007);
- (b) Direct deposition on plant leaves damages terrestrial vegetation (Moldan and Cerny, 1994; Warby, 2007);
- (c) There is an alteration of soil properties, with specific effects of depletion of exchangeable base cations due to accelerated leaching and the decrease in the base saturation and cation exchange capacity (CEC) (Kirchner and Lydersen, 1995). Other soil impacts observed are mobilisation of Aluminium (Al), Manganese (Mn) and Hydrogen ions (H<sup>+</sup>) and an increased accumulation of N and S in the soil (Warby, 2007); and
- (d) The degradation of buildings and other man-made structures, such as statues, due to acid attack (Moldan and Cerny, 1994; Warby, 2007).

On the other hand, atmospheric deposition has been shown to have the positive impact of increasing crop productivity, especially for N deposition (Reuss and Johnson, 1986). Nitrogen is an essential plant nutrient and its deposition can have a fertilising effect in areas where it is deficient.

Most of the above mentioned detrimental impacts have been experienced in the temperate climates of the northern hemisphere countries, such as the United States, Canada, Europe and Asia. The climatic conditions in these areas are different from those in southern hemisphere countries such as South Africa. For instance, the South African Highveld has seasonally contrasting climate, characterised by summer rain and dry winters (Igbafe, 2007), leading to soils experiencing seasonal wetting and drying cycles that affects their response to atmospheric deposition. The South African Highveld is also characterised by semi-arid grassland biomes, with different soil types compared to temperate climates, hence the soils will respond differently to acidification.

Some impacts of atmospheric deposition have also been observed in the South African Highveld, an area which accounts for approximately 90% of the country's emissions of sulphur dioxide (SO<sub>2</sub>) and oxides of nitrogen (NO<sub>x</sub>) (Josipovic *et al.*, 2011). According to Josipovic *et al.* (2011), industrial centres in the Highveld have the highest total acidic deposition rates and are likely to exceed the critical loads for soils in the area. The critical load concept refers to the concentration of one or more pollutants below which significant harmful effects to the environment do not occur (Kuylenstierna *et al.*, 2001; Josipovic *et al.*,



2011). The assessment of critical loads is based on mapping total deposition together with soil sensitivity, which, in turn, is based on buffering capacity and showing areas where total deposition is greater than the soil's buffer capacity (Kuylensstierna *et al.*, 2001; Josipovic *et al.*, 2011). The results of such work are presented as a map, showing areas where critical loads have been exceeded (Figure 1.1). The map shows that there is a high risk of detrimental environmental impacts from atmospheric deposition in the Mpumalanga Province

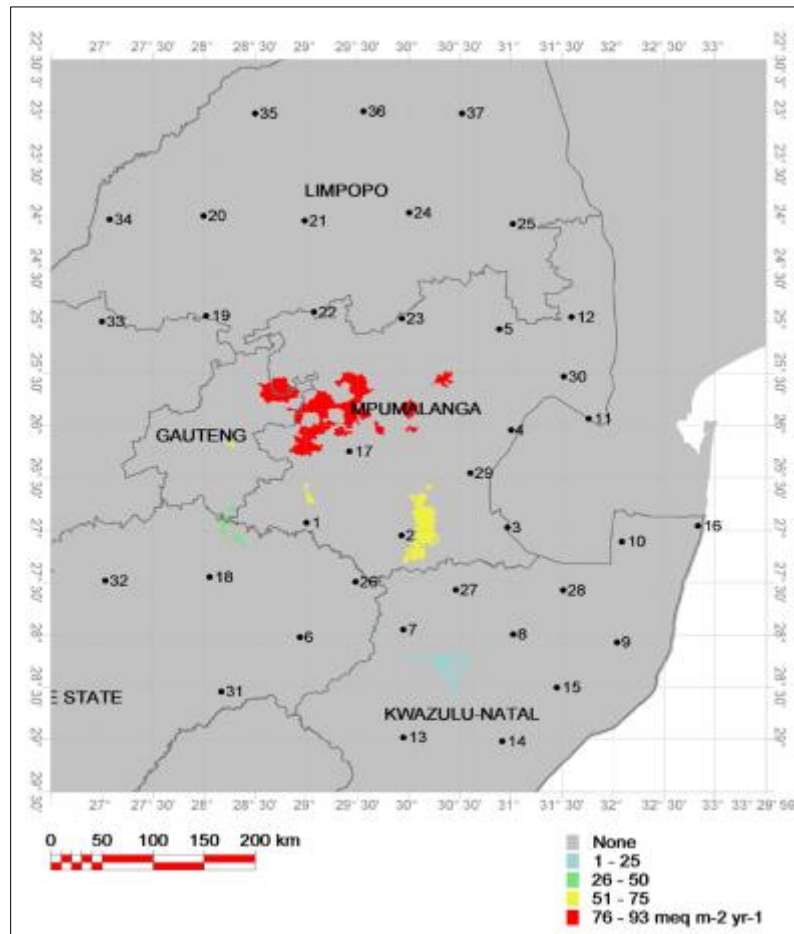


Figure 1.1 Map showing areas in South Africa where acidic critical loads have been exceeded (adapted from Josipovic, *et al.*, 2011). 1 meq m<sup>-2</sup> yr<sup>-1</sup> is equal to 1 mmol<sub>c</sub>m<sup>-2</sup>yr<sup>-1</sup>

The red areas in Figure 1.1 show that the central Mpumalanga Highveld has a high potential for the exceedance of critical loads, whilst the yellow areas indicate intermediate risk to the exceedance of critical loads (Josipovic, *et al.*, 2011).

In order to reduce atmospheric deposition and avert the exceedance of critical loads in South Africa, some measures have been proposed. These include, but are not limited to, the use of

filter bags in furnaces to capture and collect particulate matter, scrubber systems that further convert oxides of sulphur to form gypsum salts that can be collected for use in road construction and cleaner production and environmental management systems (von Blottnitz, *et al.*, 2009). However, implementing the above mechanism remains a challenge due to the lack of government capacity to monitor and control emissions, as well as cost constraints on industry to implement the control mechanisms (von Blottnitz, *et al.*, 2009). Therefore, both government and industry have to strike a balance between meeting the country's energy needs and protecting the environment. The latter usually suffers, as environmental pollution from atmospheric emission is still prevalent in the country, hence it is expected that the trend of the impacts experienced by developed countries will also be experienced in South Africa, if it is not already being felt. It is therefore important to assess the impacts of atmospheric deposition at the South African level. Effects of acid rain might only become evident in years to come, hence it is worth assessing now, so as to predict the extent of damage that might occur.

The impact of atmospheric deposition on surface water can be monitored directly by measuring changes in surface water quality, whilst those on soils can be determined by measuring the base stripping susceptibility of soils exposed to atmospheric deposition, in addition to measuring other indicative parameters such as CEC, pH and  $Al^{3+}$  leaching. Base stripping is a function of prevailing soil conditions, such as:

- (a) redox conditions,
- (b) pH,
- (c) carbon dioxide partial pressure,
- (d) microbial activity,
- (e) organic matter, and
- (f) texture and mineralogy.

The above soil conditions influence the release of bases and solutes from the top organic layer down the profile and ultimately into surface water and are hence directly linked to the acidification of surface waters (Kitchner and Lydersen 1995; Warby, 2007). The base stripping and leaching mechanisms can be investigated in the laboratory by making use of column leach tests. These tests assist in gaining an understanding of the rates of release of cations and anions and how this can affect water quality in a catchment area. The results of such tests are presented in the form of breakthrough curves, which show changes in

concentration of anions and base cations over time, with increasing throughflow pore volumes. Pore volume is the sum of volumes of all pores in a material such as soil occupied by air or fluid. In breakthrough curve analysis, pore volume represents the amount of water displaced from pore spaces at a given time. The leaching behaviour determined in the laboratory can then be used to estimate processes under field conditions and to infer the impact of atmospheric deposition on surface water quality.

Given that most atmospheric deposition research has been conducted in northern hemisphere temperate climates, and that the response to atmospheric deposition is expected to be different in the semi-arid grasslands of the South African Highveld, the aim of this research is, therefore, to determine the impacts of atmospheric deposition on soils and water in the semi-arid grassland areas of the South African Eastern Highlands. This is achieved by investigating the leaching characteristics and susceptibility to acidification, of soils exposed to atmospheric deposition in the Sandspruit Catchment, and to determine the influence of deposition on catchment water quality. The study utilises column leach tests using a distilled water solution and simulated acid rain solution to determine the soil leaching characteristics. Focus will be placed mainly on S and N in the making of a simulated acid rainwater solution because, according to Moldan and Cerny (1994), the most extensively studied elements are S and N, which are the main contributors to acidification in the form of strong acids,  $\text{H}_2\text{SO}_4$  and  $\text{HNO}_3$ . Carbon forms a weaker acid than these two, which results in the short-term acidification of surface waters and contributes to the soil organic pool, whilst S and N have long-term impacts. The simulated acid rainwater will be used to determine the leaching characteristics of selected soils from the South African Highveld and how these leaching characteristics are influenced by soil redox conditions and the pH of the rainwater solution. Column leach tests are chosen as they can mimic the movement of soil solution under field conditions in the laboratory and are more representative of in-situ leaching characteristics compared to other soil extraction tests (Goswami and Mahanta, 2007)

The research questions are posed as follows:

- (a) What are the leaching characteristics of selected catchment soils in the eastern highlands of South Africa after treatment with simulated acid deposition/rain and distilled water (control treatment) in laboratory column leach tests?
- (b) What is the relationship between the measured leaching characteristics and soil leach column conditions, such as redox potential, pH, CEC and organic matter content?

- (c) Are there any differences in leaching characteristics based on slope position (crest and toe slope)?
- (d) Is there a link between the leach column test results and measured stream water chemistry under field conditions?

Given the above research questions, the next chapter contains a comprehensive literature review of the impacts of atmospheric deposition and how it influences soil chemistry and, ultimately, surface water chemistry. The literature review will also focus on column leach tests as a tool to investigate the impacts of atmospheric deposition.

Chapter 3 contains a full description of the methods used to address the research questions. This includes the soil sampling protocol, basic soil characterisation and the leach column setup, as well as the stream water sampling protocol.

Chapter 4 presents and discusses the soil characterisation and column leach test results. The basic soil characteristics are presented in tabular form, whilst the column leach test results are presented as breakthrough curves.

Chapter 5 presents and discusses the surface water quality results. These are presented in graphical format, showing trends in pH, redox potential, EC, base and sulphate concentrations with time.

Chapter 6 contains the overall discussion, conclusion and recommendations.

## 2. LITERATURE REVIEW

The purpose of this literature review is to define atmospheric deposition and to establish its causes and impacts. These impacts are discussed in relation to soil and water acidification, and their relation to soil properties and biogeochemical cycling of N and S. A review of leach tests is also evaluated, with emphasis on column leach tests as a method to determine the leaching characteristics of soil caused by acid deposition.

### 2.1 Atmospheric Deposition

Scorgie and Kornelius (2009) defined atmospheric deposition as a process through which above-ground particles emitted from various sources are transported and deposited on ecological surfaces. These surfaces include vegetation, soils, water and man-made infrastructure, such as buildings, statues and vehicles. The emissions are deposited by various processes, depending on the nature of the particles and the prevailing environmental conditions.

The two main processes of deposition are dry and wet deposition (Moldan and Cerny, 1994; Ross and Lindberg, 1994). Dry deposition refers to the process in which particles settle on surfaces in the absence of moisture as either gasses or particulate matter (Ross and Lindberg, 1994). As emissions occur from the source, the density of the pollutant can increase, forcing the pollutants to settle on the earth's surfaces. Dry deposition also occurs when gaseous particles on solid surfaces attract each other through adsorption and become concentrated on a surface to form a thin film (Scorgie and Kornelius, 2009). Figure 2.1 illustrates the occurrence of dry deposition.

Wet deposition refers to the process whereby atmospheric emissions interact with precipitation before being deposited on ecological surfaces (Scorgie and Koernelius, 2009). Precipitation can be in the form of rain, snow or sleet, depending on climatic conditions, where deposition occurs. Precipitation interacts with atmospheric emissions, resulting in the change of chemical composition and the formation of acid rain (Moldan and Cerny, 1994; Ross and Lindberg, 1994; Warby, 2007). The main constituents of acid rain are sulphuric acid ( $\text{H}_2\text{SO}_4$ ) and nitric acid ( $\text{HNO}_3$ ), formed by the interaction of the oxides of sulphur and

nitrogen with water vapour and sunlight (Likens *et al.*, 2005; Warby, 2007). The occurrence of precipitation as acid rain can also be referred to as acid deposition (Scorgie and Koernelius, 2009). Figure 2.1 illustrates the wet deposition mechanisms.

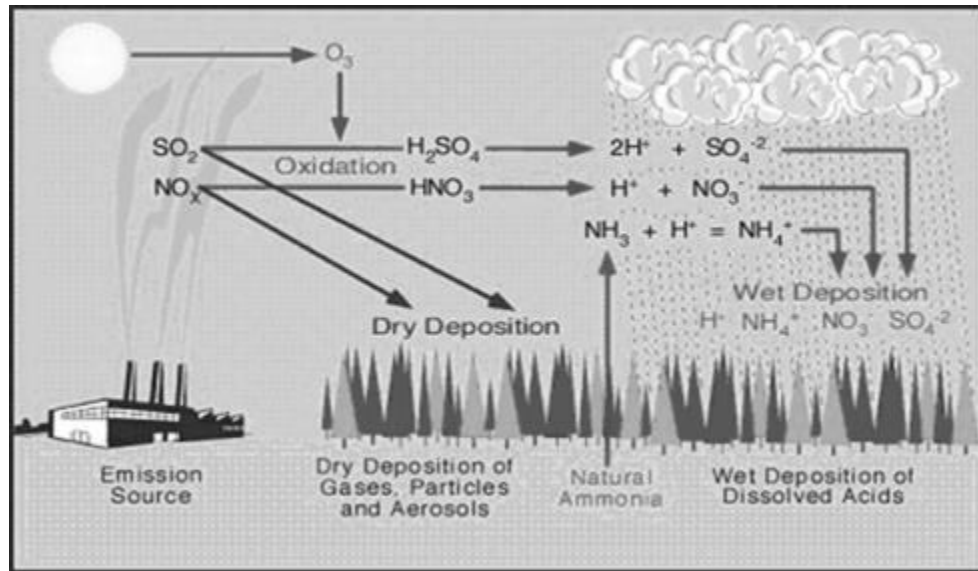


Figure 2.1 Dry and wet deposition (Csaba and Csaba, 2011)

The sources of atmospheric emissions and the formation of acid deposition are discussed in the next section.

### 2.1.1 Sources of atmospheric emissions

Sources of atmospheric emissions are both natural and anthropogenic. Anthropogenic sources of emissions depend on the activities or land use patterns in an area. On the other hand, natural sources depend on the geological, climatic and biological conditions found in an area. As the focus of the study is S and N, this section will discuss the various natural and anthropogenic sources of these elements.

As highlighted by Scorgie and Kornelius (2009), anthropogenic sources of atmospheric emissions are:

- (a) **Industrial and commercial activities:** Businesses, schools and hospitals utilise or burn coal in their processes. In industry, coal is used for electricity generation and to fire boilers that produce steam for production, laundry and heating purposes.
- (b) **Electricity generation by coal-fired power stations:** The majority of power stations in South Africa are coal-fuelled and are located in the Eastern Highlands of South

Africa (Josipovic *et al.*, 2011). These facilities make the highest contribution of S and N deposition.

- (c) **Waste treatment and disposal:** This includes the use of incinerators, landfills and waste-water treatment plants. Incinerators make use of high temperatures to burn waste from hospitals, industrial and domestic facilities. This results in the production of emissions that settle in surrounding areas. Landfill sites are utilised to bury waste in the ground and emissions are the result of decomposition of the buried waste. Waste-water treatment facilities also result in emissions of S and N from biological processes that occur during the treatment process (Kennedy, 1986).
- (d) **Residential:** The burning of paraffin, coal, liquified petroleum (LP) gas and biomass (firewood) for fuel results in the release of emissions into the atmosphere. The significance of this source of emission is based on location, with urban areas contributing less due to use of electricity, compared to rural areas where the use of paraffin and firewood is high (Scorgie and Kornelius, 2009).
- (e) **Transport:** According to Scorgie and Kornelius (2009), transportation services are the second highest anthropogenic contributor of S and N in the atmosphere, due to the use of petrol and diesel in vehicles.
- (f) **Mining:** Mining processes utilise coal to fuel boilers that generate steam for processing ore. Dust contributes to atmospheric emissions, with the main elements released being dependent on the ore being mined. For example, iron pyrites ore contains ferrous sulphide, which, when released as dust, can breakdown to form sulphur dioxide and contribute to acid deposition (Kennedy, 1986). Although, the contribution of mining was not quantified by Scorgie and Kornelius (2009) for the South African context, it contributes to atmospheric deposition in mining areas.
- (g) **Agriculture:** Agricultural activities contribute to atmospheric deposition from crop residues, fertilisers and cattle dung/livestock manure. However, the contribution of S and N from agricultural sources was not considered by the study done by Scorgie and Kornelius (2009). This might have been as a result of agriculture contributing directly to S and N concentrations in soils and water, without first being emitted into the atmosphere.

The main anthropogenic sources in both developed and developing countries of S and N are coal burning facilities. For example, coal burning facilities in the United States contribute 70% of total S and N emissions (Mast *et al.*, 2001). Contributions by various sources in South

Africa are illustrated in Figure 2.2, and show that the main sources of S and N are power generation processes (96.9% for S and 76.9% for N). The statistics are attributed to the use of coal as fuel for these activities.

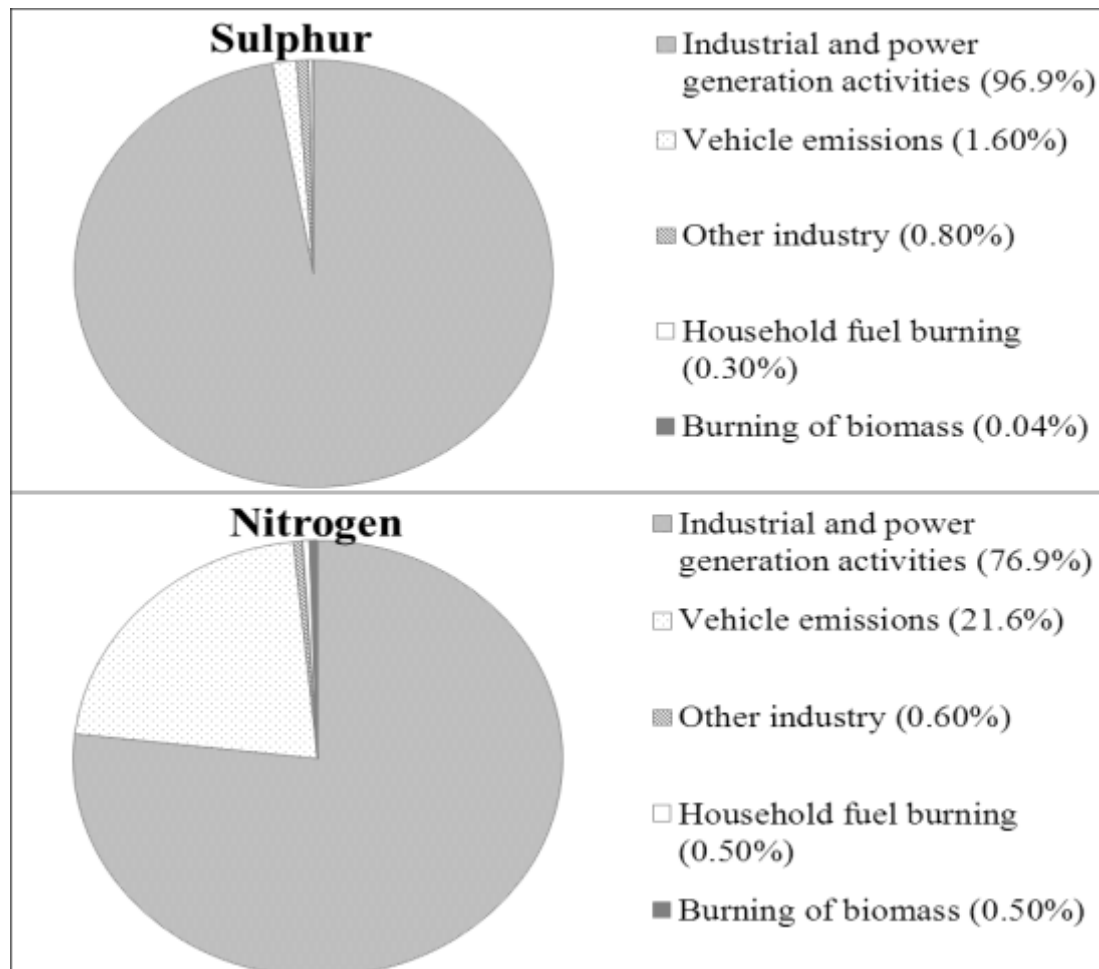


Figure 2.2 Contribution to atmospheric deposition of S and N by source in Mpumalanga, South Africa (adapted from Scorgie and Kornelius, 2009)

The difference between South Africa and developed countries, such as the United States, is attributed to the emission reduction measures that were introduced in the 1970s (Warby, 2007).

Natural sources of emissions that contribute to atmospheric deposition include:

- (a) **Biological release from microorganisms:** This occurs mostly in soils and is related to biogeochemical processes that govern S and N cycles. One such process is the release of S and N from the decomposition of organic matter in soil (Kennedy, 1986).



Some of these biological processes that contribute to S emissions occur in wetlands (Mast *et al.*, 2001).

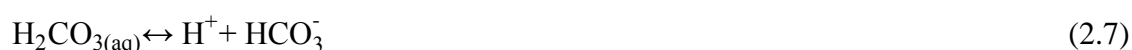
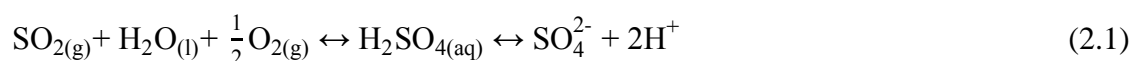
- (b) **Wildfires:** Wildfires result in the burning of vegetation and other biomass and result in the release of S and N that are organically bound in plant matter (Kennedy, 1986; Carpenter *et al.*, 1998; Scorgie and Kornelius, 2009).
- (c) **Lightning:** Lightning from thunderstorms results in nitrogen fixation through the formation of nitrogen oxide from gaseous nitrogen found naturally in air (Kennedy, 1986; Carpenter *et al.*, 1998; Scorgie and Kornelius, 2009).

By understanding the sources that are prominent in an area, the most likely impact to result from deposition can be investigated so as to ensure that all potential sources of atmospheric deposition are explored and that greater importance is not placed on one source only. Analysing the different sources of pollutants from an area also helps to distinguish between the processes that occur naturally in the environment and those that result from human interference, which hence allows for the quantification of the contribution to ecosystem damage by human activity.

The acidification of soil and water is also attributed to acid rain from these sources and its formation is discussed in the following section.

### 2.1.2 Formation of acid rain

Acid rain is a result of the interaction of S and N oxides with precipitation (Moldan and Cerny, 1994; Warby, 2007). The interactions with precipitation are shown in the following chemical equations:





According to the equations, acidification is caused by the dissociation of sulphuric, nitric or carbonic acid to form the acidic hydrogen ( $\text{H}^+$ ) ion and sulphate, nitrate or carbonate ion. The concentration of the dissociated hydrogen ion gives an indication of acidity (Warby, 2007). The pH of rainfall will depend on the concentration of  $\text{H}^+$  in the rain and will therefore determine the extent of the impact it will have on soil and water.

Cases of atmospheric deposition resulting in the formation of acid rain were investigated in the United States. Likens *et al.* (1996) showed that there is a relationship between the pollutant emissions of  $\text{SO}_2$  and  $\text{NO}_x$  and the resulting concentration of  $\text{SO}_4^{2-}$  and  $\text{NO}_3^-$  found in precipitation in the Hubbard Brook Experimental Catchment, and that the emissions led to the formation of acid rain. The acid rain was due to the biogeochemistry of  $\text{SO}_2$ , which contributes 55-75% of the acidity (Likens *et al.*, 1996). Records show that acid rain with a low pH of between 4.05 and 4.30 was observed in the United States around 1960 (Likens and Bormann, 1995).

In South Africa, rainfall acidity was measured at Amersfoort in the eastern Highveld and was found to be an average of pH 4.35, a value comparable to those obtained in the United States (Scorgie and Kornelius, 2009). This has given rise to the investigation of the impact of acid rain in the South African context and is the focus of this research.

Having discussed the formation of acid rain and its effect on rainwater pH, the following section describes the soil chemical parameters that determine fate of S and N in the environment.

## **2.2 Soil Chemical and Physical Parameters**

Soils are important in investigating the impacts of atmospheric deposition as they receive, transport and process atmospheric inputs and will therefore influence catchment water quality. During the transportation process, various biogeochemical processes occur and change the chemical parameters of the soil and soil water that contribute to rivers and streams (Essington, 2004). The biogeochemical processes are a result of interaction between the soil and atmospheric pollutants.

The main soil chemical characteristic that influences the transformation of atmospheric pollutants is its cation exchange capacity (CEC) (Mulder and Cresser, 1994; Beukes, 1995). CEC is defined as the total sum of exchangeable cations that a soil can absorb and release (Beukes, 1995). Exchangeable cations include but are not limited to  $\text{Ca}^{2+}$ ,  $\text{Mg}^{2+}$ ,  $\text{Na}^+$  and  $\text{K}^+$ . Similar to CEC is the anion exchange capacity (AEC), which refers to the total amount of exchangeable anions (Mulder and Cresser, 1994), such as fluoride ( $\text{F}^-$ ), chloride ( $\text{Cl}^-$ ), sulphate ( $\text{SO}_4^-$ ) and nitrate ( $\text{NO}_3^-$ ). In atmospheric deposition from coal-based industries, the anions usually investigated are sulphate and nitrate. Soil organic matter also contributes to the CEC of soils and hence helps in regulating atmospheric deposition (Mulder and Cresser, 1994; Beukes, 1995; Essington, 2004). Exchangeable cations and cation exchange capacity are related to the leaching status of a soil. The leaching status is expressed as the base saturation, which is the total sum of exchangeable base cations as a percentage of CEC (Beukes, 1995). Soils with high base saturation are expected to have low leaching status, as shown in Table 2.1. Soils with high CEC have a low leaching status. This was shown by Clayton *et al.*, (1991) after exposing Canadian soils to elevated levels of S deposition and to pH below 3.5. The soils with high CEC and base saturation were able to buffer changes in soil pH from the elevated S deposition. Bohan *et al.*, (1997) also showed that Chinese soils with higher CEC are less susceptible to acidification from simulated acid rain, compared to those with lower CEC.

Table 2.1 Base saturation as an indicator of leaching status (Hazeth and Murphy, 2007)

<b>Base Saturation Range (%)</b>	<b>Leaching Status</b>
70 - 100	Very weakly leached
50 - 70	Weakly leached
30 - 50	Moderately leached
15 - 30	Strongly leached
0 - 15	Very strongly leached

Another parameter that determines chemical reactions in soil is the redox status. The redox status of a soil is an indication of the oxidation and reduction condition and is measured in mV and symbolised by Eh (Lindsay, 1979). Different soil conditions are observed over various redox ranges, as shown in Table 2.2.

Table 2.2 Soil condition at various redox potential ranges (Macías and Arbestain, 2010)

<b>Soil Redox Potential Range (mV)</b>	<b>Soil Condition</b>
> +400	Aerated soil
+100 to +400	Moderately reduced
-100 to +100	Reduced
-300 to -100	Highly reduced
+300 to +500	Cultivated soils

Redox potential (Eh) is highly variable in soils and is driven by the level of aeration. The soil pH can also affect (Eh) through release and acceptance of electrons (Husson, 2013). The variability can occur at daily and seasonal cycles, depending on the moisture regime of the soil, with flooding and drying cycles resulting in most variations (Husson, 2013). Oxidation and reduction reactions control electron transfers in soil, directly impact microorganisms involved in soil processes and determine the fate of pollutants (McBride, 1994). The redox potential and pH both govern chemical reactions and the pH and redox can be plotted together as Eh and pH diagrams (also referred to as Pourbaix diagrams), to show the species of elements that are dominant over a given range of pH and Eh values, as illustrated in Figure 2.3 (Husson, 2013). The speciation of elements such as S, N, Fe and Mn are affected by Eh and pH conditions, as can be seen by the Pourbaix diagrams. On the other hand, elements such as K, Na and Al are not directly affected by Eh as there is only one possible redox state (+1 for K and Na and +3 for Al) and the main driver of their solubility is mostly pH (Husson, 2013). The redox potential and pH of a soil receiving atmospheric pollutants determines the solubility of compounds in soil and hence affects their movement in soil.

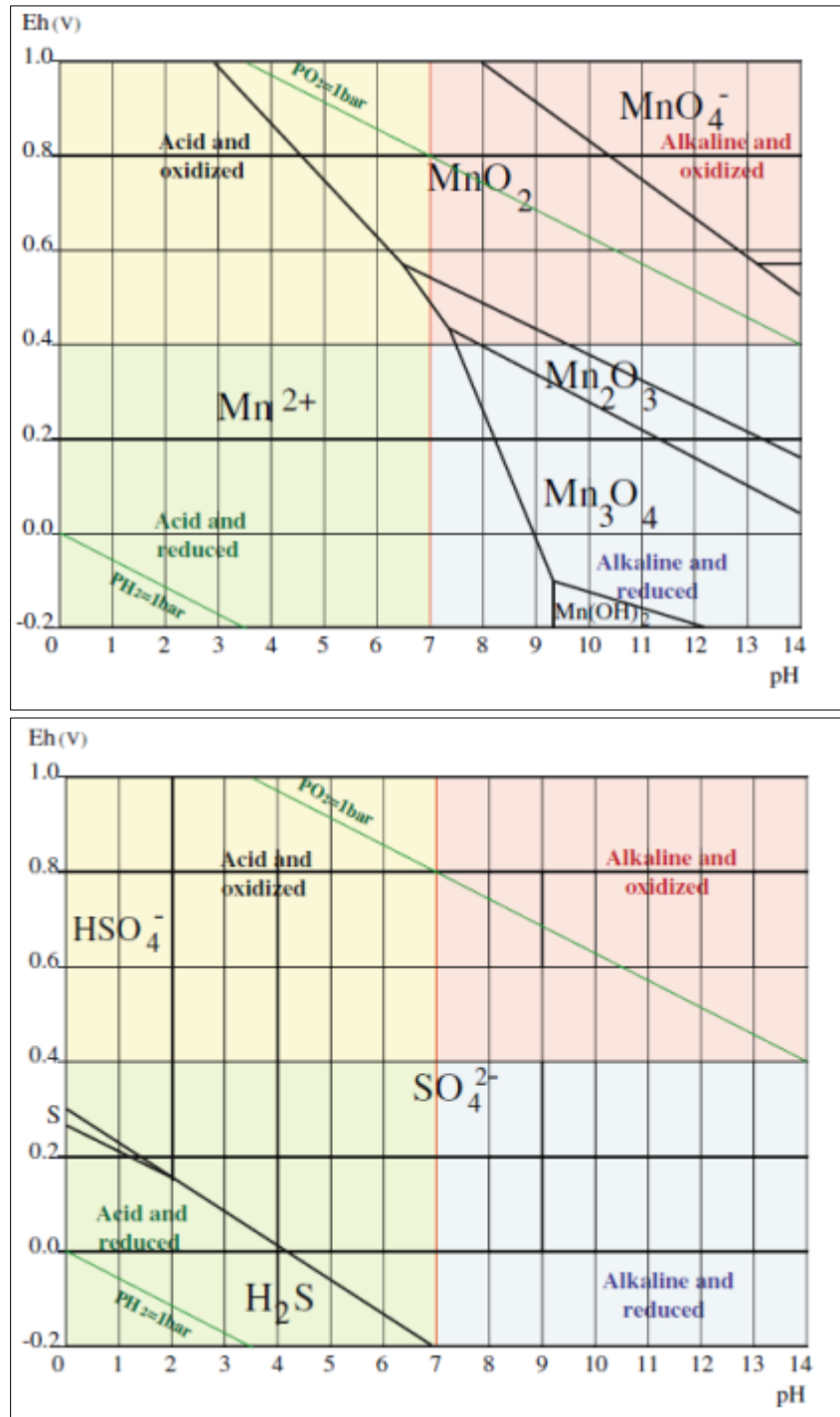


Figure 2.3 pH and redox potential (Eh) diagram showing the reduction sequence of Mn (top) and S (bottom) in water at different pH and redox conditions (Husson, 2013)

The physical parameters of soil that determine the impact of atmospheric deposition include soil depth and texture (Essington, 2004). Soil depth determines the impact on chemical parameters such as clay and organic matter content, as it is related to the amount of litter

found in a soil. Soil texture determines the CEC of a soil and hence the soil's response to atmospheric deposition.

## **2.3 Biogeochemical Nutrient Cycles**

Biogeochemical processes and nutrient cycles are important in soil and water acidification studies, as they influence the types and amounts of components that result in acidification. An understanding of these cycles provides an insight into the sources of N and S, the various forms in which they are found, their solubility, adsorption and desorption characteristics. All these characteristics influence the eventual fate of these elements and the extent to which they cause soil and water acidification. Sulphur and nitrogen also contribute to the anion pools in soil and anion exchange capacity.

### **2.3.1 Sulphur cycle**

Sulphur interactions with soil in the environment involve the adsorption of S by soil particles and its subsequent release (Figure 2.4). The adsorption of inorganic S into the soil matrix results in the retention of S and regulates the amounts released into water (Edwards, 1998). Adsorption can be non-specific and occurs through electrostatic forces that hold the negatively-charged sulphate ion on positively-charged soil organic matter surfaces, silicate and oxide surfaces. This type of adsorption is pH-dependent and increases with an increase in pH. The other type of adsorption occurs through ligand exchange, whereby sulphate ions are specifically absorbed by replacing  $\text{OH}^-$  and water from Al oxides and hydroxides (Edwards, 1998). Under low sulphate concentration, adsorption occurs on positive sites, thereby displacing water molecules, whilst under high sulphate conditions adsorption occurs on neutral sites, thereby replacing  $\text{OH}^-$  ions (Edward, 1998). In some instances, adsorption can be reversible, such as when sulphate or base cation concentrations increase in soil solution (Reuss and Johnson, 1986). This desorption mechanism increases the amount of sulphate in the soil solution and results in the potential leaching of sulphate (Fey and Guy, 1993; Hultberg *et al.*, 1994; Edwards, 1998).

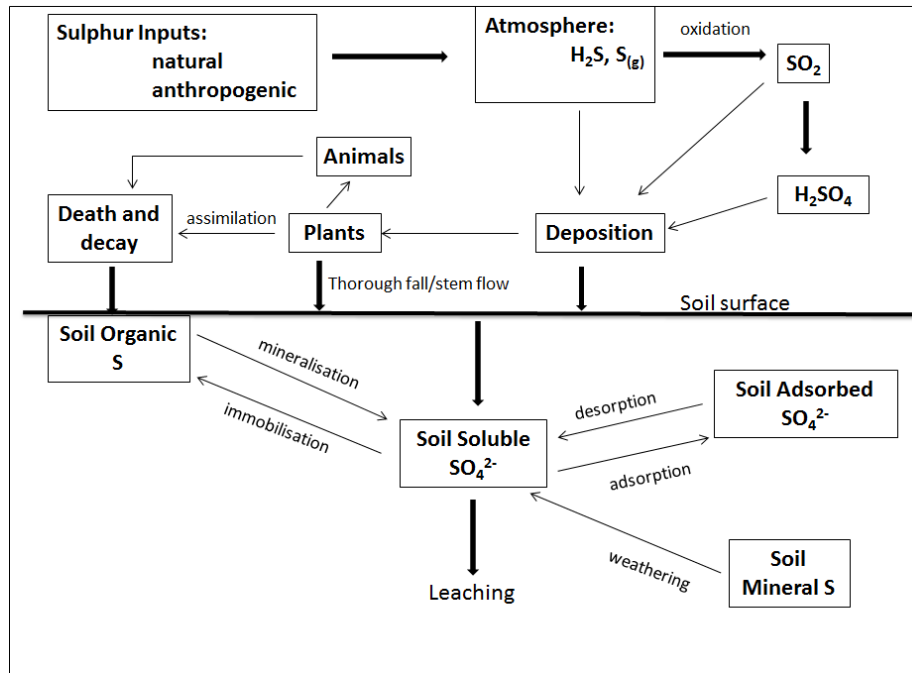


Figure 2.4 Sulphur cycle (adapted from Johnson, 1984; Reuss and Johnson, 1986)

Soil microorganisms play a crucial role in S retention by either immobilising sulphur or mineralising it into a different form (Hultberg *et al.*, 1994). Immobilisation occurs through aerobic and non-aerobic microbial respiration (Edwards, 1998). The soil microorganisms utilise the S in electron exchange reactions and this results in S being immobilised as microbial biomass and becoming part of the soil organic matter. On the other hand, organic S from microorganisms and decaying plants can be oxidised into smaller S compounds through depolymerisation to form highly mobile sulphate and ester-sulphate molecules (Edwards, 1998). These mineralisation and immobilisation processes are driven by the amount of S in the system. If S is low, immobilisation will proceed to meet the microbial needs and if S is higher than required mineralisation will occur, increasing the chances of S loss from the soil to ground and surface water (Edwards, 1998).

The retention mechanisms of S, described above, are important in regulating S from atmospheric deposition. However, the ability of a soil system to retain S can be reached under conditions of high atmospheric deposition, resulting in the leaching of sulphate to ground and surface water (Johnson, 1984). The addition of sulphate to a soil system under atmospheric deposition will result in the following changes in soil solution chemistry, as discussed below:

- a) The  $\text{SO}_4^{2-}$  front moves down the soil profile (Reus and Johnson, 1986).

- b) The concentration of  $\text{SO}_4^{2-}$  in the soil increases. In leaching studies, this is indicated by a reduction of  $\text{SO}_4^{2-}$  concentration in collected leachate, signifying that adsorption mechanisms are immobilizing the  $\text{SO}_4^{2-}$  in the soil matrix (Bohan *et al.*, 1997).
- c) There is a slight drop in pH (unlikely to exceed 0.2 or 0.3 units), as indicated by studies done, by OK *et al.*, 2007; Liu *et al.*, 2010 and Hedl *et al.*, 2011).
- d) Increase in soil solution concentration of  $\text{Ca}^{2+}$ ,  $\text{Mg}^{2+}$  and or ionic  $\text{Al}^{3+}$  (Clayton *et al.*, 1991; Bohan, *et al.*, 1997).

### 2.3.2 Nitrogen cycle

The nitrogen cycle is illustrated in Figure 2.5. The conversion of gaseous N into organic compounds occurs through biological fixation (nitrogen fixing bacteria) or physical processes (lightening) (Söderlund and Svensson, 1976).

The organic nitrogen compounds are part of plant and microbial proteins, which, upon decomposition, result in the formation of ammonia ( $\text{NH}_3$ ) (Reuss and Johnson, 1986). The ammonia gas goes through the process of ammonification, which involves the protonation of ammonia/and or the reaction with water to give the ammonium ion ( $\text{NH}_4^+$ ), a process mediated by bacteria (Bernhard, 2010). The  $\text{NH}_4^+$  ion can be directly taken up by plants or, if in excess of plant requirements, is converted to nitrate ( $\text{NO}_3^-$ ) (Gundersen and Bashik, 1994). Nitrate is highly mobile in water and can either be taken up by plants or, if in excess, leach to ground water accompanied by base cations (Gundersen and Bashik, 1994; Mulder and Cresser, 1994). Nitrate leaching is based on the soil system. Nitrogen-limited soils will not result in  $\text{NO}_3^-$  leaching, whilst N rich systems will be subject to the leaching of  $\text{NO}_3^-$  (Reuss and Johnson, 1986).



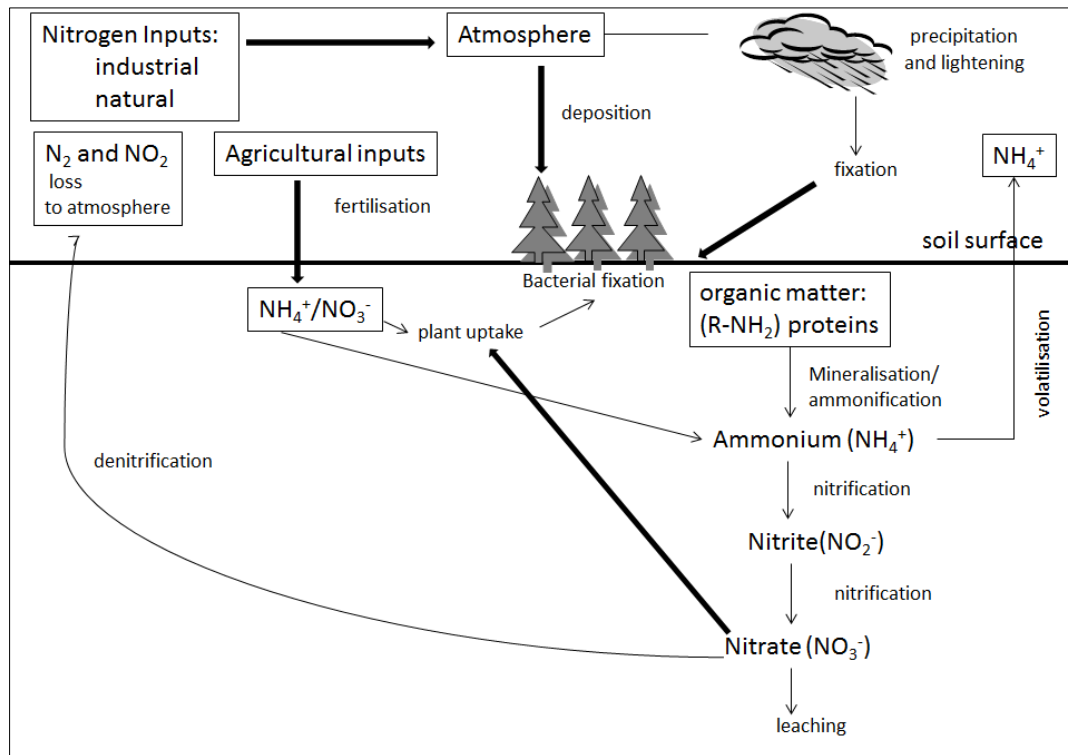


Figure 2.5 Nitrogen cycle (adapted from Söderlund and Svensson, 1976; Gundersen and Bashik, 1994; Bernhard, 2010)

A reverse process, denitrification, converts the ( $\text{NO}_3^-$ ) to  $\text{N}_2$  or  $\text{N}_2\text{O}$  and occurs when there is excess ( $\text{NO}_3^-$ ) after plant uptake and bacterial assimilation (Bernhard, 2011). The process is facilitated by facultative anaerobic bacteria, which can use nitrate as an electron acceptor instead of oxygen (Söderlund and Svensson, 1976). Nitrogen can also be lost to the atmosphere through ammonia volatilisation (Gundersen and Bashik, 1994). These N losses are significant in ecosystems that have limited nitrogen. As highlighted, N is a growth-limiting nutrient under low concentrations, with losses from the system only occurring when N is in excess.

The leaching potential of N makes it a major pollution problem, with agricultural systems contributing significantly as a result of the use of fertilisers. Atmospherically-derived N has also been identified as a contributor of ground and surface water pollution (Gundersen and Bashik, 1994). Nitrogen deposition leads to acidification by accelerating plant growth, resulting in more uptake of base cations (Reuss and Johnson, 1986).

Nitrogen deposition can occur as either nitric acid ( $\text{HNO}_3$ ), ammonium sulphate  $[(\text{NH}_4)_2\text{SO}_4]$  and/or ammonium nitrate ( $\text{NH}_4\text{NO}_3$ ) and the soil nitrogen cycle will respond differently to these inputs, as indicated in Figure 2.6.

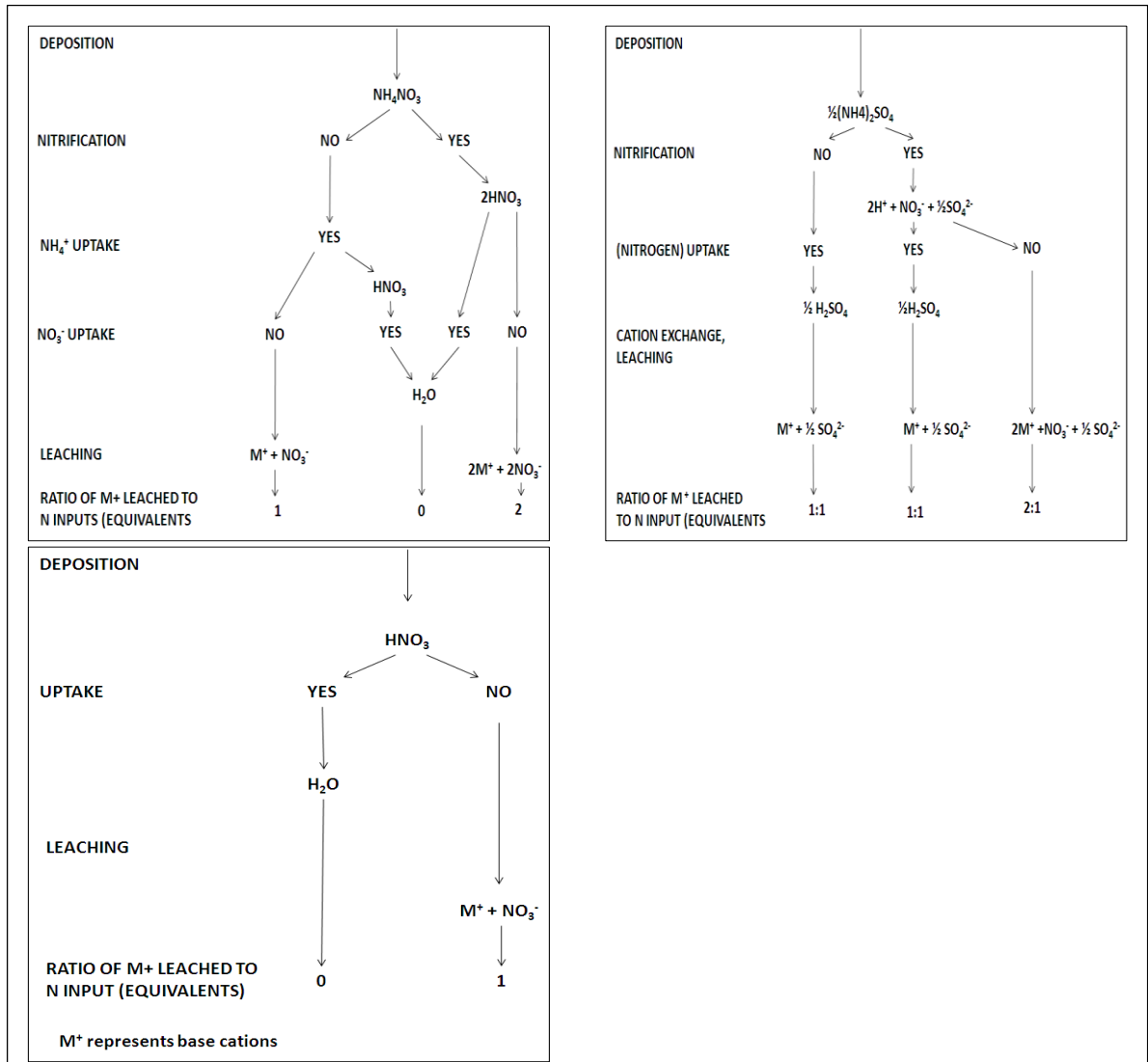


Figure 2.6 Impacts on soil N system associated with  $\text{NH}_4\text{NO}_3$  (top left),  $(\text{NH}_4)_2\text{SO}_4$  (top right) and  $\text{HNO}_3$  (bottom left) (adapted from Reuss and Johnson, 1986)

If deposition occurs as  $\text{HNO}_3$ , leaching or the neutralisation of the acidity is dependent on mobility and the availability of  $\text{NO}_3^-$  for plant uptake. On the other hand, if deposition occurs as  $\text{NH}_4\text{NO}_3$ , the impact on the soil will be dependent on whether or not nitrification, plant uptake, or both occur. A case whereby nitrification initially occurs, with no plant uptake, will result in more loss (2 equivalents) compared to a scenario where both nitrification and uptake occur, resulting in a lower loss (0 equivalents) of  $\text{NO}_3^-$ . Artificial addition of  $\text{NH}_4\text{NO}_3$  was done for over 10 years in the Rocky Mountains, USA, and the results showed decreases in pH

and acid buffering capacity, and an increase in exchangeable cations (Lieb *et al.*, 2011). Deposition as  $(\text{NH}_4)_2\text{SO}_4$  results in more complex reactions, which are governed by the ratio of  $\text{NH}_4^+$  to  $\text{SO}_4^{2-}$ . The  $\text{NH}_4^+$  ion can either be taken up by plants or undergo nitrification; either way, this will result in the formation of  $\text{H}_2\text{SO}_4$ , leading to base cation leaching according to the charge balance principle. The highest amount of leaching will be expected under conditions of nitrification and no plant uptake, as a combination of  $\text{SO}_4^{2-}$  and  $\text{NO}_3^-$  result in more base cations leaching (Reuss and Johnson, 1986).

The soil characteristics defined in this section determine how soils will respond to acid deposition and the leaching characteristics and the subsequent impacts on surface water. These parameters also determine the degree to which soils and surface water can buffer the impacts of atmospheric deposition. The next section therefore, describes the soil buffering mechanisms in response to atmospheric deposition.

## 2.4 Soil Buffering Mechanisms in Response to Atmospheric Deposition

Mayer (1998) highlighted that acidification is a slow and progressive process, which begins in the top horizon and moves down the soil profile, until it reaches ground and surface water. However, soils have various buffer mechanisms to acidic input, which are highlighted below:

- a) Carbonate mineral buffering: occurs in calcareous soils with high Ca and Mg carbonates and pH above 7 (McBride, 1994).
- b) Exchangeable base cation buffering: occurs in soils with intermediate pH ranges (5.5 to 7.0) (Bohan *et al.*, 1997; Mayer 1998), as indicated by the equation below.



where,  
Ca = all base cations in soil.

Exchangeable Ca bound to soil exchange surfaces is replaced by  $\text{H}^+$  ion. This results in the neutralisation of the acidity and the release of exchangeable Ca into the soil solution. Soils with high organic matter and CEC should have high buffering capacity due to higher exchangeable bases available on exchange surfaces to neutralise acidity. The neutralised acidity is temporarily stored on exchange sites; the reverse (release of  $\text{H}^+$  ions and adsorption of exchangeable Ca) can occur when pH increases.

- c) The above is an over-simplification of the buffering response of soils, as it does not represent the role of  $\text{Al}^{3+}$  ions. The adsorbed  $\text{H}^+$  in Equation 2.6 reacts with aluminosilicates consuming the  $\text{H}^+$  ion and releases Al from mineral complexes into soils (McBride, 1994; Bohan, *et al.*, 1997; Larssen, *et al.*, 1999).



The reaction buffers the soil at pH 4.5 to 5.0 range and results in high Al concentration in soil solution. At pH higher than 5.0 Al precipitates as a solid  $\text{Al}(\text{OH})_3$  and generates 3 moles of acidity.



- d) With continuous acidification Al will be depleted and Fe will begin to play a role in acid buffering. The reaction occurs at pH values lower than 3 and is shown below (Lindsay, 1979).



## 2.5 Impacts of Atmospheric Deposition

Atmospheric deposition impacts can either be beneficial or detrimental to the environment. The impacts are dependent on the receiving environments' characteristics, such as elevation, slope, aspect, vegetation cover and the location of the catchment in relation to the source of emissions (Ross and Lindberg, 1994). These characteristics determine the amount of emissions deposited in a particular area. For instance, vegetation intercepts emissions before they reach soil surfaces and regulates soil concentrations of C, S and N through plant uptake. Other determinants of environmental impact are relationships of base and acidic ions in precipitation and those in soil and water located in a catchment (Ross and Lindberg, 1994). Such ions include, but are not limited to,  $\text{H}^+$ ,  $\text{NH}_4^+$ ,  $\text{Mg}^{2+}$ ,  $\text{Ca}^{2+}$ ,  $\text{K}^+$ ,  $\text{Na}^+$ ,  $\text{SO}_4^{2-}$ ,  $\text{NO}_3^-$ ,  $\text{Cl}^-$  and  $\text{HCO}_3^-$ . These ions occur naturally in soil or water and have a buffering effect on the impacts of atmospheric deposition, hence determining the extent of the impacts.

The impacts of atmospheric deposition on both soils and water are dependent on the acid neutralising capacity (ANC), which refers to the ability of soil or water to neutralise acidity

(Warby, 2007). On soils, the ANC is dependent on processes such as mineral weathering, cation exchange and immobilisation of S and N through nutrient cycles. On the other hand, the ANC of surface water is mostly governed by stream flows and the concentration of cations and anions in water, parameters which are dependent on seasons (Driscoll *et al.*, 2001). However, in catchment studies, it is difficult to distinguish between the contribution to ANC for the entire catchment, as both soil and surface water processes contribute to buffering the effects of acidification but, at different levels.

Studies have been done on the impact of acid deposition on water (Kitchner and Lydersen, 1995; Likens *et al.*, 1996; Carpenter *et al.*, 1998; Likens *et al.*, 2005; Warby, 2007; Novak *et al.*, 2000) and on soils (Fernandez-Sanjurjo *et al.*, 1997; Mayer, 1998; OK *et al.*, 2007; Liu *et al.*, 2010; Hedl *et al.*, 2012), and the findings of these studies will be discussed in the following sections.

### **2.5.1 Impacts on soils**

The buffering mechanisms, as well as the impacts of atmospheric deposition, have been observed in various places. Mayer (1998) observed the impacts of atmospheric deposition on forest soils in Germany, where base leaching was seen as a function of soil type and mineralogy. Different soil types and mineralogy resulted in different responses to acid deposition. In this German case, atmospheric deposition also resulted in the leaching of heavy metals, such as Cd, Zn and Co, that are toxic to plants. Cases of soil acidification were also reported in the eastern Sudetes Mountains of the Czech Republic (Hedl *et al.*, 2011). The study compared recent soil characteristics, such as pH, with those obtained from the area forty years before. The study also described differences in acidification between catchments at high altitudes and between different soil horizons. The results showed a decline in pH across all sites, due to atmospheric deposition from increased industrial activity in the area. Lower pH values were obtained at lower altitudes, with beech forests, compared to higher altitudes, with coniferous forests. Comparisons of acidification down a soil horizon showed that low pH was obtained in upper soil horizons, compared to the lower horizons. However, as organic matter content changed with sites, decreases in pH were lower at those sites with high organic matter content (Hedl *et al.*, 2011). This study shows that the acidification of soil is a combination of factors, such as slope position, vegetation type and cover and soil profile position, as well as organic matter content, all of which determine the soil type. Investigation

of the long-term impacts of N on soils was done through the experimental additions of N to three soils in the Dinghushan Biosphere Reserve of China. The study site experiences a subtropical monsoon humid climate and consists of three forests at different stages of succession. The soils in the area were lateritic red soils, with a depth of less than 30 cm (Liu *et al.*, 2010). The study area was chosen, as soils showed a decline in pH over time from the 1980s to late 2005 and also had low exchangeable  $\text{Ca}^{2+}$  and high exchangeable Al, all indications of soil acidity. Plots were established in the area and N added to them to simulate the deposition of N. After this, soil and soil water samples at 20 cm depths and at five intervals over five years were collected for analysis of pH. The addition of N to the soils in the reserve resulted in further acidification due to increased N loading. This was attributed to the already observed low pH and base saturation and high exchangeable Al, which reduced the CEC of the soils and made them susceptible to acid deposition. The extent of acidification also differed with forest type, with the forest at an earlier succession stage experiencing higher declines in pH compared to the mature forests (Liu *et al.*, 2010). This study showed the link between acidification and vegetation type, that is, mature forests are more effective at bio-cycling, hence they can resist acidification. Continued atmospheric deposition, in this case simulated by the addition of N, results in a decline in soil pH and soil exchangeable  $\text{Ca}^{2+}$ , which makes soils lose their productivity.

The impacts of atmospheric deposition in Canada were investigated in two catchment areas located in Alberta, Canada (OK *et al.*, 2007). The areas under investigation consisted of mineral soils, luvisolic and boralf and two different forest types dominated by jack pine and aspen. Climatic conditions are cold with low precipitation (OK *et al.*, 2007). Soil samples were collected by horizon and subjected to measurements of soil pH, base saturation, Al saturation and acid buffering capacity. These parameters were utilised as an indicator of the level of acidification within the catchments' chemical characterisations. The soil pH of the two catchments ranged from 2.83 to 2.91 and showed an increasing trend moving down the soil profile (OK *et al.*, 2007). The base saturation and  $\text{Al}^{3+}$  ion concentration showed that the forest soils had undergone acidification. Both soils also showed low CEC, an indication that if the rate of atmospheric deposition was not reduced, the ecosystems would become damaged due to acidification. In this case the role of vegetation in soil acidification was not clearly indicated. The study showed the usefulness of using pH, base saturation and  $\text{Al}^{3+}$  concentration to infer the impacts of acidification of forest soils.

Fernandez-Sanjurjo *et al.* (1997) investigated the impacts of atmospheric deposition on small catchment slate soils with different forms of vegetation (deciduous, pine and heath) in north-western Spain. The study involved extracting soil solutions through the column displacement method and the leachate analysed for pH, base cations and Al. The results showed base cation depletion, which was attributed to atmospheric deposition. Chloride and sodium ions were common in all soil horizons due to the proximity of the sea that was influencing the concentration of these ions. Sulphate ion was found to be bound in the organic horizon and inorganic Al was also dominant, an indicator of acidification. This study highlights the importance of identifying all possible sources that can contribute to acidification, so that conclusions on the actual contribution of acidification by atmospheric emissions can be determined and not assumed. The sulphate that was found in the organic soil horizon could have been from the sea.

Investigations on the impact of atmospheric deposition on soils where mostly done in northern hemisphere countries, such as the United States, Canada, Europe and Asia (Fernandez-Sanjurjo *et al.*, 1997; Mayer, 1998; OK *et al.*, 2007; Liu *et al.*, 2010; Hedl *et al.*, 2012). The climatic conditions in these areas are different from those in southern hemisphere countries such as South Africa. For instance, the South African Highveld has seasonally contrasting climate, characterised by summer rain and dry winters (Igbafe, 2007). This results in soil wetting and drying cycles that affect the response to atmospheric deposition. Soils in the South African Highveld range from clay to sandy and those characterised as sandy are more susceptible to acidification from atmospheric deposition (Lorentz *et al.*, 2010). The South African Highveld is characterised by grassland biomes, hence the soil response to acidification will differ to those in temperate forests. There is a high likelihood that South African soils will respond differently to atmospheric deposition, compared to those in the northern hemisphere.

Soil processes have an impact on water quality as they receive, transform and release pollutants into water; and are governed by climatic and soil conditions, as well as soil type. The next section will therefore focus on the impacts of atmospheric deposition on water.

### 2.5.2 Impacts on surface water

The impacts of atmospheric deposition on surface water in the United States are well documented. Long-term studies were undertaken in the Hubbard Brook Catchment from 1963, to determine the impact of atmospheric deposition on different ecosystem processes. The studies undertaken in the Catchment showed relationships between S and N concentrations, with declining rain water pH. The low pH of rain water subsequently altered the quality of stream water in the Catchment by causing declines in surface water pH. The concentration of S in the atmosphere was found to have a positive correlation to sulphate concentration in stream water (Likens, 2004).

Links with atmospheric deposition and surface water quality in catchments at the Czech-German border, central Europe, were investigated by Novak *et al.* (2000). The results showed a correlation between sulphate and nitrate from atmospheric deposition with surface water pH values of 5.4, demonstrating the onset of acidification. Nitrate and sulphate contributed 61 and 27% of the anion exchange capacity. This showed the negative impacts of atmospheric deposition on surface water quality. The correlation of atmospheric deposition and surface water quality was shown by the concentration of  $\text{NO}_3^-$  and total N in atmospheric deposition and in oxidised N in surface water systems (Carpenter *et al.*, 1998). Thus, N in the atmosphere contributed to N found in river systems, resulting in the reduction of water quality. Nitrogen is an essential element for plant growth, thus if concentrations in surface water are high it shows that there is excess N in the soil resulting in eutrophication of water (Jenkins *et al.*, 1997). Subsequently, eutrophication results in negative impacts through the increased costs of water treatment and the reduction of aquatic biodiversity.

On the other hand, the relationship between atmospheric deposition and surface water quality is not always detrimental. For example, Neal *et al.* (1995) show that the impacts of acidification in southern Europe are different from those observed in the United States. In southern Europe, atmospheric pollutants are buffered by alkaline dust from industrial emissions found in the area, resulting in the deposition of neutral salts. Consequently, changes in water chemistry are minimal, showing that the water has a high acid neutralising capacity from the neutral salts, providing a scenario where high atmospheric deposition does not result in changes in stream water quality. The alkaline dust improved the fertility of soils in this Catchment.



The above-mentioned studies focused on the impacts of increased atmospheric emissions on water quality. Other studies investigated the impact of emission reduction on water quality, with the aim of finding out if recovery of acidified waters would occur. This was due to the introduction of the Clean Air Act of 1970 in the United States, which sought to reduce the concentration of SO<sub>2</sub> and particulate matter emitted by industry (Likens *et al.*, 1996). This led to a decline in sulphate in both precipitation and surface waters.

Kitchner and Lydersen (1995) also showed a decline in the sulphate and nitrate in surface water due to emission reductions in Norwegian catchments. However, this was not followed by an improvement in the water quality, as there were still high concentrations of Ca and Mg in the water. Kitchner and Lydersen (1995) attributed this to the loss of base cations from the soil under acid conditions and argued that although the decline of Ca and Mg in water did not occur, the conditions would have deteriorated further than what they did, if emissions had not been reduced. The study sought to correlate the reduction of atmospheric S with an improvement in water quality. However, the results showed that the improvement in water quality did not occur as rapidly as expected. The S reductions slowed down the rate of acidification, which would have been much more pronounced if atmospheric S concentrations had not been reduced. This was deduced, by making use of acid-base mass balances to calculate the loss of Ca and Mg under high emission scenario.

Warby (2007) also investigated the impact of decreasing atmospheric deposition on stream water quality in the north-eastern parts of the United States. The study involved the investigation of surface water quality from 1984 to 2001, by using parameters such as acid neutralising capacity, pH, Ca<sup>2+</sup>, SO<sub>4</sub><sup>2-</sup> and NO<sub>3</sub><sup>-</sup> concentrations. The surface water concentration of Ca<sup>2+</sup> and SO<sub>4</sub><sup>2-</sup> decreased, whilst the NO<sub>3</sub><sup>-</sup> results were not significant enough, to infer if any change had occurred. There were increases in pH and ANC, showing slight, but not complete recovery from acidification. These results draw attention to the link between atmospheric deposition and surface water chemistry, a process that can be extrapolated when using a South African catchment.

The impacts and ecosystem risk and sensitivity to atmospheric deposition mentioned above, were investigated, using various methodologies. One method of assessing risk to environmental pollutants is leach tests and these are discussed in the following section.

## 2.6 Leach Tests

Leach tests are procedures that seek to mimic the movement of soil solution under field conditions in the laboratory (Goswami and Mahanta, 2007). The procedures were developed to monitor and understand the leaching of pollutants within the environment. The purposes of leach procedures were to determine the amounts of pollutants released through leaching and how chemical parameters, such as pH and redox conditions affected the leaching process (Fallman and Aurell, 1996). The results from the leach tests are used to determine risk to the environment from pollutants such as mine and construction waste and to also determine the risk of ground water contamination (Guyonnet, 2010). The complex nature of environmental systems and pollutants has thus led to the development of various leach tests, classified according to the purpose of results.

Van der Sloot (1996) defined two classification systems for leach tests. One is to either obtain an understanding of equilibrium conditions at the end of leaching and the other is to gain an understanding of the dynamic processes during leaching. Examples of equilibrium tests were cited as batch tests, whilst dynamic tests were diffusion tests and column leach tests. The other classification system, cited by van der Sloot (1996) was based on the intended use of the results. Identified under this system were characterisation tests for wastes, legal compliance tests for government waste disposal, re-use regulations and the verification of on-site conditions (for mine dumps and landfill sites). An example of a characterisation test is the Synthetic Precipitation Leaching Procedure, which is done according to the United States Environmental Protection Agency EPA Method 1312 (Hagemen, 2003). Governments and international regulatory agencies have developed standardised regulatory tests to assess risk to the environment and the results can be compared. Examples of regulatory tests are:

- (a) EP-toxicity Test or Characteristic Leaching Procedure (TCLP) done according to (EPA) Method 1311 (Hagemen, 2003).
- (b) German Leach Test(DIN 38414) S4 (van der Sloot, 1996)
- (c) Column Leach Test (van der Sloot, 1996)

The results of these tests, based on leaching properties, are dependent on the physical and chemical parameters of waste and soils (van der Sloot, 1996). Physical parameters refer to particle size and porosity and chemical parameters refer to pH, redox, organic matter and concentration of elements. However, it is difficult to take into consideration the impact of all

these parameters by conducting one leach test. For example, the regulatory tests, highlighted above, do not consider the redox conditions of the material being tested and how it will affect leachate concentration (van der Sloot, 1996). Other conditions that affect the release of leachate are the fraction of pollutant/substance available for leaching, the solubility of material, chemical speciation in solid and liquid phase and the concentration gradient between pore water.

The impacts of atmospheric deposition have been investigated, by making use of column leach tests (Fey and Guy, 1993; Lorentz *et al.*, 2010). The following section will therefore discuss column leach tests.

### 2.6.1 Column leach tests

When analysing the behaviour of substances in soils, it is important to note that the soil solution is under the influence of gravity. One such method to mimic this influence of gravity is the column leach test (Goswami and Mahanta, 2007). Column tests include both water-saturated and unsaturated conditions, depending on the amount of leaching liquid used. The advantage of using this method is that the leachate can be collected at intervals during the test, thus it does not interfere with the chemical equilibrium within the column. The disadvantage is that it does not reflect the influence of redox conditions (Fallman and Aurell, 1996).

#### 2.6.1.1 Breakthrough curves

The results of column leach tests are in the form of breakthrough curves (BTCs) that show changes in solute concentration over time or at different pore volumes (Nielsen and Biggar, 1962; Andreiadis, 2005; Rogerio, 2007). Breakthrough curves are usually represented as graphs, with pore volume or time on the horizontal axis and relative concentration or concentration of solute on the vertical axis. Relative concentration is defined as:

$$\text{Relative concentration} = \frac{C}{C_0} \quad (2.10)$$

Where  $C$  is the concentration of solute in collected leachate at the bottom of column

$C_0$  is the concentration of solute in leaching liquid (initial concentration)

The shape of a BTC explains how a solute moves through a soil column and a breakthrough curve for a non-reactive or conservative solute, such as chloride, is used as a reference point to describe solute movement (Rao, 1974). A BTC for a conservative solute in soil shows a symmetrical S-shape (Chu, 2004), with the area under the BTC curve showing the volume of solute lost to leaching and the area above the curve showing the volume of solute adsorbed by the soil matrix (Andreiadis, 2005). This gives an indication of the adsorption and desorption characteristics of a leaching liquid passing through soil.

There are several types of BTCs and the three main categories are piston flow BTCs, BTCs for a non-reactive solute and delayed BTCs (Rogerio, 2007). Piston flow is represented by Curve (a), Curve (b) represents solute movement through dispersion, with no interaction between solute and solid (soil) phase, characteristic of a non-reactive solute, and Curve (c) represents a delayed response due to variations in pore velocity in the column (Figure 2.7) (Nielsen and Biggar, 1962). During piston flow, the solute does not interact with the soil matrix and assumes all pores have the same size. The piston flow BTC is a theoretical curve, as such conditions do not exist under field conditions. In the field, water flow is affected by different pore sizes, giving rise to un-uniform water flow. A more realistic curve arises due to water reaching the bottom of the column at different rates, as it passes through pores of different sizes. This is common for a non-reactive solute and a typical conservative solute would reach the relative concentration of 0.5 at pore volume 1 (Nielsen and Biggar, 1962). The assumption used in describing the above-mentioned three types of BTCs is that solute movement is a result of advection and dispersion processes. Advection is the bulk movement of solute at a velocity similar to the flow rate of water in the soil and dispersion describes the spreading of solute as it moves through a porous media such as soil (Knox *et al.*, 1993).

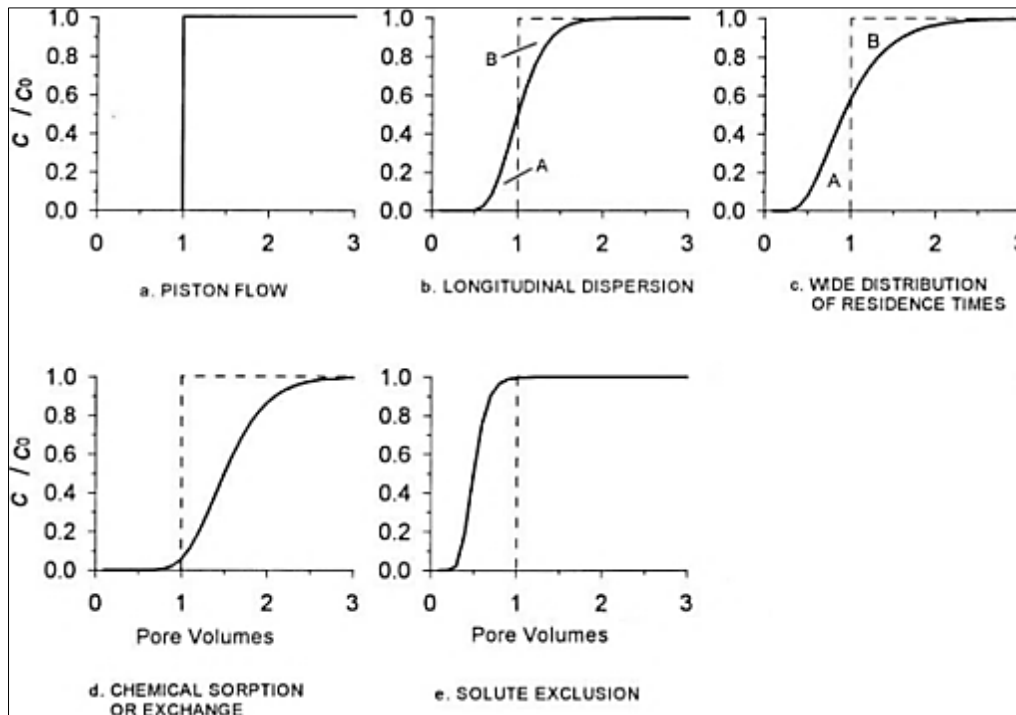


Figure 2.7 Typical Breakthrough curves for column leach tests (adapted from Nielsen and Biggar, 1962)

The other types of BTCs are represented by Curves (d) and (e) which show delayed responses (Figure 2.7 d and e). Curve (d) shows a delayed response due to chemical and physical interactions between the solute and solid (soil) matrix. Curve (e) represents a delayed BTC due to incomplete mixing between the solute-soil matrix, owing to stagnant (dead) pore spaces. Curve (e) results in an increase in solute concentration (Nielsen and Biggar, 1962). The differences between Curves (a), (b) and (c), from (d) and (e), are because there is no interaction between solute and solid matrix in Curves (a), (b) and (c), whilst for (d) and (e) there is some interaction between the solute and solid matrix. This is shown by the areas marked A and B in Figure 2.7 (a and b), whereby the area under the BTC, up to one pore volume, is the same as the area above the curve, for all times greater than one pore volume (Nielsen and Biggar, 1962).

The above-mentioned breakthrough curves represent a scenario, where a solute of known concentration (a tracer solute) is leached through a non-contaminated solid matrix. In the case of contaminated soil, where the solute or element of concern is already in the soil matrix, the expected breakthrough curve shapes will be the inverse of those described in Figure 2.7. The inverted curves are shown in Figure 2.8. Curve (a) represents a non-reactive (conservative) solute, which reaches a relative concentration 0.5 at 1 pore volume. Curve (b) represents a

BTC that has the symmetry point shifted to the left. This indicates that the solution is exiting the column at a later stage than the non-reactive solute and that the solute concentration is being reduced by adsorption or precipitation processes. Curve (c) represents early breakthrough, whereby a relative concentration of 0.5 is reached before 1 pore volume, as all macro and micro pores are participating and the tail represents the dissolution of solute from pore spaces (Rao, 1974)

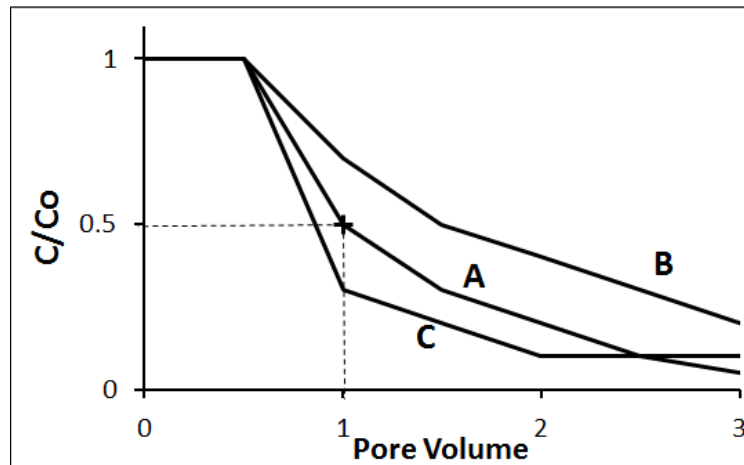


Figure 2.8 Inverted breakthrough curves for contaminated soil (adapted Rao, 1974)

The shape of BTCs is important as it allows for the interpretation of column leach test results and gives an indication of the transport processes occurring within soil columns.

Fey and Guy (1993) undertook column leach tests that sought to simulate the impact of acid rain on South African soils. They did this by allowing a simulated solution of acid rain to pass through a soil column and analysed the effluent for cations and anions. This allowed for the determination of the impacts of acid rain on different soil types.

The objective of the Fey and Guy (1993) study was to investigate the response of soils from the Vaal Catchment to sulphur loads from atmospheric deposition and the subsequent impacts on the Catchment's water quality. The response of the Vaal Catchment was compared to other soils obtained from the Natal region, a low atmospheric deposition zone. The study involved sampling soil profiles in the Vaal Catchment and Natal region. Column leaching was done using tubes packed with both bulk samples obtained from the A horizon, whilst those for the B horizon were obtained from soil profiles that had been dug up. Firstly, the samples were "stripped" with distilled water until constant electrical conductivity (EC) values were obtained. Secondly, the samples were saturated with acid suspension solution until

breakthrough was achieved, as indicated by constant EC values. Thirdly, the same samples were saturated with distilled water to determine S desorption behaviour. During the three stages, leachate was obtained and analysed for EC, pH, anion and cation composition.

The results showed that S retention was low, which means that S from atmospheric deposition would have an impact on water quality in the Vaal Catchment. In addition, the results showed that soil acidity is related to the sulphate retention capacity of the soil and that water quality showed signs of being affected by the atmospheric addition of S in the Catchment area.

Although the study gave some insight into the S retention capacity of catchment soils, it had some shortcomings. Firstly, soil samples were obtained from disturbed areas, such as road under-cuttings. Their properties could have been altered and were not truly representative of the soils found in the Vaal Catchment. Secondly, during the leach column tests the soil was first saturated with distilled water and not truly representative of processes that occur naturally in the environment. Thirdly, although soil characterisation was done at the start of the investigation, S adsorption reactions could not be correlated to initial soil characteristics, except for pH. The level of S adsorption showed a strong correlation with pH, allowing pH to be used to extrapolate S adsorption in other soils outside the Vaal catchment.

Besides the above shortcomings, Fey and Guy (1993) concluded that the sulphur retention of soils in the Vaal Catchment was correlated to the increase in Total Dissolved Solids (TDS) in the Vaal Catchment waters.

A follow-up study to the Fey and Guy (1993) work was conducted by Lorentz *et al.* (2010). This study was done using soil from the Sabie and Sandspruit Catchments in the Mpumalanga Province, South Africa. Leach column tests were performed separately for soils obtained from 0-100 mm and 100-200 mm depths. The leaching solutions used were distilled water and simulated acid rain applied to different soil samples. The difference with the Fey and Guy (1993) study was that the soils were not first “stripped” and leached with distilled water before saturation with simulated acid suspension. Another difference was that soils from two different horizons were not packed in the same column, but that leaching was done separately. In addition, two solutions were used in separate replicate columns, a simulated acid rain solution and distilled water. The soils were initially packed in an unsaturated state, allowed to equilibrate, and then the resident liquid was displaced upwards by the ingress of

an invading solution (simulated acid rain or distilled water) from the base. Instead of adding distilled water to determine desorption behaviour, the leach columns were subsequently allowed to evaporate and dry for four months before being leached a second time with the simulated acid rain or distilled water, something closer to field conditions (Lorentz *et al.*, 2010). Differences in soil sampling from the Fey and Guy (1993) study were that soil samples were obtained from undisturbed areas and at three different slope positions in the same catchment. This was done so as to account for the catena effect on a soils' response to acid deposition. The results obtained from the breakthrough curves show that simulated acid rain results in base stripping from the soils, as indicated by the measured cation concentration in the leachate.

Of particular interest was that the release of S and Mn did not follow the expected trend and questions on the conditions governing the observed breakthrough were posed. Figure 2.9 shows the concentration of S and Mn, following a similar declining trend with time. The breakthrough curve did not pass through the relative concentration of 0.5 at pore volume 1, like the conservative species. This could be attributed to different sorption mechanisms for S and Mn. The adsorption of S is dependent on many variables, such as pH, redox conditions, temperature and microbial conditions, which vary with slope position, hence the need to extend leach column tests with simulated acid rain to include other slope positions, such as crest and midslope.

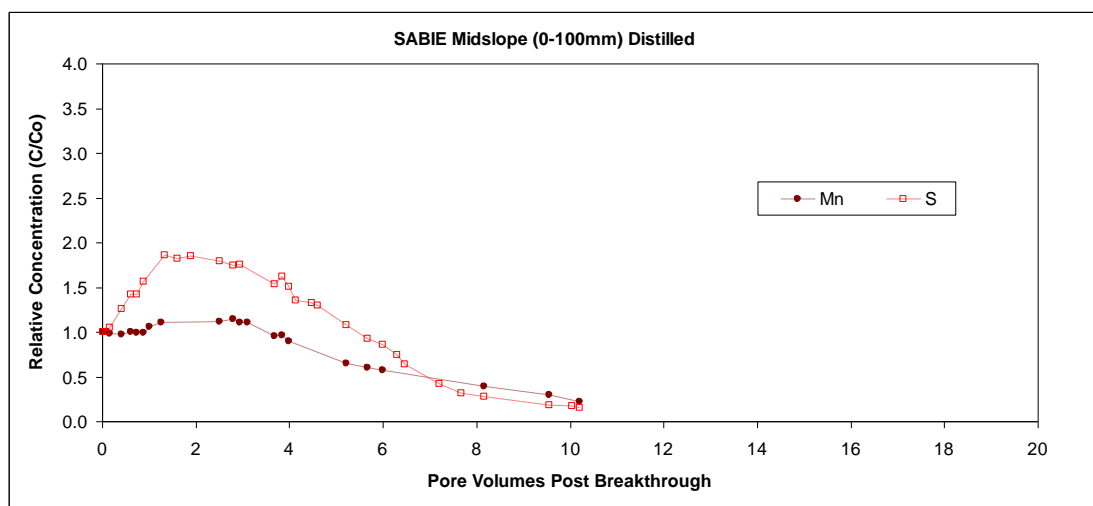


Figure 2.9 Breakthrough curve for S and Mn for Sabie Midslope (0-100mm) leached with distilled water (Lorentz *et al.*, 2010)



Given the leaching characteristics of S and Mn shown in Figure 2.1, there are still unanswered questions, such as; could this unexpected response have been due to prevailing redox conditions under saturated conditions and the effect of soil organic matter and microbial activity? This necessitates the investigation of soil redox conditions, organic matter and soil microbial activity and how they affect column leach breakthrough curves.

## **2.7 Conclusion**

Given the scenario that atmospheric deposition is expected to increase in South Africa, it is important to determine the impacts of this acidification and the leaching characteristics of predominant soil types and use this information to estimate the long-term impacts of acid deposition on soil and water. Emphasis is placed on soil and water, as they are essential resources that require proper management to ensure the continuation of agricultural and industrial production systems. As part of ecosystems, soils and water have natural buffering capacities to counter the effects of atmospheric pollutants, and so these capacities need to be evaluated.

The impacts of atmospheric deposition also need to be investigated from a local South African semi-arid perspective, as most other investigations were conducted in temperate climates. The investigation will be conducted from a small catchment perspective, by looking at responses of at least two different soil types to simulated acid rain along different slope positions.

The following chapter describes the methodology that will be utilised to answer the research question.

## **3. METHODOLOGY**

### **3.1 Introduction**

This chapter contains a description of the study site and methods used during the course of the research to meet the objectives of the study. Leaching characteristics were determined by conducting soil column leach tests with simulated rainwater and distilled water solutions. Basic soil characterisation was conducted to aid in interpreting the column leach test results and the methods used are described, together with the soil sampling protocol utilised (Sections 3.3 to 3.5). The sampling and analysis protocols used to determine catchment water chemistry are described (Section 3.5).

### **3.2 Site Description**

The study site is located in the Eastern Highlands, Mpumalanga Province, South Africa, where a research catchment was established on Mr Wessel Oosthuizen's second farm. This Catchment was referred to as "Wessel's Farm" during the course of the research. The research Catchment (latitude -27.2323 S; longitude 29.9177 E) is approximately 14 km north of Volksrust (Figure 3.1) and is in the headwaters of the Sandspruit Catchment, which feeds into the Klip River Catchment. The area is characterised by mixed grasslands, with mostly sourveld species, and is currently utilised as pasture for cattle ranching. The geology comprises fine sedimentary rock of the Karoo system and the soils are thin and sandy. The mean annual precipitation of the area is 770 mm (WRC, 2009). The site was chosen for its close proximity to coal-fired power stations, which contribute to the atmospheric deposition of oxides of S and N. The closest power station was identified as the Majuba Power station, which is approximately 24 km south-east of the research Catchment.

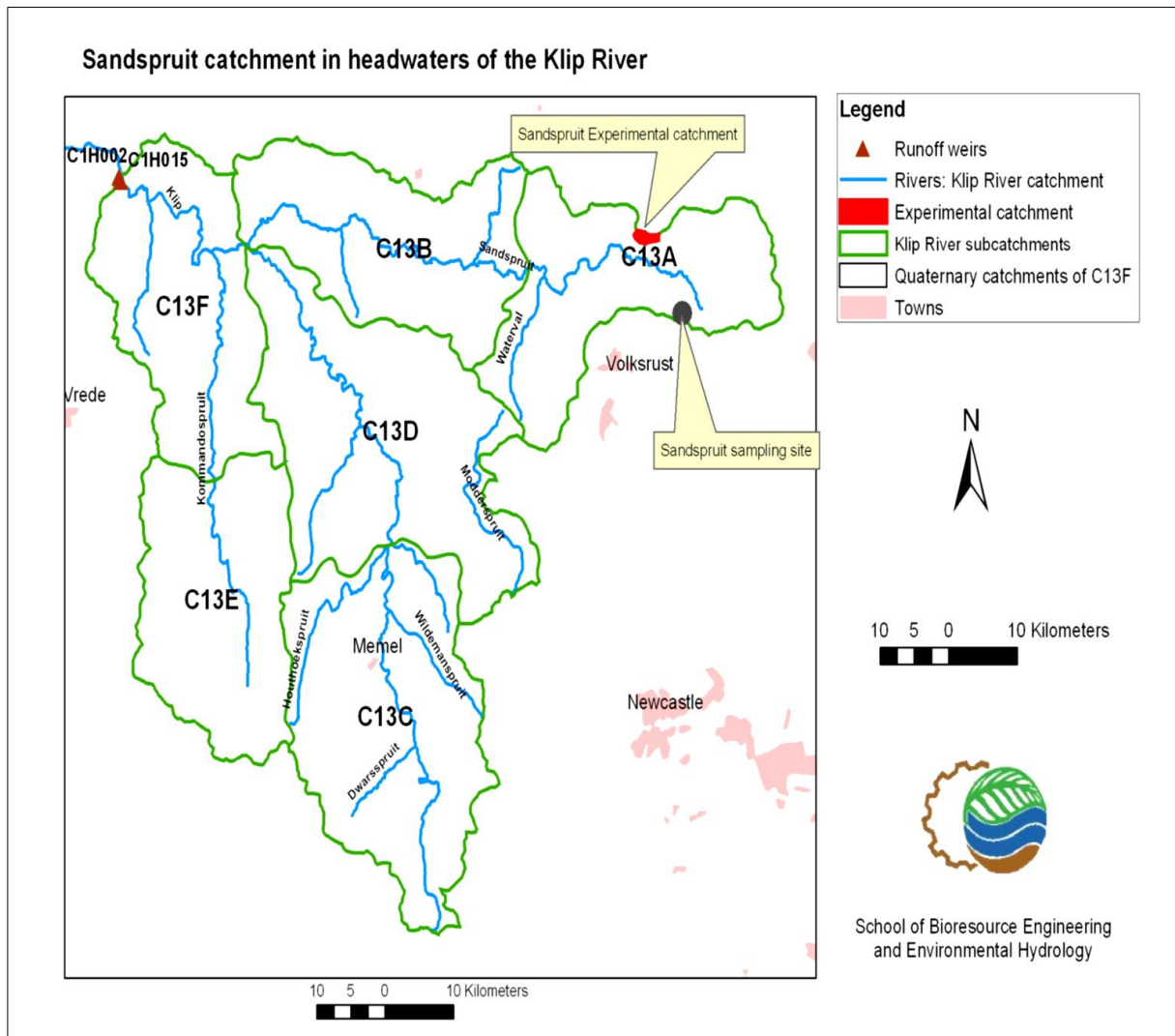


Figure 3.1 Location of the Sandspruit Experimental Catchment (Lorentz, et al., 2010)

### 3.3 Soil Sampling

The first soil sampling exercise was conducted during the third week of February 2012. Soil samples were obtained from three different hillslope positions within Wessel’s Farm, that is, the crest (lat. -27.236840; 29.922010), the mid-slope (lat. -27.234740; 29.916780) and the toe slope (lat. -27.234180; 29.915040). These positions were chosen to take account of changes in soil characteristics that occur with changes in the slope gradient (catena effect). This first soil sampling site was located on a transect, where a weather station had been installed, and was thus referred to as the “weather station” transect (Figure 3.2). The second soil sampling analysis was conducted in February 2013 and was done on another transect near the windmill on the research catchment (Figure 3.2) and was thus referred to as the “windmill site”. The

windmill site was sampled from two slope positions, that is, the crest (lat. -27.235400; 29.934650) and the toe (lat. -27.235660; 29.932650), as the transect was short and disrupted by a road.

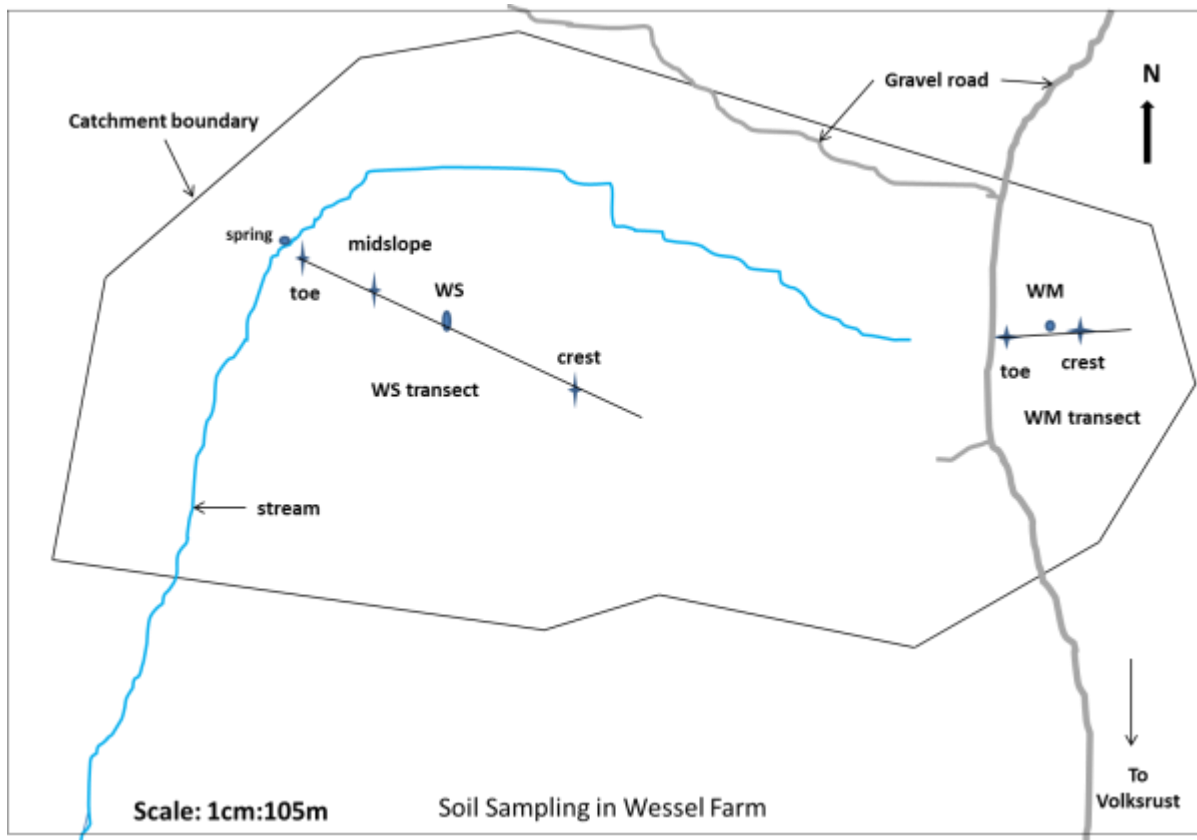


Figure 3.2 Map of the Sandspruit Research Catchment showing, soil sampling positions in relation to the weather station, windmill and spring

At each slope position, bulk samples were obtained from the 0-100 and 100-200 mm depths, using a shovel from a (1 x 1) m quadrant. Sampling was continued by augering at 200 mm incremental depths until saprolite was reached (Figure 3.3) and these samples kept for future column tests. Core (7.5 cm in diameter and 5.0 cm in height) samples were also taken at soil depths of 0-100 mm and 100-200 mm, in triplicates, for the determination of bulk density and saturated hydraulic conductivity.



Figure 3.3 Soil sampling using an auger (left) and soil cores (right)

After sampling, the soil was air-dried and aggregates were broken up to pass through a 2 mm sieve, before analysis for selected soil parameters and packing for column leach tests, as discussed in the following sections.

### 3.4 Soil Characterisation

Soil characterisation was done for selected parameters, so as to obtain a reference point for processes occurring in the soil before exposure to various leaching liquids.

The following soil chemical characteristics were determined;

- (a) Soil pH, using both a water and 1M KCl 1:2.5 soil to liquid extract (Thomas, 1996). A calibrated CRISON pH meter was used to measure the pH of the extracts.
- (b) Soil Electrical Conductivity (EC) in a 1:2.5 soil to water extract with a calibrated HANNA EC meter (Rhoades, 1996). The EC meter had a temperature sensor and readings were standardised to 25°C.
- (c) Exchangeable Ca, Mg, Na, K, Al, Mn and Fe; and effective cation exchange capacity (CECe) using, the BaCl<sub>2</sub> Compulsive Exchange Method (Hendershot and Duquette, 1986; Sumner and Miller, 1996). The CECe is a rapid estimate of CEC and has been used for regulatory purposes, hence used in this study for comparison with results obtained from other studies. The cations were extracted by a 0.1 M BaCl<sub>2</sub> solution and the exchangeable cation concentration was determined using the Varian ICP OES machine. The CEC was determined by the summation of exchangeable bases, Al, Mn and Fe.
- (d) Soil acidity and exchangeable Al by the KCl Method (van Reeuwijk, 2002). Soil acidity was determined by extracting the soil with a 1M KCl solution, followed by

titration with 0.1 M NaOH. Exchangeable Al from the extract was determined using the Varian Inductively Coupled Plasma – Optical Emission Spectrometer (ICP OES) machine.

- (e) Organic Carbon was determined using the Walkley Black Method, which involves wet oxidation of organic carbon by dichromate and subsequent oxidation-reduction with an Fe<sup>2+</sup> solution (The Non-Affiliated Soil Analysis Work Committee, 1990).
- (f) Soluble anions and cations were determined from a saturated paste extract (van Reeuwijk, 2002). The saturated paste extract pH and EC were determined using a CRSION pH meter and HANNAH EC meter, respectively. Soluble anions, chloride, nitrate-N, sulphate and the cation ammonium-N were determined by the Thermoscientific Gallery Discrete Calorimetric Analyser and cations (Ca, Mg, Na, K, Al, Mn and Fe) were determined using the Varian ICP OES machine. The paste saturation percentage was determined by taking a sample of the saturated paste and determining the water content using the gravimetric method. This was to enable the concentration of cations and anions to be calculated on a mass basis.

The following soil physical characteristics were determined.

- (a) Bulk density using the core method (Tan, 2005).
- (b) Moisture content by oven-drying (van Reeuwijk, 2002).
- (c) Particle size distribution and soil textural classification, by using the Hydrometer Method. Dispersion was done with 4% sodium hexametaphosphate buffered in 1% sodium carbonate (Calgon solution) (Tan, 2005).
- (d) Saturated Hydraulic Conductivity of undisturbed core samples was determined by the Constant Head Method (Reynolds, 1993).

### **3.5 Column Leach Tests**

Column leach tests were conducted with soils from the two hillslope transects, that is, the weather station and windmill transects. For each transect, soils from the crest and toe slope positions were used. The midslope position was rejected because the textural classification was the same as that of the toe soils and leach columns were to be conducted on samples exhibiting different soil textural classifications.

Eight PVC plastic columns 110 mm in diameter and 205 mm in length were packed with soils from the crest (4 columns) and the toe slope (4 columns) positions from the weather station site on Wessel Farm. The column dimensions were chosen so as to reduce boundary flow effects and column dispersivity. This eight-column set-up was repeated for the windmill transect. No replicates for each column treatment were done, according to Malmstrom *et al.*, (2006), who carried out leaching experiments with the same size columns without any replicates. Surface soils (0-100 mm) were used for packing columns to the required bulk density equivalent to that measured by the core method and water content (Table 3.1). The soil was first wet to 50% saturation level using distilled water or simulated rainwater, according to the treatment type and left to equilibrate for 24hrs. The soil was then packed in quarterly increments, and compressed using a wooden board to ensure that all the soil would fit into the column. Discs of stainless steel mesh, milk filter, coarse sand or diatomaceous earth were placed at both ends of the columns, depending on whether the column treatment was aerated or non-aerated (Figure 3.4).

Table 3.1 Soil physical parameters used to pack and run leach columns

	Weather Station Site		Windmill Site	
	Crest	Toe	Crest	Toe
Bulk density (g/cm <sup>3</sup> )	1.4	1.4	1.2	1.4
Assumed particle density (g/cm <sup>3</sup> ) (Tan, 2005)	2.65	2.65	2.65	2.65
Porosity	0.47	0.47	0.56	0.49
Water content (50% saturation)	0.24	0.24	0.28	0.25
Volume of column (cm <sup>3</sup> )	1732.5	1732.5	1732.5	1732.5
Mass of air dried soil to pack (g)	2692.31	2595.29	2387.25	2622.97
Saturated hydraulic conductivity (cm/hr)	0.023	0.018	5.960	2.352
Flow rate applied to columns (cm <sup>3</sup> /hr)	1.62	1.62	22.32	22.32

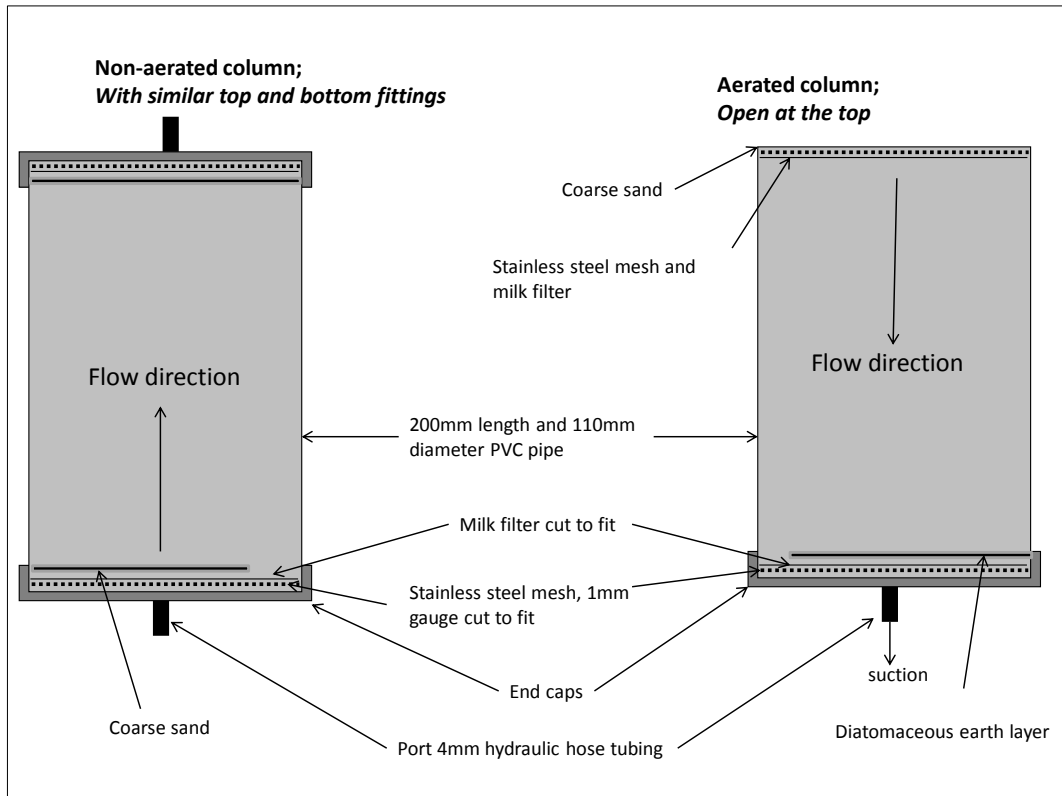


Figure 3.4 Components used in packing aerated and non-aerated columns

After packing, the columns were placed on a wall bracket and treatments applied (Table 3.2). The aerated columns were left open at the top and leaching liquid was applied from the top (Figure 3.5). They were placed higher than the non-aerated columns to ensure the leachate outlet was at least 1 m from the collection point to allow for 1 m suction at the base of the column. The non-aerated columns were closed and sealed on both ends, pumping was from the bottom and leachate was collected from the outlet point at the top of the column (Figure 3.5 and Figure 3.6).



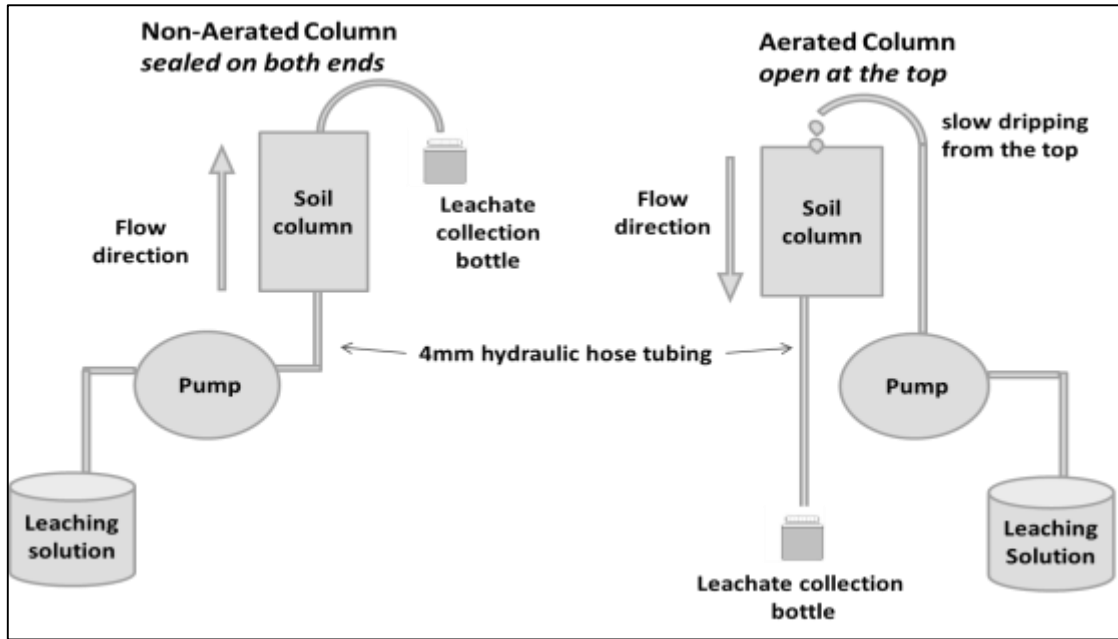


Figure 3.5 Leach column set-up showing direction flow of leaching liquid in the column and leachate collection positions



Figure 3.6 Eight columns mounted on the wall bracket, with 4 aerated columns (top) and 4 non-aerated columns (bottom)

A flow rate of  $1.62 \text{ cm}^3/\text{hr}$  was applied to all weather station columns and  $22.32 \text{ cm}^3/\text{hr}$  for all windmill columns. This was based on half the measured saturated hydraulic conductivity of the soil samples, as shown by the following equation:

$$Q = \left( \frac{K_{\text{sat}}}{2} \right) \times \text{cross sectional area of column} \quad (3.1)$$

Where:  $Q$  = flow rate ( $\text{cm}^3/\text{hr}$ )

$K_{sat}$  = saturated hydraulic conductivity (cm/hr)

The  $K_{sat}$  for the weather station samples was divided by a factor of 2, to ensure that the non-aerated columns did not become flooded. For windmill soils, the  $K_{sat}$  was much higher than the weather station soils, therefore, to avoid flooding, the  $K_{sat}$  was divided by a factor of 10. This was determined from prior column leach tests conducted by Lorentz *et al.*, (2010). The peristaltic pump could not allow for different flow rates for each of the eight columns, hence the lowest  $K_{sat}$  between crest and toe slope was utilised for each eight-column setup.

Two leaching solutions were used for each eight-column setup, that is, distilled water and simulated rainwater (Table 3.2). Distilled water was used as the control, whilst simulated rainwater was used to simulate leaching characteristics under acid deposition.

Table 3.2 Leaching liquid and level of aeration applied to both set of columns (weather station and windmill soils). Each setup consisted of 8 columns as indicated in the right hand column

<b>Soil Sample</b>	<b>Aeration</b>	<b>Leaching liquid</b>
Crest	Aerated	Distilled water
		Simulated Rainwater
	Non-Aerated	Distilled water
		Simulated Rainwater
Toe	Aerated	Distilled water
		Simulated Rainwater
	Non-Aerated	Distilled water
		Simulated Rainwater

The simulated rainwater was prepared, based on measured rain water chemistry from Amersfoort, as shown in Table 3.3 and had a pH of 4.35 (Lorentz *et al.*, 2010). The distilled water had a pH of 7.05.

Table 3.3 Rainwater chemistry for Amersfoort, Mpumalanga, and the simulated rainwater used in the column leach experiments

Rainwater chemistry for Amersfoort (after Mphepya, 2002).		Simulated rainwater chemistry used in the column leach experiment (after Lorentz, <i>et al.</i> , 2010)	
Cations ( $\mu\text{mol/l}$ )	Anions ( $\mu\text{mol/l}$ )	Cations ( $\mu\text{mol/l}$ )	Anions ( $\mu\text{mol/l}$ )
H <sup>+</sup> : 44.9	CH <sub>3</sub> COO <sup>-</sup> : 6.1	H <sup>+</sup> : 44.9	CH <sub>3</sub> COO <sup>-</sup> : 6.1
Na <sup>+</sup> : 9.3	HCOO <sup>-</sup> : 7.6	Na <sup>+</sup> : 9.3	HCOO <sup>-</sup> : 7.6
NH <sub>4</sub> <sup>+</sup> : 22.3	SO <sub>4</sub> <sup>-</sup> : 59.1	NH <sub>4</sub> <sup>+</sup> : 22.3	SO <sub>4</sub> <sup>-</sup> : 59.1
K <sup>+</sup> : 4.7	Cl <sup>-</sup> : 9.8	K <sup>+</sup> : 4.7	Cl <sup>-</sup> : 8.4
Ca <sup>++</sup> : 18.7	NO <sub>3</sub> <sup>-</sup> : 25.0	Ca <sup>++</sup> : 18.7	NO <sub>3</sub> <sup>-</sup> : 25.4
Mg <sup>++</sup> : 6.7		Mg <sup>++</sup> : 6.7	
$\Sigma$ 106.6	$\Sigma$ 107.6	$\Sigma$ 106.6	$\Sigma$ 106.6

The acid rain was made from 1.341 g (NH<sub>4</sub>)<sub>2</sub>SO<sub>4</sub>, 0.517 g HCOONa, 2.208 g Ca(NO<sub>3</sub>)<sub>2</sub>·4H<sub>2</sub>O, 0.859 g Mg(NO<sub>3</sub>)<sub>2</sub>·6H<sub>2</sub>O, 0.099 g NaCl, 0.107 g NH<sub>4</sub>Cl, 0.350 g KCl, 6.1 ml 1 M acetic acid and 19.4 ml H<sub>2</sub>SO<sub>4</sub>. The reagents were mixed in 1 L deionised water. This solution was 1000 times the concentration needed and had to be diluted to make a bulk solution used for leaching. The bulk sample was made from mixing 20 ml of the stock solution in 20 L deionised water.

Leachate from the weather station columns was collected daily, whilst that from the windmill soils was collected at 4-hour intervals during the day and at 8-hour intervals during the night. The sample collection period was based on the expected pore volumes after breakthrough occurred and was calculated from the flow rate and the total column pore volume. A minimum of 0.1 pore volumes (approximately 40 cm<sup>3</sup>) was deemed as a sufficient volume for the pH, EC, redox potential, base cation and heavy metal analysis, and anion analysis.

Upon collection, the sample was measured to determine the exact pore volume. The collected leachate was analysed for pH, redox potential, electrical conductivity (EC), sulphur, base cations and heavy metals (Al, Mn and Fe). Selected samples were also analysed for nitrate, ammonium, chloride and sulphate.

### 3.6 Catchment Water Sampling and Analysis

Water was sampled within the established research catchment located on Wessel's Farm. The samples were taken on 18 March 2011, 23 June 2011, 25 August 2011, 3 November 2011, 31

and January 2012. Samples were extracted from the stream, spring and borehole within Wessel's Farm and also from tributaries to the Sandspruit River itself, up to the confluence with the Klip River (Figure 3.7). The surface water samples were taken just below the surface and as far away from the stream bank as possible by immersing rinsed 250 ml polyethylene bottles. Borehole samples were taken from the tap at the reservoir outlet, whilst the spring samples were taken from spring outlet.

The pH and EC of the samples was measured in-situ and kept at less than 4 °C for the laboratory analysis of sulphate and nitrate, using a calibrated HACH DR/2000 Spectrophotometer and base cations (Ca, Mg, Na and K) analyses, using the VARIAN ICP OES machine.

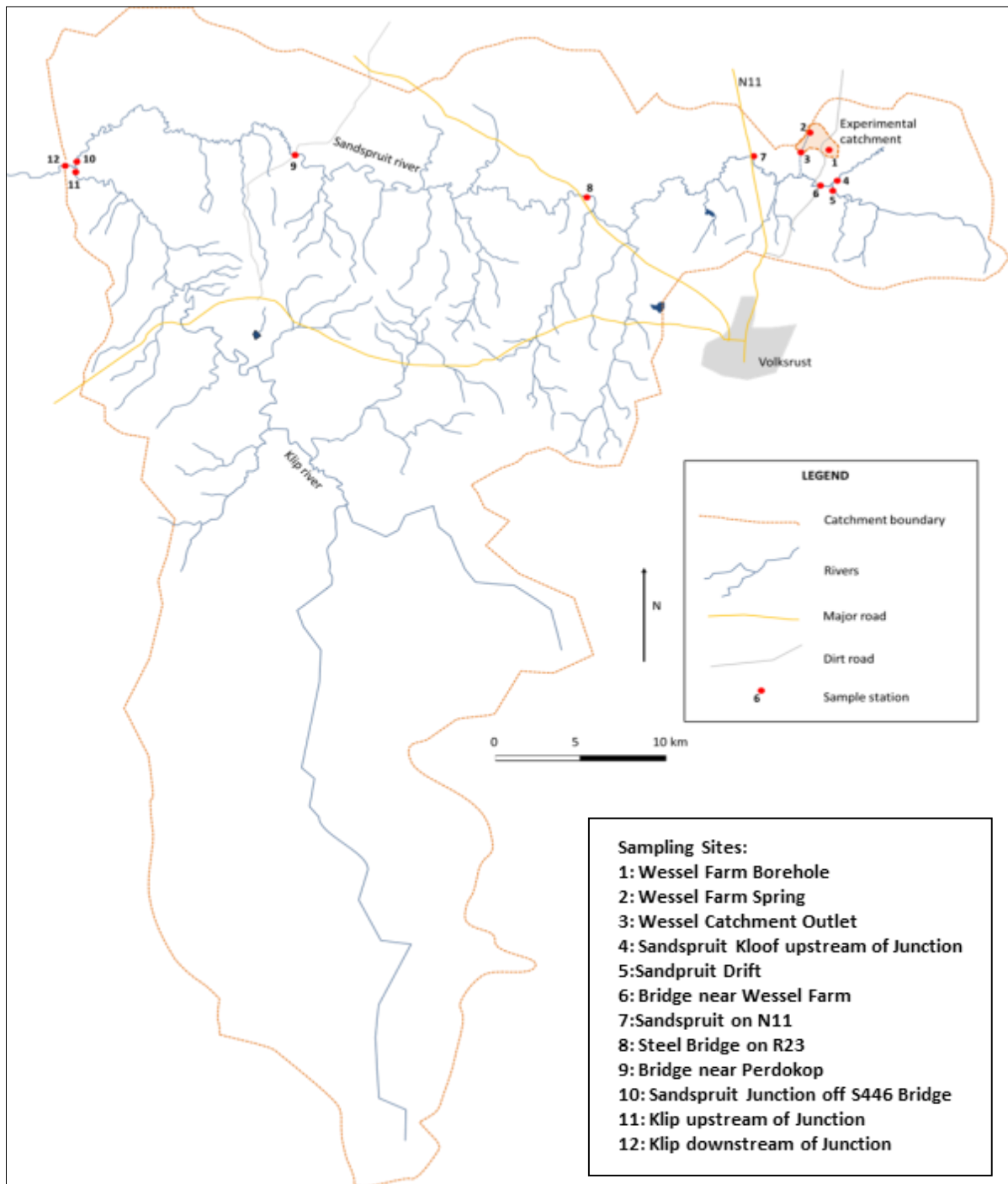


Figure 3.7 Map indicating the location of surface water sampling positions in the Sandspruit Catchment

## **4. THE LEACHING BEHAVIOUR OF SANDSPRUIT CATCHMENT SOILS EXPOSED TO SIMULATED ACID RAIN AND DISTILLED WATER**

### **4.1 Introduction**

This chapter consists of a summary of results for, and a discussion on, the chemical and physical characteristics of soil, as well as the leach column test results for the weather station (WS) and windmill (WM) soil columns.

### **4.2 Soil Characterisation**

The physical and chemical characteristics of soil are summarised in Table 4.1. The pH results for all samples range from slightly acidic (greater than 6.0) to moderately acidic (between 5.6 and 6.0). The exchangeable acidity results are low, as the values are directly related to soil pH. The exchangeable acidity represents acidity from the hydrolysis of exchangeable  $Al^{3+}$  ions on soil exchange surfaces, and is an indicator of the amount of soluble Al in the soil. The exchangeable acidity also represents acidity from  $H^+$  ions from the hydrolysis of organic matter. The soils have high organic matter content, greater than 4% for all cases, as summarised in Table 4.1. This explains the values of exchangeable acidity observed in the WM toe slope and WS crest and toe even though  $Al^{3+}$  is below detection limits in all the cases. The electrical conductivity of the 1:2.5 soil extract is low, ranging from 0.023 to 0.083 mS/cm, indicating non-saline conditions.

The exchangeable bases and cation exchange capacity results, obtained from extraction with 0.1M  $BaCl_2$  solution, are summarised in Table 4.2. Exchangeable Ca and Mg are more abundant than the other exchangeable cations. Sodium is detectable in the WS toe slope sample only and is below detection limits in the rest of the soils, which is again an indication of non-saline soil conditions. Aluminium is detectable in the WM crest slope sample only and is below detection limits in the rest of the soil samples. The absence of Al in most of the samples is due to the soil pH being above 5.5, where Al occurs in an insoluble state. Manganese is below detection level in only one sample, that is, the WM toe slope, with the

rest of the samples having low Mn concentrations. The WS soils have high CECe values above 20cmol<sub>c</sub>/kg, indicating high buffering capacity, a characteristic of soils with high clay and organic matter content. On the other hand, the WM soils have moderate CECe, indicating a moderate buffering capacity. However, all samples have very high base saturation (greater than 80%), indicating very weakly leached soils, with very low Al<sup>3+</sup> ion concentrations.

Table 4.1 Soil physical and chemical characteristics determined in a 1:2.5 extract. All soil samples were obtained from the 0-100mm depth

Site	Slope position	Bulk density (g/cm <sup>3</sup> )	Particle size distribution			Soil Texture (USDA)	Saturated hydraulic conductivity (cm/hr)	Organic matter content (%)	pH <sub>water</sub> 1:2.5	pH <sub>KCl</sub> 1:2.5	EC <sub>2.5</sub> (mS/cm)	Exch. Acidity (cmol <sub>c</sub> /kg soil)	Exch. Al <sup>3+</sup> (cmol <sub>c</sub> /kg soil)
			Sand (%)	Silt (%)	Clay (%)								
<b>Weather Station</b>	Crest	1.40	53	22	25	Sandy Clay Loam	0.02	9.1	5.8	4.5	0.08	0.04	*
	Toe	1.40	33	26	41	Clay	0.02	5.3	6.2	4.9	0.05	0.08	*
<b>Windmill</b>	Crest	1.16	54	22	24	Sandy Clay Loam	5.96	6.6	6.4	4.9	0.03	0.11	0.12
	Toe	1.35	53	27	20	Sandy Loam	2.35	4.1	5.7	4.6	0.02	0.15	*
<b>Standard deviation</b>								2.1	0.3	0.2	0.01	0.1	0.1

\*below detection limit

Table 4.2 Soil exchangeable bases and effective cation exchange capacity determined by extraction with 0.1M BaCl<sub>2</sub> solution

Site	Slope position	Depth (mm)	Exch. Ca <sup>2+</sup>	Exch. Mg <sup>2+</sup>	Exch. Na <sup>+</sup>	Exch. K <sup>+</sup>	Exch. Al <sup>3+</sup>	Exch. Mn <sup>2+</sup>	Exch. Fe <sup>2+</sup>	CECe (cmol <sub>c</sub> /kg soil)	Base Saturation (%)
			(cmol <sub>c</sub> /kg soil)	(cmol <sub>c</sub> /kg soil)	(cmol <sub>c</sub> /kg soil)	(cmol <sub>c</sub> /kg soil)	(cmol <sub>c</sub> /kg soil)	(cmol <sub>c</sub> /kg soil)	(cmol <sub>c</sub> /kg soil)		
<b>Weather Station</b>	Crest	0-100	16.3	6.8	*	0.4	*	0.05	*	23.5	99.8
	Toe	0-100	15.9	8.1	0.02	0.4	*	0.06	*	24.4	99.7
<b>Windmill</b>	Crest	0-100	10.4	4.7	*	0.3	0.04	0.05	*	15.5	99.3
	Toe	0-100	6.5	2.3	*	0.3	*	*	*	9.3	98.4
<b>Standard deviation</b>			3.7	2.0	0.01	0.1	0.02	0.04	0.0		

\*below detection limit



The results for water soluble cations and anions, determined by the saturated paste extract procedure, are summarised in Table 4.3. The EC results of all the soil samples are below 4 mS/cm, indicating non-saline conditions. The EC results obtained from the saturated paste extract are higher than those obtained from the 1:2.5 extract. However, the results of the saturated paste are widely accepted, as the saturated paste is a standardised method of determining EC and soluble anions and cations, hence the results can be used for comparison purposes (Rhoades *et al.*, 1999). The pH<sub>water</sub> measured in the saturation extract is higher than that obtained in the 1:2.5 soil to water ratio. This was contrary to expectation, as the pH<sub>water</sub> in a saturation extract is expected to be lower than in the 1:2.5 extract, due to a low dilution and higher concentration of H<sup>+</sup> ions.

Table 4.3 Water soluble cations and anions from saturated paste extract

Site	Weather Station Site		Windmill Site		Standard Deviation
	Crest	Toe	Crest	Toe	
<b>Slope Position</b>	Crest	Toe	Crest	Toe	
<b>Soil Depth (mm)</b>	0-100	0-100	0-100	0-100	
<b>pH</b>	6.2	6.3	6.5	7.0	0.5
<b>EC (mS/cm)</b>	0.54	0.24	0.19	0.22	0.14
<b>Sulphate (cmol/kg soil)</b>	0.06	0.01	0.05	0.06	0.2
<b>Chloride (cmol/kg soil)</b>	0.04	0.02	0.03	0.03	0.08
<b>Ammonia-N (cmol/kg soil)</b>	0.022	0.003	0.002	0.003	0.07
<b>Nitrate-N (cmol/kg soil)</b>	0.0006	0.0008	0.0008	0.0006	0.003
<b>Ca (cmol/kg soil)</b>	0.35	0.01	0.05	0.04	1.04
<b>Mg (cmol/kg soil)</b>	0.18	0.03	0.03	0.02	0.59
<b>Na (cmol/kg soil)</b>	0.04	0.04	0.02	0.01	0.15
<b>K (cmol/kg soil)</b>	0.006	0.002	0.003	0.005	0.02
<b>Al (cmol/kg soil)</b>	*	0.01	0.02	0.03	0.01
<b>Mn (cmol/kg soil)</b>	0.004	0.001	0.001	0.001	0.002
<b>Fe (cmol/kg soil)</b>	0.00	0.00	0.01	0.01	0.01
<b>Saturation percentage (%)</b>	68.0	48.6	68.9	48.2	9.3

\*below detection limit

Calcium, Mg and Na concentrations in the saturation paste are highest in the WS crest soil and lowest in the WM toe soil. Potassium concentration is highest in the WS crest soil and lowest in the weather station toe soil. Aluminium and Fe concentrations are highest in the WM toe soil and lowest in the WS crest soil. Manganese concentration is highest in WS crest soil and has the same concentration as the rest of the samples. Generally, Ca and Mg concentrations are greater than those of the other exchangeable bases. This is expected, as Ca and Mg are generally in higher abundance in soils, with the exception of sodic soils, where

Na is more abundant than Ca and Mg. Na is low in concentration, indicating non-saline conditions. Aluminium concentration is low across all the samples, indicating that soil pH is not low enough, to cause the release of soluble Al.

Sulphate concentration is higher than ammonium and nitrate, as it is deposited in greater abundance than the nitrogen component of atmospheric deposition. Ammonia-N and nitrate-N were low for all samples, as N is an essential nutrient taken up by plants. The nitrate-N values obtained for these samples indicate that N is not in excess of that required by plants and microorganisms.

### 4.3 Leach Column Results Expressed as Concentration

The results of the measurements and analysis conducted on collected leachate samples from the leach columns are presented in the following sections.

The first sets of results under discussion are those for EC, pH and redox potential. The results are presented as curves, with pore volume on the horizontal axis and EC, pH and redox potential on the vertical axis. The results for base cations, Mn, Al, Fe, S,  $\text{NO}_3^-$  and  $\text{NH}_4^+$  are presented as breakthrough curves (BTCs), with the pore volume on the horizontal axis and concentration in mg/L on the vertical axis. The pore volume is derived from the equation below:

$$\text{pore volume} = \frac{\text{cumulative sample volume}}{\text{total column volume}} \quad (4.1)$$

The BTCs describe the different types of solute movement within soils. For results presented in this chapter, the breakthrough curves of base cations, Mn, Al, Fe, S,  $\text{NO}_3^-$  and  $\text{NH}_4^+$  are compared with the breakthrough curves for chloride ( $\text{Cl}^-$ ). Chloride is a non-reactive solute, hence the shape of its BTC has been used as a reference point for describing solute movement. The results are also presented in tabular form, showing the type of BTCs for each soil column treatment, the breakthrough concentration and the maximum concentration for each element. The type of breakthrough curve was derived from plotting the results as relative concentration ( $C/C_0$ ) against pore volume and these graphs are shown in the Appendices section (Appendix 1 to 11). There are several types of BTCs and the leach column results are grouped into five categories, each representing behaviour similar to typical BTCs, as illustrated in Figure 4.1. Curves 1, 2 and 3 are described under Section 2.6.1.1,

whilst Curves 4 and 5 are not typical BTCs described in the literature review. Curve 4 usually represents breakthrough behaviour for tracer leach column studies. Although the leach columns conducted for this research were not tracer studies, there are some BTCs which show this type of behaviour.

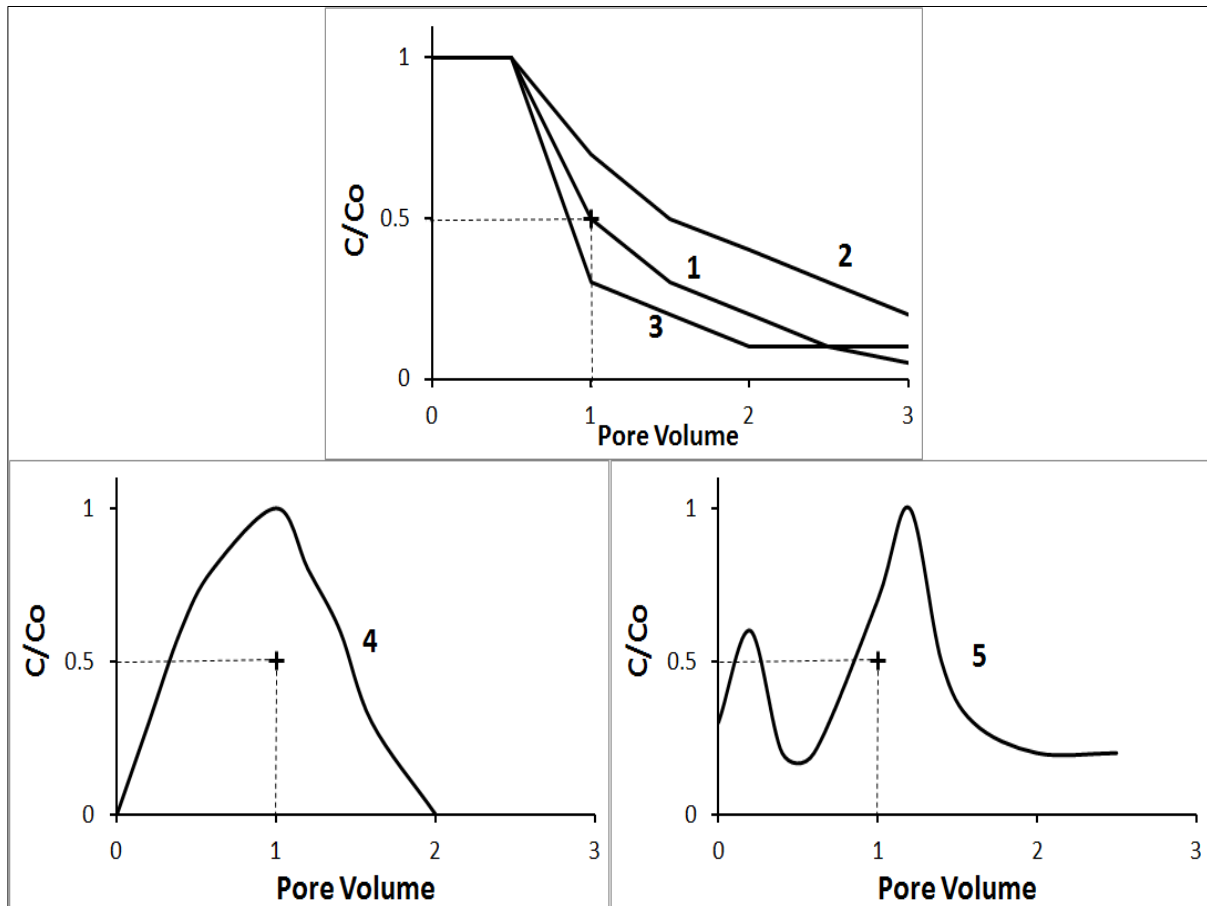


Figure 4.1 Typical BTCs used to group WS and WM column leach test results. Curves 1, 2, 3 are illustrated on the top graph, Curve 4 on the bottom left and Curve 5 on the bottom right

The leach column test results are further expressed as cumulative mass, to determine the actual amount of solutes (in terms of mass per kg of soil) leached from the columns.

### 4.3.1 Electrical conductivity

The leachate electrical conductivity (EC) values from WS soils are higher in non-aerated crest columns than in crest aerated columns throughout the leaching period (Figure 4.2: left). The leachate from WS crest soils has EC values that follow a bell-shaped breakthrough

curve, indicating an initial increase, followed by a decline in EC values as leaching progresses (Figure 4.2: left top), whilst that of WS toe soils follows a continuously declining trend for aerated columns and an initial decline, followed by an increase, for non-aerated columns (Figure 4.2: left bottom).

Leachate collected from WM aerated columns from both crest and toe soil has higher EC values for aerated columns than non-aerated columns from breakthrough up to 0.50 pore volumes for crest soils and 1.00 pore volumes for toe soils (Figure 4.2: right). Thereafter, the values for all eight WM columns become similar throughout the leaching period, showing BTCs with a tail, characteristic of Curve 3 (Figure 4.1). This indicates solution moving into dead pore spaces and being released slowly by diffusion. Unlike the WS soils, there is no difference in leachate EC values arising, due to the use of the two leaching solutions. Both distilled water and simulated rainwater treatments result in the same EC values and BTC shapes.

Comparing the two soils, both WS crest and toe soils result in leachate with higher EC values, indicating that WS soil column leachates have more salts than WM soil column leachates. This is attributed to the initial soil conditions for the two hillslope sites, which show that WS soils have more cations and anions than WM soils, as illustrated by the basic soil characterisation results (Table 4.2 and Table 4.3). Furthermore, higher EC values from the WS soil column leachate indicate more loss of cations and anions from the soil system and potential loading into ground and surface water.

When comparing the leaching behaviour between different hillslope positions (crest vs. toe), based on the EC results, the leaching of cations and anions for both WS and WM sites is higher at the crest slope position than at the toe slope position. This is due to the different soil textures. The WS hillslope crest soil is characterised as sandy clay loam (24.70% clay), whilst the toe soil is classified as clay (41.01% clay). Clay has a higher CEC and buffering capacity than sandy clay loam. On the other hand, the leaching levels of WM crest and toe soils cannot be easily distinguished, as the soils have almost equal amounts of clay and the same clay buffering capacity. The WM crest soil is classified as sandy clay loam (23.79% clay) and the toe soil as sandy loam (20.48% clay).

The EC results show the general leaching characteristics of the soils. The specific processes involved in soil columns can be explained further by looking at the pH and redox of the

leachates, as these parameters influence the solubility and leaching characteristics of cations and anions.

### 4.3.2 pH and redox potential

The breakthrough leachate sample pH values for the sixteen columns, for both WS and WM soils, are shown in Table 4.4. The lowest breakthrough pH value of 5.7 is obtained from WS toe simulated rainwater non-aerated column, whilst the highest pH value of 8.1 is obtained from WM crest simulated rainwater aerated column. The leachate sample with the highest pH goes against expectation, as the simulated rainwater solution has lower pH and would be expected to result in leachate with lower pH. This is because the soil from this sampling position has the highest  $pH_{water}$  of 6.4, compared to the other soil samples (Table. 4.1) and requires more acidity for the pH to go down, that is, the soil has a higher buffering capacity to the added acidity.

Table 4.4 Breakthrough sample pH, EC and redox potential values for all leach columns

Site	Slope Position	Leaching solution	Level of aeration	pH	Redox potential(mV)	EC (mS/cm)
Weather Station	Crest	Distilled Water	Aerated	6.5	177	0.9
			Non-aerated	6.2	189	0.5
		Simulated Rainwater	Aerated	6.4	174	0.8
			Non-aerated	5.8	218	1.3
	Toe	Distilled Water	Aerated	6.7	169	0.7
			Non-aerated	6.1	184	0.6
		Simulated Rainwater	Aerated	7.3	51	0.8
			Non-aerated	5.7	244	0.5
Windmill	Crest	Distilled Water	Aerated	7.5	215	0.6
			Non-aerated	7.1	291	0.2
		Simulated Rainwater	Aerated	8.1	217	0.3
			Non-aerated	7.8	236	0.3
	Toe	Distilled Water	Aerated	7.1	224	0.5
			Non-aerated	6.4	287	0.4
		Simulated Rainwater	Aerated	7.4	215	0.5
			Non-aerated	7.2	230	0.4

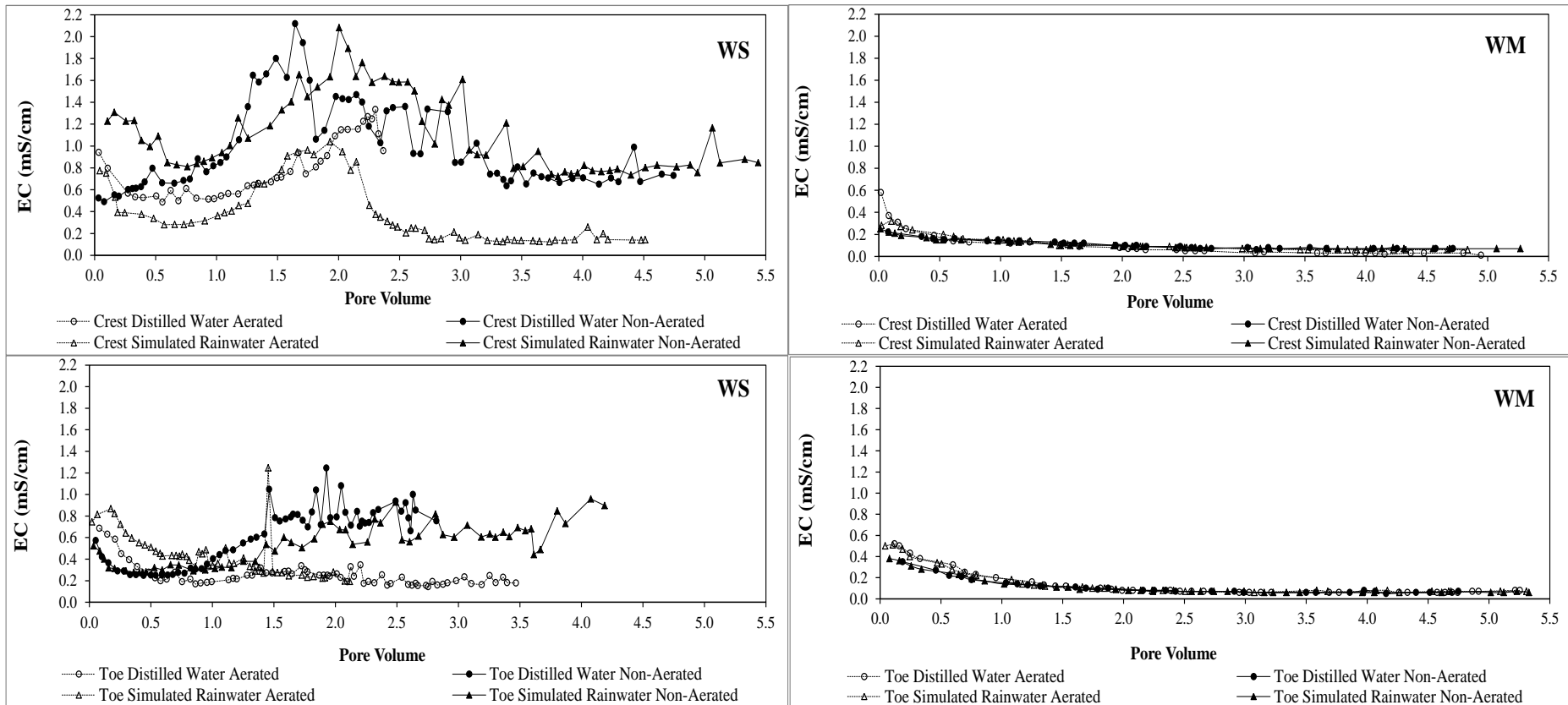


Figure 4.2 Leachate EC breakthrough curves for WS (left: crest above, toe below) and WM (right: crest above, toe below) soil columns

For WS soil columns, the leachate pH values range between 5.7 and 8.5, whilst for WM soil columns, the pH values range between 5.8 and 8.1. The pH values for leachate collected from WS soil columns show an initial increase from breakthrough, to around 0.30 pore volumes, and then fluctuates from alkaline to slightly acidic conditions (Figure 4.3: left). The initial increase and then decline in pH is the same as that observed by Cho *et al.*, (2003) after leaching of soil with SAR.

The pH values for leachate collected from WM soil columns show an initial decline in pH from breakthrough to around 0.70 pore volumes, followed by an increase for crest soils and a decline for toe soils (Figure 4.3: right). The WM crest soil columns show more variation from alkaline to slightly acidic, whilst leachate from the WM toe soil columns are slightly acidic throughout the leaching process. The decrease in leachate pH values for the WM toe soils is similar to studies done by OK *et al.* (2007), Liu *et al.* (2010) and Hedl *et al.* (2011).

The redox potential of leachate collected from WS columns starts with positive values, followed by fluctuating behaviour (Figure 4.4: left). The redox potential values of leachate from non-aerated columns gradually declines to negative values, indicating a transition from oxidising to reducing conditions during the leaching process. The exception is leachate from crest distilled water, which increases to positive values (Figure 4.4: left). The leachate from WS crest simulated rainwater and WS toe distilled water aerated columns remains positive throughout, showing that the columns are under oxidising conditions throughout the leaching process (Figure 4.4: left).

Another point to note is the breakthrough redox potential values for the WS crest simulated rainwater aerated column, which unlike the other columns, had a significantly lower breakthrough redox potential value of 51 mV (Figure 4.4: left bottom). This late breakthrough is attributed to the slow movement of leaching liquid through the column and could have resulted in restricted water movement, leading to low redox potential values. The breakthrough for the column occurred 13 days after the other columns.

The redox potential for leachate from all WM crest and toe soils fluctuates between +150 and +300 mV, which reflects oxidising conditions in all columns throughout the leaching period (Figure 4.4: right). However, there is one exception, where the redox potential in leachate from the crest distilled water non-aerated column drops to 118 mV at 3.10 pore volumes (Figure 4.4, top right).

The main contributing factor to the differences in redox potential values between WS and WM soil columns is the different pore velocity applied under each setup. The pore velocity applied to the soil columns is obtained from the following equation:

$$\text{Pore Velocity, (cm/hr)} = \frac{\text{Flow rate, Q (cm}^3\text{/hr)}}{\text{Column cross sectional area, A (cm}^2\text{)}} \quad (4.2)$$

The pore velocity applied to the WS soil columns is 0.02 cm/hr, whilst that applied to the WM soils columns is 0.3 cm/hr, 15 times more than in WS soils. For the WS soil columns, the slow leach velocity resulted in the redox potential differences between aerated and non-aerated columns. The non-aerated columns became anaerobic over time, whilst the aerated columns remained aerobic (Figure 4; left). On the other hand, there is no difference between the redox potential from the WM aerated and non-aerated columns (Figure 4.5; right). The high pore velocity applied to these soil columns did not allow for anaerobic conditions to develop during the leaching period.



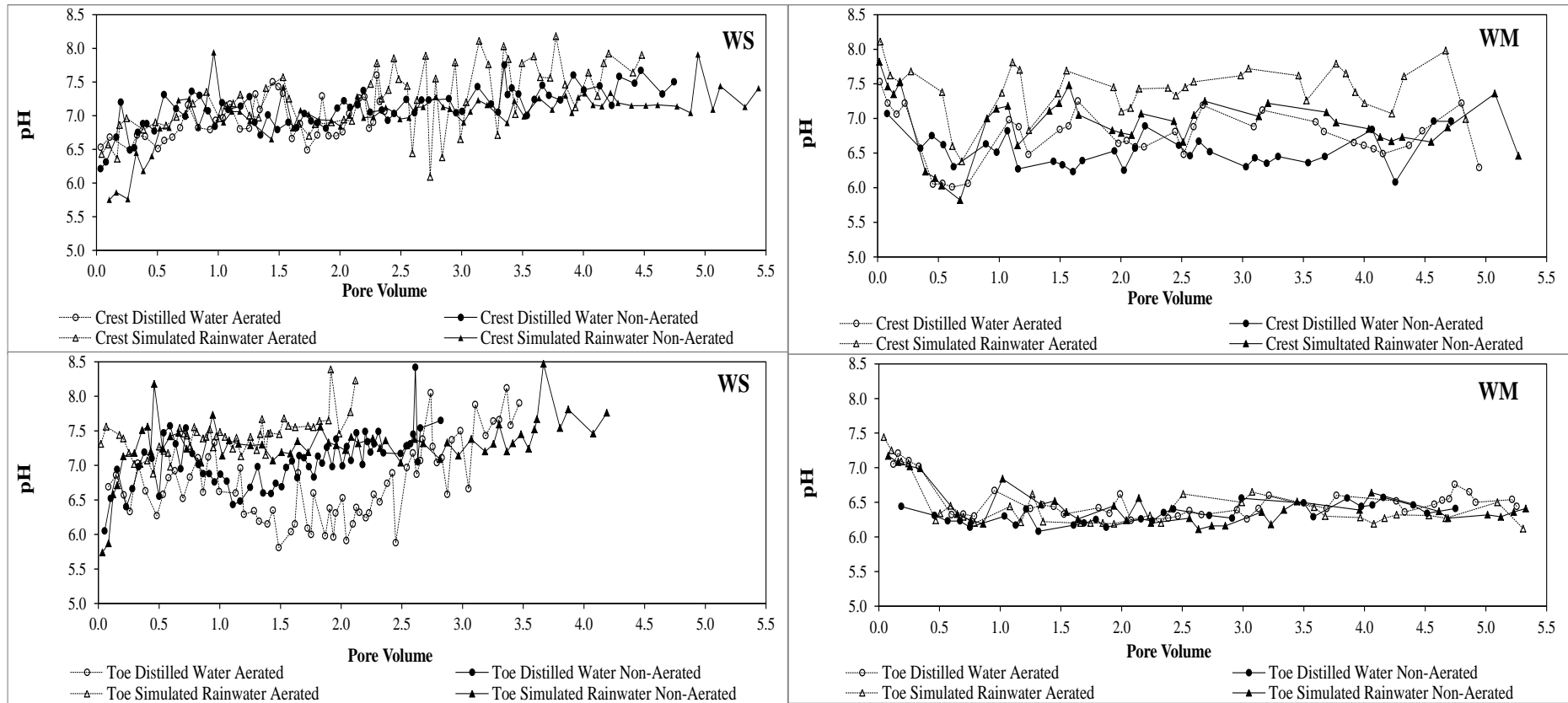


Figure 4.3 Leachate pH breakthrough curves for WS (left: crest above, toe below) and WM (right: crest above, toe below) soil columns

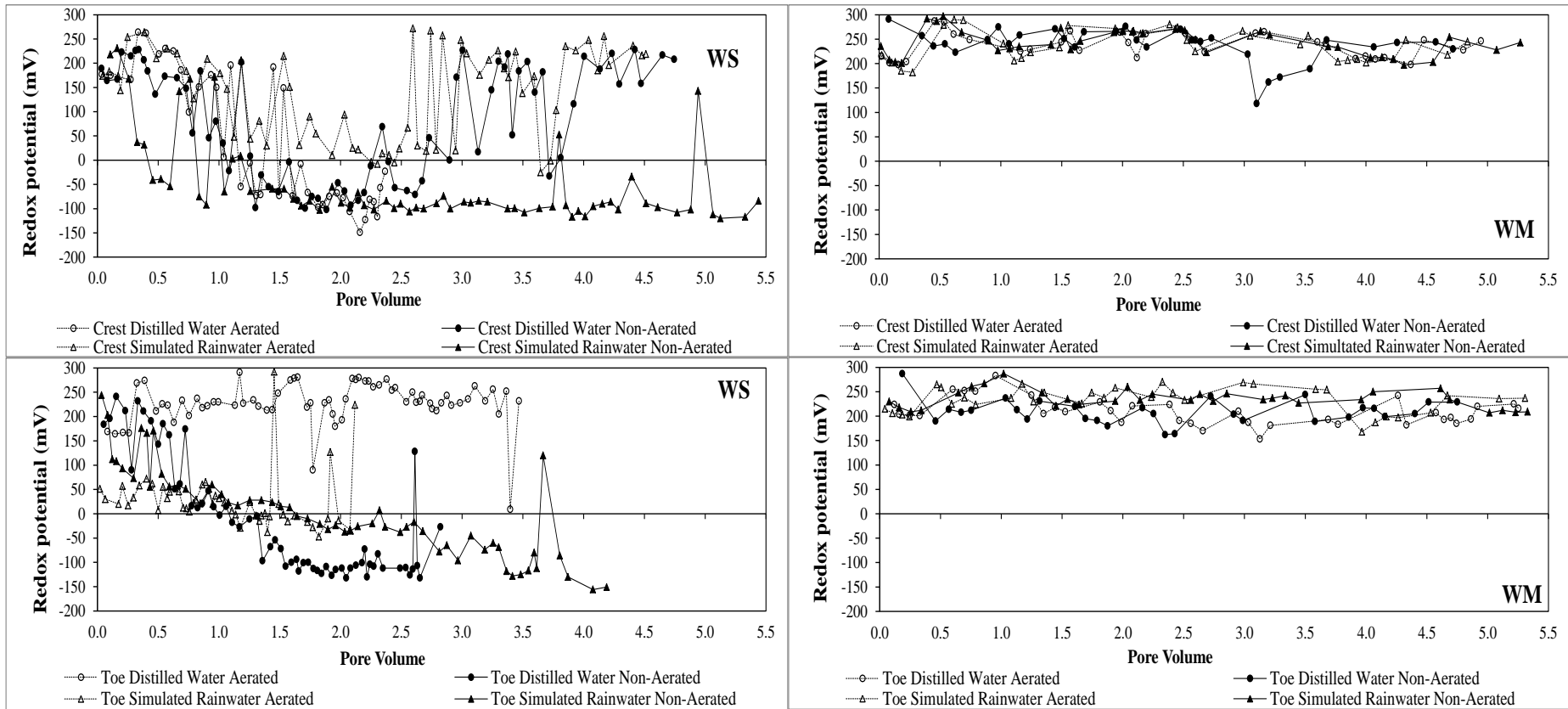


Figure 4.4 Leachate redox potential breakthrough curves for WS (left: crest above, toe below) and WM (right: crest above, toe below) soil columns

Plotting pH and redox potential graphs also shows that leachate from all 16 columns fall in the same pH region, but different redox potential regions, due to the wide variation in leachate redox potential values (Figure 4.5). Plotting pH and redox potential graphs is also significant, as it shows the behaviour of metal and non-metal species with changing pH and redox conditions, and it highlights the sequence of reduction for the various pH and redox conditions. From the column pH and redox potential diagrams, it is expected that, for those columns transitioning from oxidising to reducing conditions, nitrogen as nitrate is reduced to ammonia and sulphate to hydrogen sulphide. The behaviour of base cations (Ca, Mg, Na and K) is not directly affected by changes in redox; hence their behaviour is determined by accompanying anions, such as nitrate and sulphur. For the columns under oxidising conditions, nitrogen as nitrate and sulphur as sulphate are available in solution. The pH and redox potential diagrams show that, WS soil leach columns are alkaline-aerobic, whilst WM soil leach columns are acidic-aerobic. These combinations result in different solubility and leaching characteristics of cation and anions, which are observed in the BTCs discussed later on.

### **4.3.3 Chloride breakthrough curve**

Chloride is a non-reactive (conservative) solute, hence its BTC can be used as a reference, to describe the behaviour of other elements in soil solution. Chloride leachate concentration was measured for WM soils only, as reagents for the analysis were not available at the time of conducting WS column tests. The  $\text{Cl}^-$  BTCs for the WM soils are illustrated in Figure 4.6 and all eight BTCs show the same behaviour. The BTC shape is Number 3 (Table.4.5) for all curves, which indicates an early breakthrough, where the relative concentration of 0.5 is reached before 1 pore volume. Under our leach column conditions, the  $\text{Cl}^-$  BTC does not show the behaviour of a typical non-reactive solute, which is represented by Curve 1 (Figure 4.1). This indicates that the micro-macro pore interactions within the WM soil columns have an impact on the transport processes occurring in the column. The long tail observed in the  $\text{Cl}^-$  BTCs is indicative of non-homogeneous conditions in the soil columns, which result in  $\text{Cl}^-$  moving from dead or micro-pore spaces and being released into the macro-pore conduits by diffusion.

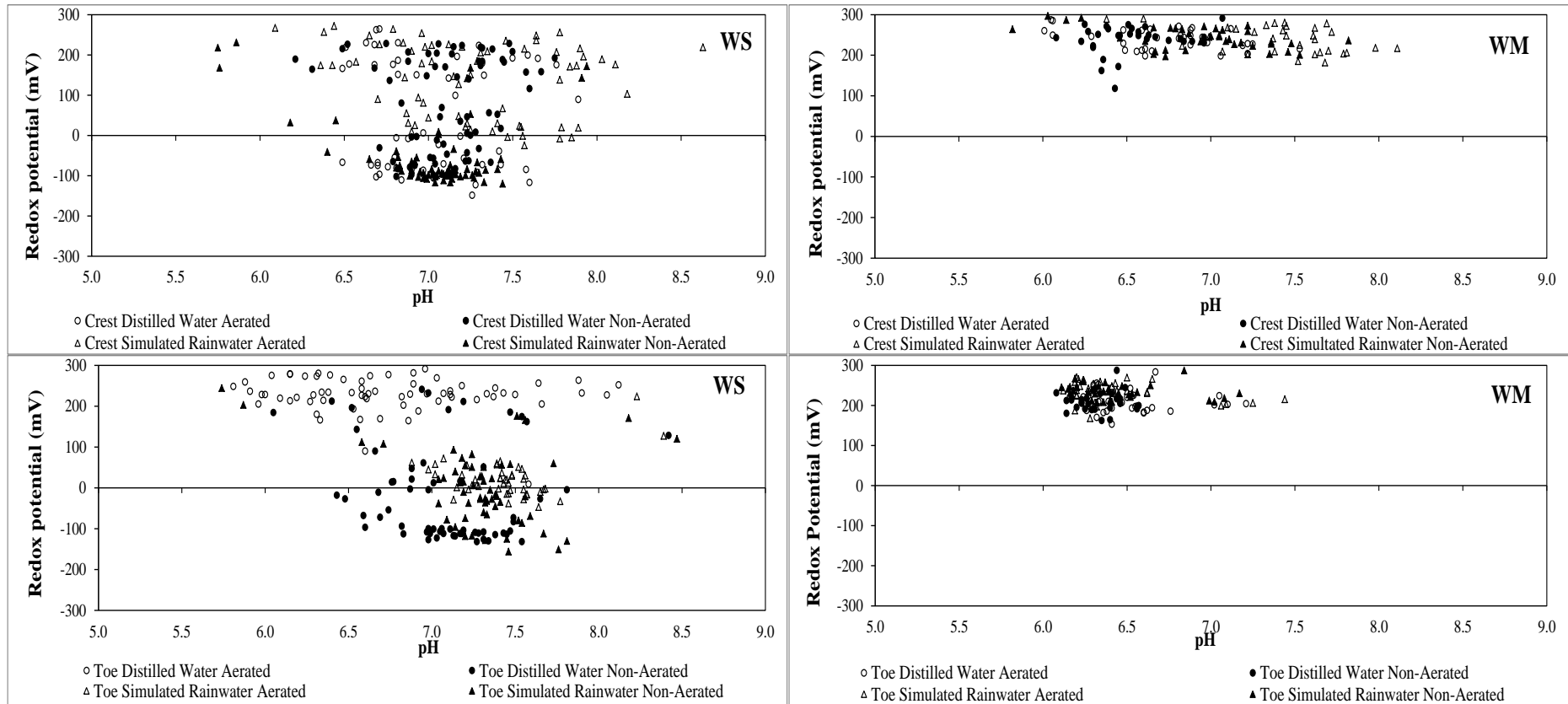


Figure 4.5 pH and redox potential diagrams for WS (left: crest above, toe below) and WM (right: crest above, toe below) leachate samples

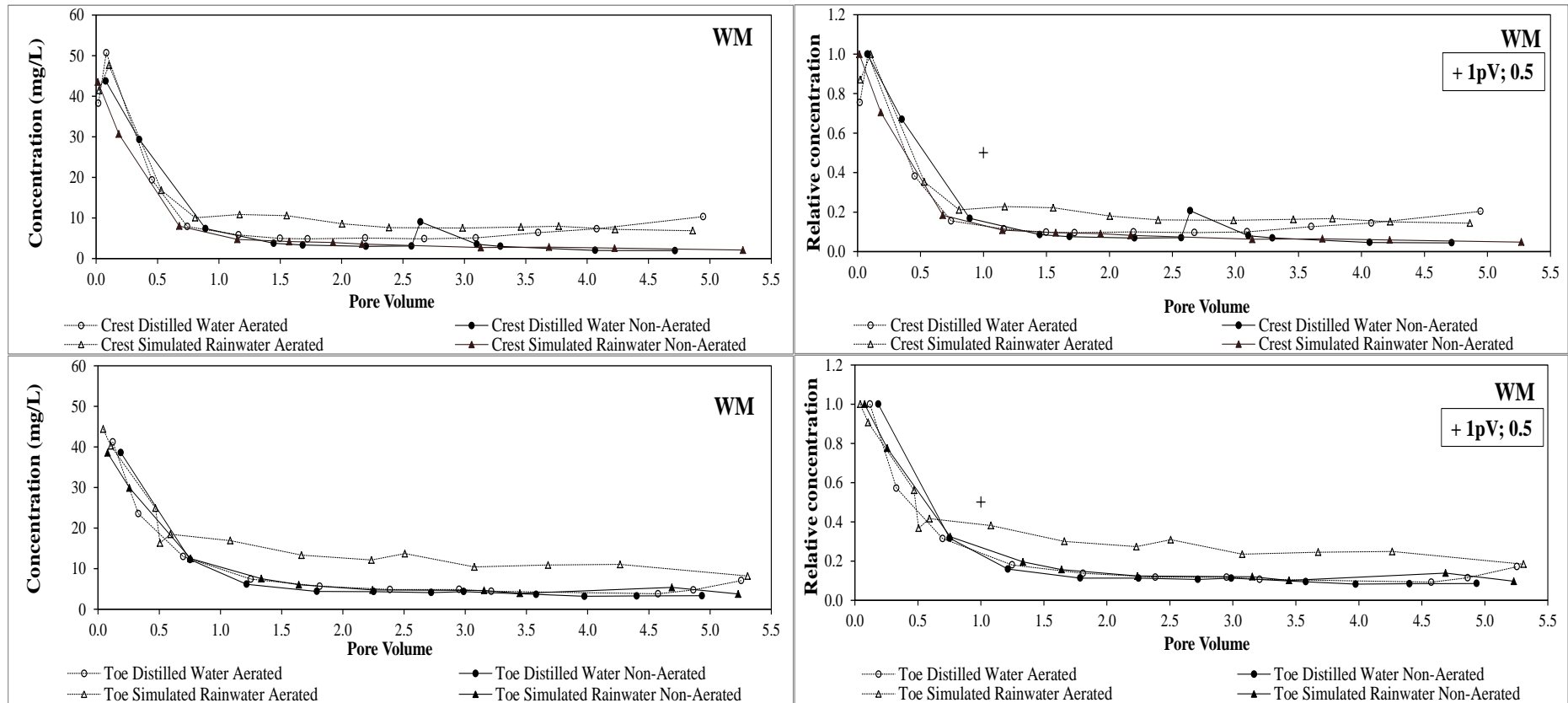


Figure 4.6 Chloride breakthrough curves for WM soil columns as concentration (left: crest above, toe below) and as relative concentration (right: crest above and toe below)

Table 4.5 Chloride BTC shape, BTC, maximum and tail (after 2.5 pore volumes) concentration for WM soil columns

Site	Slope position	Leaching solution	Level of aeration	Chloride			
				BTC shape	Breakthrough concentration (mg/L)	Maximum concentration (mg/L)	Tail concentration (2.5 pore volumes) (mg/L)
Windmill	Crest	Distilled Water	Aerated	3	38.3	50.7	4.9
			Non-aerated	3	43.7	43.7	3.1
		Simulated Rainwater	Aerated	3	41.4	47.6	7.5
			Non-aerated	3	43.5	43.5	2.7
	Toe	Distilled Water	Aerated	3	41.2	41.2	4.8
			Non-aerated	3	36.6	36.6	4.1
		Simulated Rainwater	Aerated	3	44.4	44.4	13.7
			Non-aerated	3	38.5	38.5	4.6

#### 4.3.4 Base cations

The leachate concentrations of Ca, Mg and K for all WS soil column treatments follow the same behaviour as EC and are shown in Figures 4.7, 4.8 and 4.10, respectively. These cations show the same behaviour as EC because they are the main contributors of soluble salts that are measured as EC in soil solutions. The sodium (Na) concentration from WS soil columns shows a general declining behaviour (Figure 4.9). The leachate concentrations of Ca (Figure 4.7: right), Mg (Figure 4.8: right) and Na (Figure 4.9: right) for all WM column treatments follow the same behaviour, that is, a general decline in concentration from breakthrough up to 1.00 pore volumes and thereafter constant concentrations are attained. On the other hand, K shows a different leaching behaviour, compared to Ca, Mg and Na for the WM soil columns (Figure 4.10: right).

The Ca BTC shape for the WS soil columns is Curve 5, with the exception of crest simulated rainwater non-aerated column, which is bell-shaped (Curve 4) (Table 4.6). The bell-shaped curve goes against expectation, as bell-shaped BTCs arise from the pulse or intermittent leaching of a tracer and not from the continuous leaching of already contaminated soils. This indicates some release and adsorption mechanism of Ca from organic matter within this soil column. The BTC shape Number 5 for the other columns is not representative of any typical breakthrough curves defined in literature; hence, it is difficult to explain the process behind the leaching of Ca in these columns. The Ca BTCs for all WM soil columns are similar to Curve 3, indicating an early breakthrough and the use of both micro- and macro-pores for Ca leaching in this column, similar to the processes involved in Cl<sup>-</sup> leaching. The Ca breakthrough behaviour is similar to the leaching of Zn observed by Zheng *et al.*, (2012), whereby the release of Zn occurs in stages. The first stage involves the leaching of the water soluble fraction, followed by adsorption and desorption as Zn moves down the soil profile. The last stage involves release of Zn from different fractions such as organic matter.

The Mg BTCs for the WS soil columns show similar behaviour to that of Ca from the same columns (Table 4.7) However, differences arise from the BTCs for WM soil columns, where leachate from the crest simulated rainwater aerated and toe simulated rainwater aerated columns have BTC Shape 2 and 5, respectively (Table 4.7). Shape 2 indicates that Mg is exiting the column at a later stage than non-reactive solutes, such as Cl<sup>-</sup>, and that Mg is being reduced by adsorption or precipitation processes in this column.

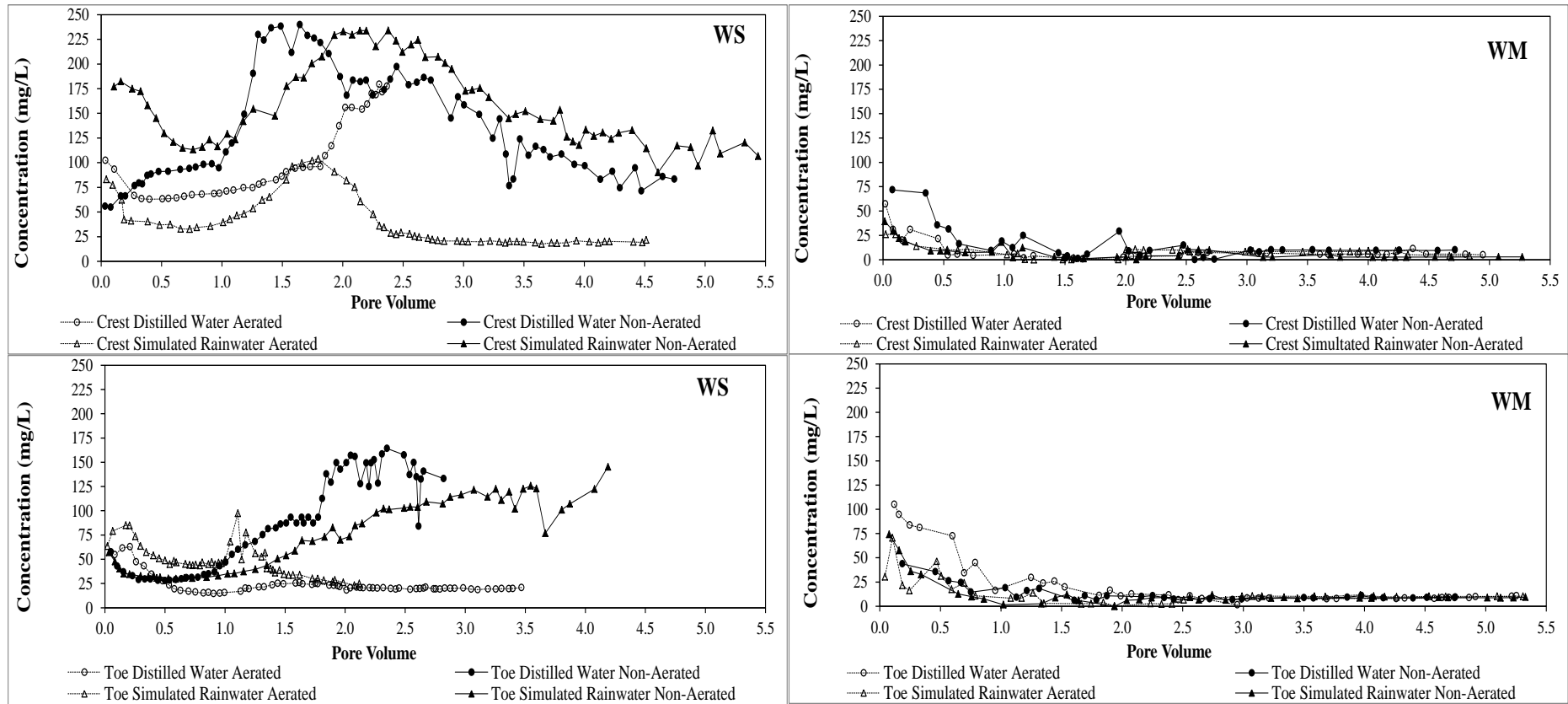


Figure 4.7 Calcium breakthrough curves for WS (left: crest above, toe below) and WM (right: crest above, toe below) soil columns



Table 4.6 Calcium BTC shape, BTC, maximum and tail (after 2.5 pore volumes) concentration for WS and WM soil columns

Site	Slope position	Leaching solution	Level of aeration	Calcium			
				BTC shape	Breakthrough concentration (mg/L)	Maximum concentration (mg/L)	Tail concentration (2.5 pore volumes) (mg/L)
<b>Weather Station</b>	Crest	Distilled Water	Aerated	5	102.4	179.5	177.5
			Non-aerated	5	55.8	239.9	197.2
		Simulated Rainwater	Aerated	5	83.0	103.8	29.1
			Non-aerated	4	177.0	234.0	212.2
	Toe	Distilled Water	Aerated	5	54.6	54.6	20.2
			Non-aerated	5	57.4	164.2	157.5
		Simulated Rainwater	Aerated	5	63.5	97.4	23.2
			Non-aerated	5	57.1	102.8	102.8
<b>Windmill</b>	Crest	Distilled Water	Aerated	3	57.3	57.3	8.0
			Non-aerated	3	71.8	71.8	14.8
		Simulated Rainwater	Aerated	3	26.0	25.7	9.8
			Non-aerated	3	39.3	39.3	10.5
	Toe	Distilled Water	Aerated	3	105.1	105.1	6.7
			Non-aerated	3	43.8	43.8	7.7
		Simulated Rainwater	Aerated	3	30.3	70.6	6.6
			Non-aerated	3	74.1	74.1	9.3

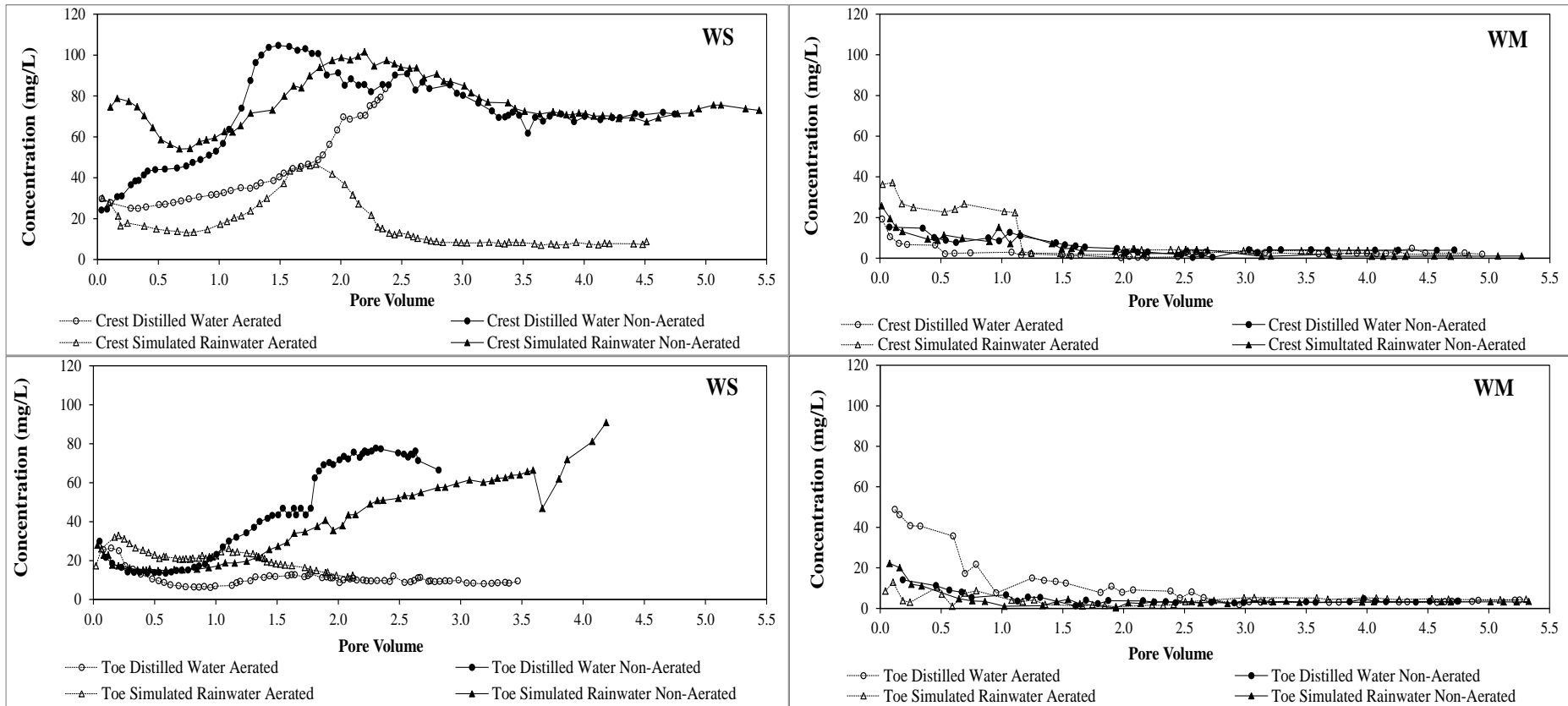


Figure 4.8 Magnesium breakthrough curves for WS (left: crest above, toe below) and WM (right: crest above, toe below) soil columns

Table 4.7 Magnesium BTC shape, BTC, maximum and tail (after 2.5 pore volumes) concentration for WS and WM soil columns

Site	Slope position	Leaching solution	Level of aeration	Magnesium			
				BTC shape	Breakthrough concentration (mg/L)	Maximum concentration (mg/L)	Tail concentration (2.5 pore volumes) (mg/L)
<b>Weather Station</b>	Crest	Distilled Water	Aerated	5	29.7	84.5	83.5
			Non-aerated	5	24.2	104.7	90.2
		Simulated Rainwater	Aerated	4	30.1	46.6	13.0
			Non-aerated	5	74.5	101.5	95.7
	Toe	Distilled Water	Aerated	5	25.5	25.5	12.0
			Non-aerated	5	29.9	77.3	75.3
		Simulated Rainwater	Aerated	5	17.3	32.9	12.4
			Non-aerated	5	27.9	52.0	52.0
<b>Windmill</b>	Crest	Distilled Water	Aerated	3	19.3	19.3	3.1
			Non-aerated	3	15.3	15.3	1.8
		Simulated Rainwater	Aerated	2	36.3	36.3	3.6
			Non-aerated	3	25.8	25.8	4.3
	Toe	Distilled Water	Aerated	3	48.8	48.8	5.0
			Non-aerated	3	14.0	14.0	2.8
		Simulated Rainwater	Aerated	5	8.6	12.9	3.3
			Non-aerated	3	22.2	22.2	3.4

The Na BTCs for leachate from WS aerated soil columns show similar behaviour to that illustrated by Curve 3, whilst the non-aerated columns show similar behaviour to Curve 5 (Table 4.8). This makes Na behaviour different from that of Ca and Mg and this is due to the differences in the chemical characteristics of these cations under different soil conditions. Ca and Mg in their ionic state, both have oxidation state +2, whilst Na has oxidation state +1, resulting in different leaching behaviour. The shape for the Na WM soil column BTCs are similar to Number 5, with the exception of toe distilled water non-aerated, which is similar to Curve 1, indicating a non-reactive solute, where the solute moves by dispersion, with no interaction with the soil. This is against expectation, as Na is not a conservative element, due to its involvement in soil ion exchange (Table 4.8). The Na concentration from the WM aerated columns from breakthrough to 1.00 pore volume for WM crest soils and to 0.60 for toe soils, is higher than Ca, Mg and K, but basic soil characterisation shows Na as the least abundant base cation (Figure.4.9: left).

The BTCs for K for leachate from all WS and WM soil columns shows similar behaviour to Curve 5, where the solute movement is not similar to the typical BTCs defined in literature (Table 4.9). Although clear BTC behaviour cannot be established, the WM soils show a steady decline in the K concentration with time. The release pattern of K can be attributed to the clay mineralogy, which was not analysed in this study.

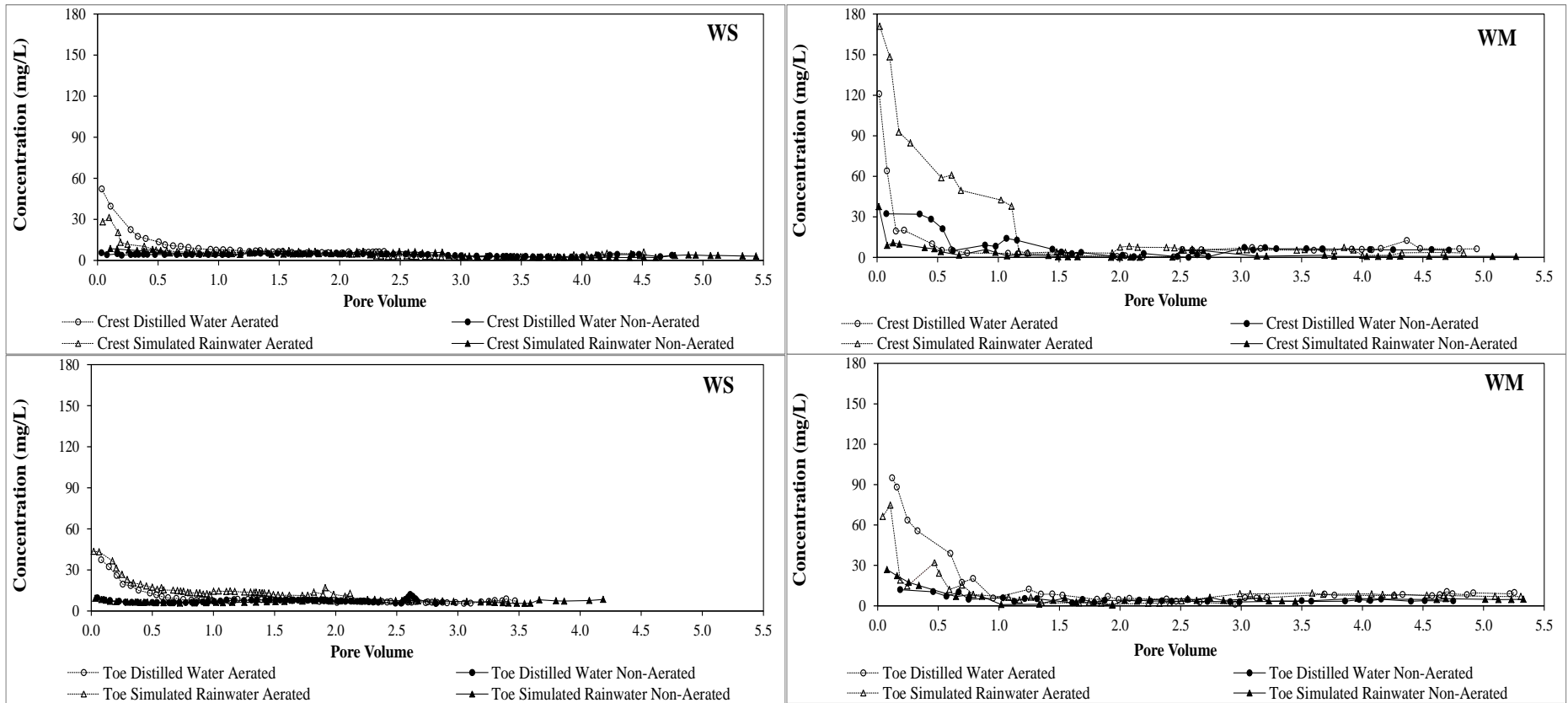


Figure 4.9 Sodium breakthrough curves for WS (left: crest above, toe below) and WM (right: crest above, toe below) soil columns

Table 4.8 Sodium BTC shape, BTC, maximum and tail (after 2.5 pore volumes) concentration for WS and WM soil columns

Site	Slope position	Leaching solution	Level of aeration	Sodium			
				BTC shape	Breakthrough concentration (mg/L)	Maximum concentration (mg/L)	Tail concentration (2.5 pore volumes) (mg/L)
<b>Weather Station</b>	Crest	Distilled Water	Aerated	3	52.2	52.2	6.5
			Non-aerated	5	5.6	5.6	4.5
		Simulated Rainwater	Aerated	3	28.1	28.1	2.8
			Non-aerated	5	8.6	8.6	6.5
	Toe	Distilled Water	Aerated	3	37.4	37.4	6.8
			Non-aerated	5	9.6	9.6	5.7
		Simulated Rainwater	Aerated	3	43.6	43.6	13.0
			Non-aerated	5	9.3	9.3	7.6
<b>Windmill</b>	Crest	Distilled Water	Aerated	3	120.9	120.9	5.8
			Non-aerated	3	32.3	32.3	0.6
		Simulated Rainwater	Aerated	3	170.9	170.9	5.3
			Non-aerated	3	37.6	37.6	5.3
	Toe	Distilled Water	Aerated	3	95.0	95.0	3.3
			Non-aerated	1	12.0	12.0	3.4
		Simulated Rainwater	Aerated	3	66.3	74.8	3.6
			Non-aerated	3	26.8	26.8	5.2

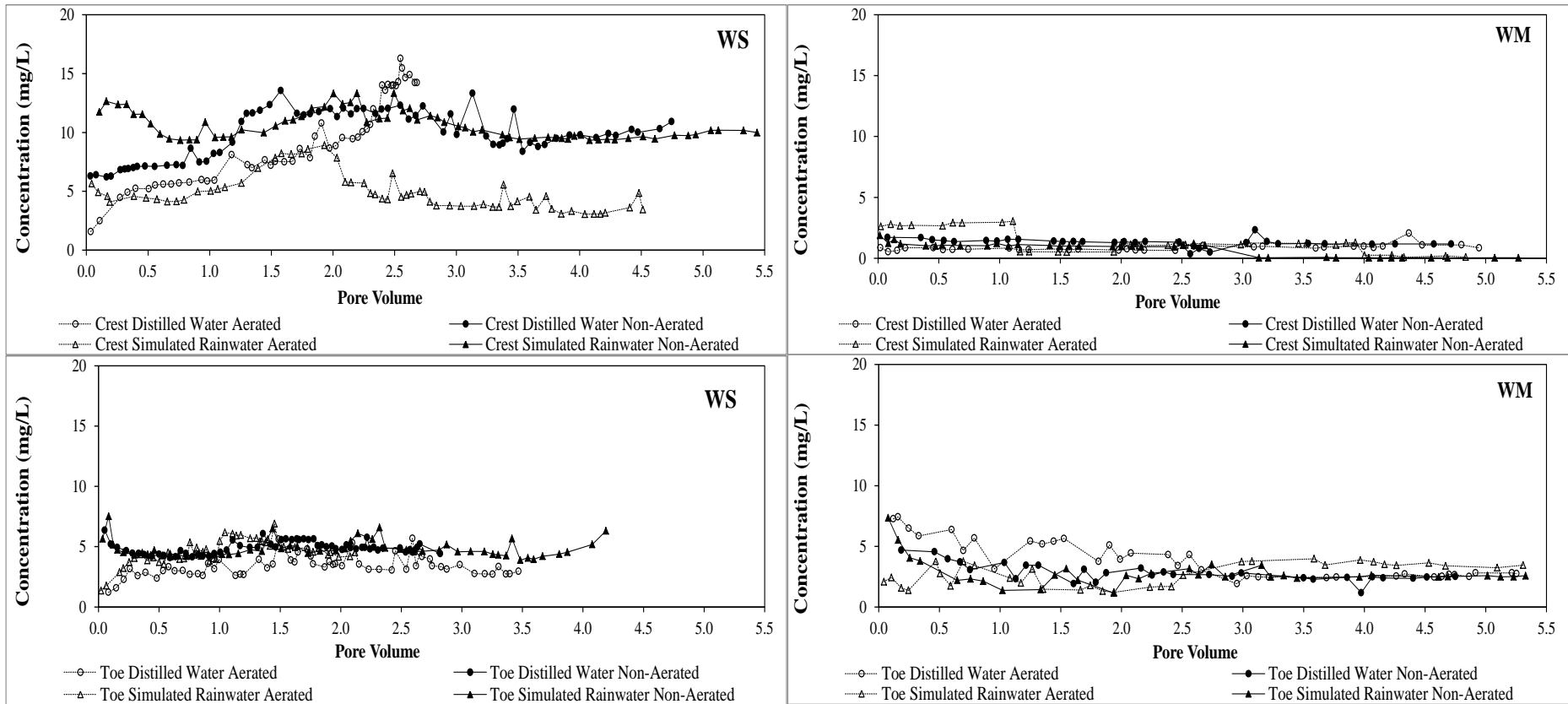


Figure 4.10 Potassium breakthrough curves for WS (left: crest above, toe below) and WM (right: crest above, toe below) soil columns

Table 4.9 Potassium BTC shape, BTC, maximum and tail (after 2.5 pore volumes) concentration for WS and WM soil columns

Site	Slope position	Leaching solution	Level of aeration	Potassium			
				BTC shape	Breakthrough concentration (mg/L)	Maximum concentration (mg/L)	Tail concentration (2.5 pore volumes) (mg/L)
<b>Weather Station</b>	Crest	Distilled Water	Aerated	5	1.6	14.0	11.1
			Non-aerated	5	6.3	13.6	12.0
		Simulated Rainwater	Aerated	5	5.7	8.9	6.5
			Non-aerated	5	11.7	13.3	13.3
	Toe	Distilled Water	Aerated	5	1.2	5.6	4.6
			Non-aerated	5	6.4	6.4	4.9
		Simulated Rainwater	Aerated	5	1.4	6.9	4.5
			Non-aerated	5	5.7	7.5	4.8
<b>Windmill</b>	Crest	Distilled Water	Aerated	5	0.9	0.9	0.6
			Non-aerated	5	1.7	1.7	1.3
		Simulated Rainwater	Aerated	5	2.6	3.0	1.1
			Non-aerated	5	1.9	1.9	1.1
	Toe	Distilled Water	Aerated	5	7.3	7.3	3.4
			Non-aerated	5	4.7	4.7	2.7
		Simulated Rainwater	Aerated	5	2.1	3.8	2.6
			Non-aerated	5	7.3	7.3	3.2



The above variations in BTC shapes for Ca, Mg, Na and K obtained from leachate from WS and WM soil columns, can be explained by the different column setups. BTC shapes are dependent on the behaviour of each element and this has been discussed above. The other factors are variations in pore velocity and solute concentrations in the leaching liquid.

The pore velocity for the WS soil columns is 0.02 cm/hr, whilst that for WM soils columns is 0.3 cm/hr, 15 times more than in WS soils. High pore velocity, as in the case of WM soil columns, steepens and shifts the BTC to the left, as indicated by BTC curves for Ca, Mg and Na (Figure 4.7: left, Figure 4.8: left and Figure 4.9: left, respectively). The impact of solute concentration on BTC is dependent on the density of the leaching liquid. The density of the leaching liquid increases as the concentration of solutes increases. BTCs steepen and translate to the left, with an increase in leaching liquid concentration. In this case, the simulated rainwater solution has more solutes than distilled water. This would be expected to result in the different shape of BTCs, however for all Ca, Mg, Na and K curves, this phenomenon is not clear, as the shape of the BTCs does not differ with the leaching liquid. The only exception is in the Mg concentration from WM soil column leachates, where leachate from the crest simulated rainwater aerated and toe simulated rainwater aerated columns have BTC Shapes 2 and 5, respectively (Table 4.7), differing with the same WM soils with distilled water as the leaching liquid.

The leaching behaviour of Ca and Mg for the WS non-aerated soil columns, which is similar to the bell-shaped BTC is attributed to changes that occur on soil ion exchange surfaces with changing redox conditions. The concentration of Ca and Mg in leachate increases with decreasing redox potential values (reducing conditions), as indicated in Figures 4.4: right, 4.7: right and 4.8: right. The reducing conditions result in Fe and Mn being released into solution and the destruction of soil cation exchange sites. This causes an increase in the concentration of Ca and Mg released into solution. The decline in Ca and Mg concentration in the WS non-aerated columns after 2.0 pore volumes (Figure 4.7 and 4.8: right), is due to the re-oxidised soil surfaces providing exchange sites for Ca and Mg, lowering their concentration in solution. The decline in Ca and Mg concentration for the non-aerated columns coincides with an increase in, or constant redox potential values after 2.0 pore volumes (Figure 4.4: right). As for the WM soil columns, the destruction of exchange sites does not occur as the columns remain oxidised throughout the leaching process.

Overall, leachates from WS soil columns have a higher concentration of base cations, with the exception of Na. This is due to WS soils having a higher initial concentration of Ca, Mg and K, as well as higher CECe (Table 4.2). This enables the WS soils to buffer the acidity from acid deposition. The buffering mechanism occurs in soils with intermediate pH ranges between 5.5 and 7.0 and is governed by the following reaction (Equation 4.3), where  $\text{Ca}^{2+}$  represents any base cation in the soil (McBride, 1994):



Acidity, in the form of  $\text{H}^+$  ions, is exchanged with the base cations on soil surfaces, resulting in the release of exchangeable bases into the soil solution and the neutralisation of the acidity. The WS soils have high a CECe and therefore a high buffering capacity, hence a greater release of Ca, Mg and K into the soil solution. This release of base cations buffers changes in acidity even under simulated rainwater solution at pH 4.35 (Figure 4.3: right). The leaching characteristics exhibited by the WS soils are similar to those obtained in studies conducted in Canada and China by Clayton *et al.* (1991) and Bohan *et al.* (1997). The studies showed that soils with high CECe and base saturation are able to buffer changes in pH resulting from atmospheric deposition. The WM soils have a lower initial base cation and CECe (Table 4.2), hence even though the above process in Equation 4.3 occurs, the base cations are depleted, resulting in lower leachate pH (slightly acidic) obtained from the WM soils (Figure 4.3: left). Nawaz *et al.*, (2012) also showed that the leaching of base cations is depended on soil characteristics such as CEC and initial base concentration in the soil.

#### 4.3.5 Aluminium, manganese and iron

The Al concentration in leachate from the WS soil columns is below detection limit, indicating that there is no soluble Al in solution, except for the toe distilled water aerated soil column, where Al is available between 0.32 and 1.00 pore volumes (Figure 4.11: left). This is due to initial soil conditions, whereby the Al concentration in the soil is initially below the detection limit before leaching commenced (Tables 4.2 and 4.3). The pH of the leachate is also not low enough to cause release of Al (Figure 4.3: left). On the other hand, the Al concentration in leachate collected from the WM crest and toe soil columns are highest in the aerated columns (Figure 4.11: right). An interesting point to note is that the Al concentration in the crest simulated rainwater aerated column starts by being higher than the other three crest columns and then sharply declines at 1.11 pore volumes to the same level as the other

three columns (Figure 4.11: left). This is due to the WM crest soil being the only one with Al present during soil characterisation, using both the KCl and BaCl<sub>2</sub> extraction methods, whilst the Al concentration for the rest of the samples was below the detection limit (Tables 4.2 and 4.3).

The Al BTC behaviour for all the WM soil columns is similar to that of Curve 5, and is not similar to any typical BTCs defined in literature. Furthermore, an increase in Al concentration in leachate is expected to be accompanied by a decrease in leachate pH, but that is not the case for the WM crest soils, where an increase in Al concentration results in an increase or no change in leachate pH (Figure 4.3: right). However, for the WM toe soil column results, the presence of Al in leachates results in leachate pH declining from neutral, to slightly acidic values (Figure 4.3: left bottom).

The leaching behaviour of Al in WM soils is explained by the following equation (Lindsay, 1979):



The equation represents the use of Al as a buffering mechanism against lowering pH due to acidification. In the case of WM soils, the Ca, Mg and Na BTCs (Figures 4.7, 4.8 and 4.9) show that the base cations are quickly depleted from the soil and hence can no longer effectively buffer the acidification through the process indicated by Equation 4.3. This results in the use of the Al buffer mechanism, where H<sup>+</sup> ions attack soil minerals releasing Al<sup>3+</sup> from mineral complexes into soil solution. This buffer mechanism also explains the differences in Al BTCs observed for WS and WM soils. For the WS soils, the pH is not low enough to result in the release of Al from soil complexes and the anaerobic conditions of the columns result in the release of Mn and Fe from Mn/Fe concretions that might be obstructing the base cations from participating in ion exchange. When Mn and Fe are released they free up the base cations to participate in buffering the soil, according to Equation 4.3, instead of using the Al buffering mechanism. Mayer (1998) obtained the same results as the WM soils, where the Al<sup>3+</sup> concentration in leachate increased, with increased atmospheric deposition.

The manganese (Mn) concentration in leachates from the WS crest soil columns follows the same behaviour as Ca, Mg and K, with the exception of crest simulated rainwater aerated column, where Mn is below the detection limits (Figure 4.12: left). The Mn concentration in leachate from the WS toe soil columns does not follow the same behaviour as Ca, Mg and K.

Manganese is only detectable in the non-aerated WS toe soil columns between 0.85 and 1.19 pore volume, whilst it is below detection limits for the aerated columns. The Mn concentration in leachate collected from all the WM crest soil columns shows similar behaviour (Figure 4.12: right). The shape for all Mn BTCs is undefined (Curve 5) (Table 4.11). From breakthrough to 2.00 pore volumes, the Mn concentration in all four WM crest soils is below detection level and becomes available at a low constant concentration of 0.62 mg/L for the rest of the leaching period (Figure 4.11: right top). For WM toe soils, Mn is present in the leachate from aerated columns from breakthrough to 1.50 pore volumes, and thereafter it decreases to below detection level. From 3.00 pore volumes, the Mn concentration for all four WM toe columns is present at a low, constant concentration of 0.71 mg/L (Figure 4.11: right bottom). The absence of Mn in solution during the first stages of leaching for WM soils, is a result of WM soils having the lowest initial Mn concentration from the saturated paste results (Table 4.3).

The iron (Fe) concentration in leachate from the WS soil columns follows the same behaviour as Mn, with a few exceptions (Figure 4.13: left). Iron is available in leachate from the WS toe distilled water aerated column between 0.30 and 1.44 pore volumes, whilst the Mn concentration is below the detection limit for the same column. The Fe concentrations in leachate from all WM crest and toe soil columns follow the same behaviour as in Al, except that Al is at a higher concentration than Fe (Figure 4.13: right).

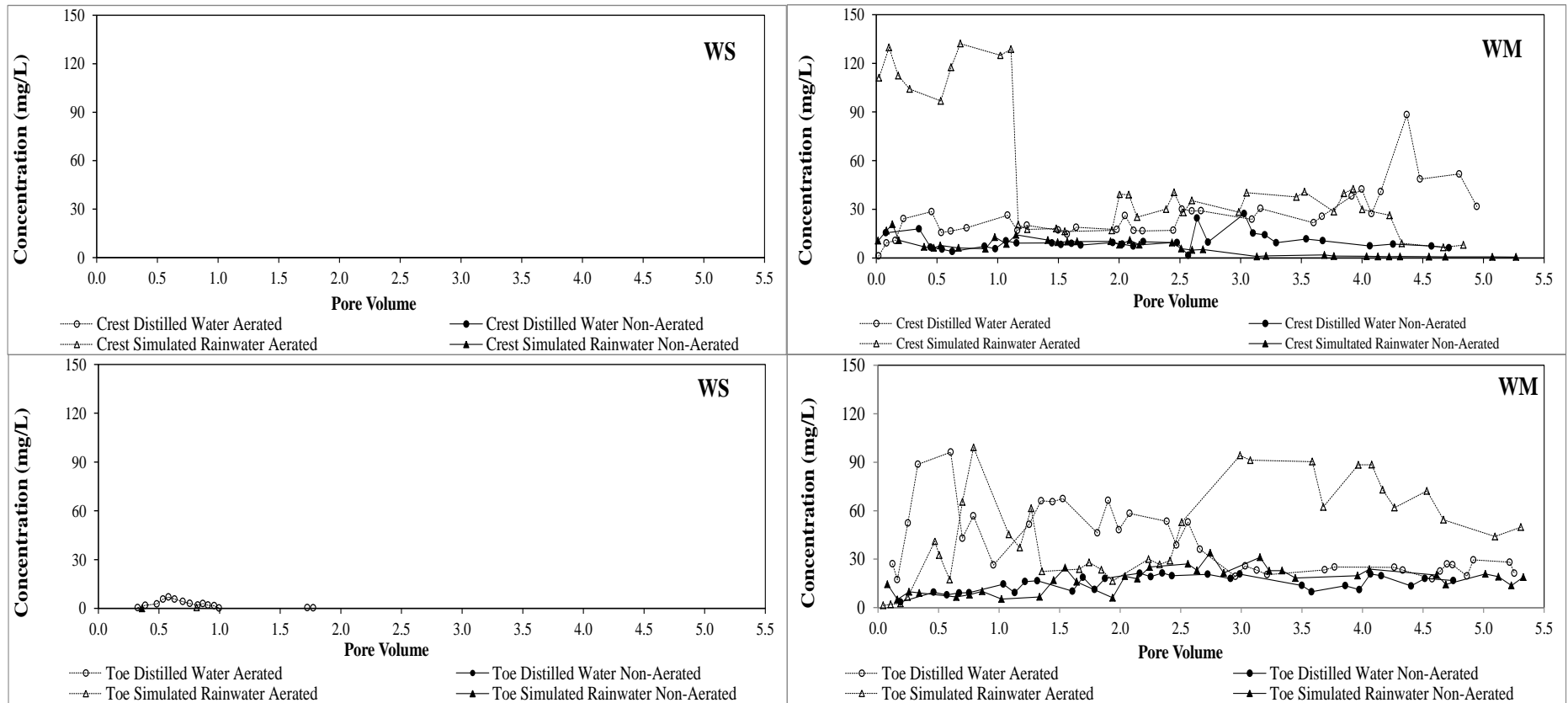


Figure 4.11 Aluminium breakthrough curves for WS (left: crest above, toe below) and WM (right: crest above, toe below) soil columns. The Al concentration for WS crest soil column leachates (left top) were all below detection limits

Table 4.10 Aluminium BTC shape, BTC, maximum and tail (after 2.5 pore volumes) concentration for WS and WM soil columns

Site	Slope position	Leaching solution	Level of aeration	Aluminium			
				BTC shape	Breakthrough concentration (mg/L)	Maximum concentration (mg/L)	Tail concentration (2.5 pore volumes) (mg/L)
<b>Weather Station</b>	Crest	Distilled Water	Aerated	*	*	*	*
			Non-aerated	*	*	*	*
		Simulated Rainwater	Aerated	*	*	*	*
			Non-aerated	*	*	*	*
	Toe	Distilled Water	Aerated	4	0.5	7.0	0.2
			Non-aerated	*	*	*	*
		Simulated Rainwater	Aerated	*	*	*	*
			Non-aerated	*	*	*	*
<b>Windmill</b>	Crest	Distilled Water	Aerated	5	1.2	30.0	30.0
			Non-aerated	5	15.5	18.0	9.3
		Simulated Rainwater	Aerated	5	111.1	132.1	40.4
			Non-aerated	5	10.6	20.8	5.7
	Toe	Distilled Water	Aerated	5	27.1	96.2	38.7
			Non-aerated	5	3.4	19.7	19.7
		Simulated Rainwater	Aerated	5	1.3	99.1	52.8
			Non-aerated	5	14.4	27.1	27.1

\*below detection limit

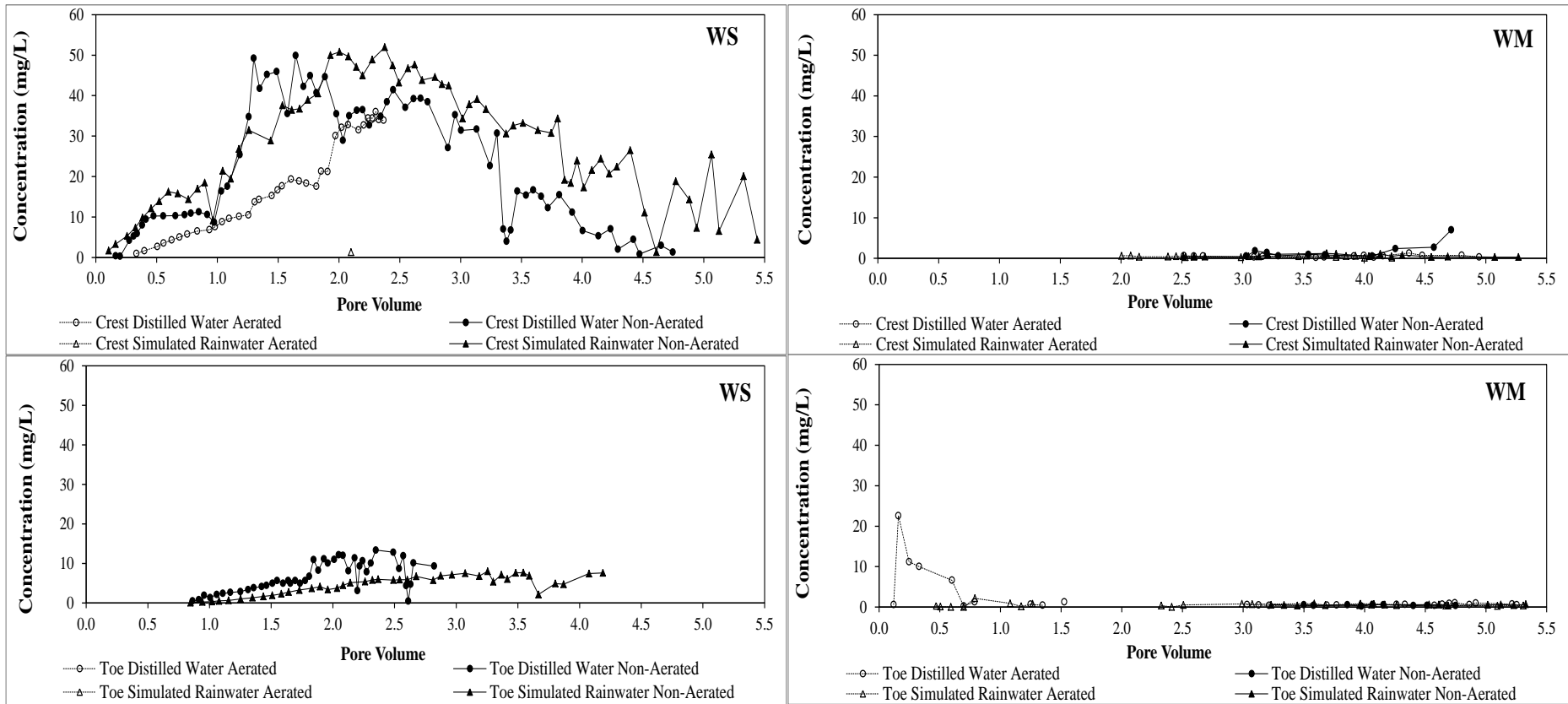


Figure 4.12 Manganese breakthrough curves for WS (left: crest above, toe below) and WM (right: crest above, toe below) soil columns

Table 4.11 Manganese BTC shape, BTC, maximum and tail (after 2.5 pore volumes) concentration for WS and WM soil columns

Site	Slope position	Leaching solution	Level of aeration	Manganese			
				BTC shape	Breakthrough concentration (mg/L)	Maximum concentration (mg/L)	Tail concentration (2.5 pore volumes) (mg/L)
<b>Weather Station</b>	Crest	Distilled Water	Aerated	5	0.9	36.0	33.9
			Non-aerated	4	0.4	49.9	41.4
		Simulated Rainwater	Aerated	*	*	*	*
			Non-aerated	4	1.7	52.0	47.4
	Toe	Distilled Water	Aerated	*	*	*	*
			Non-aerated	5	0.5	12.8	12.8
		Simulated Rainwater	Aerated	*	*	*	*
			Non-aerated	5	0.9	5.8	5.8
<b>Windmill</b>	Crest	Distilled Water	Aerated	5	0.6	0.6	0.6
			Non-aerated	*	*	*	*
		Simulated Rainwater	Aerated	5	0.6	0.6	0.5
			Non-aerated	5	0.5	0.5	0.5
	Toe	Distilled Water	Aerated	5	0.6	22.6	*
			Non-aerated	*	*	*	*
		Simulated Rainwater	Aerated	5	0.3	2.2	0.5
			Non-aerated	*	*	*	*

\*below detection limit



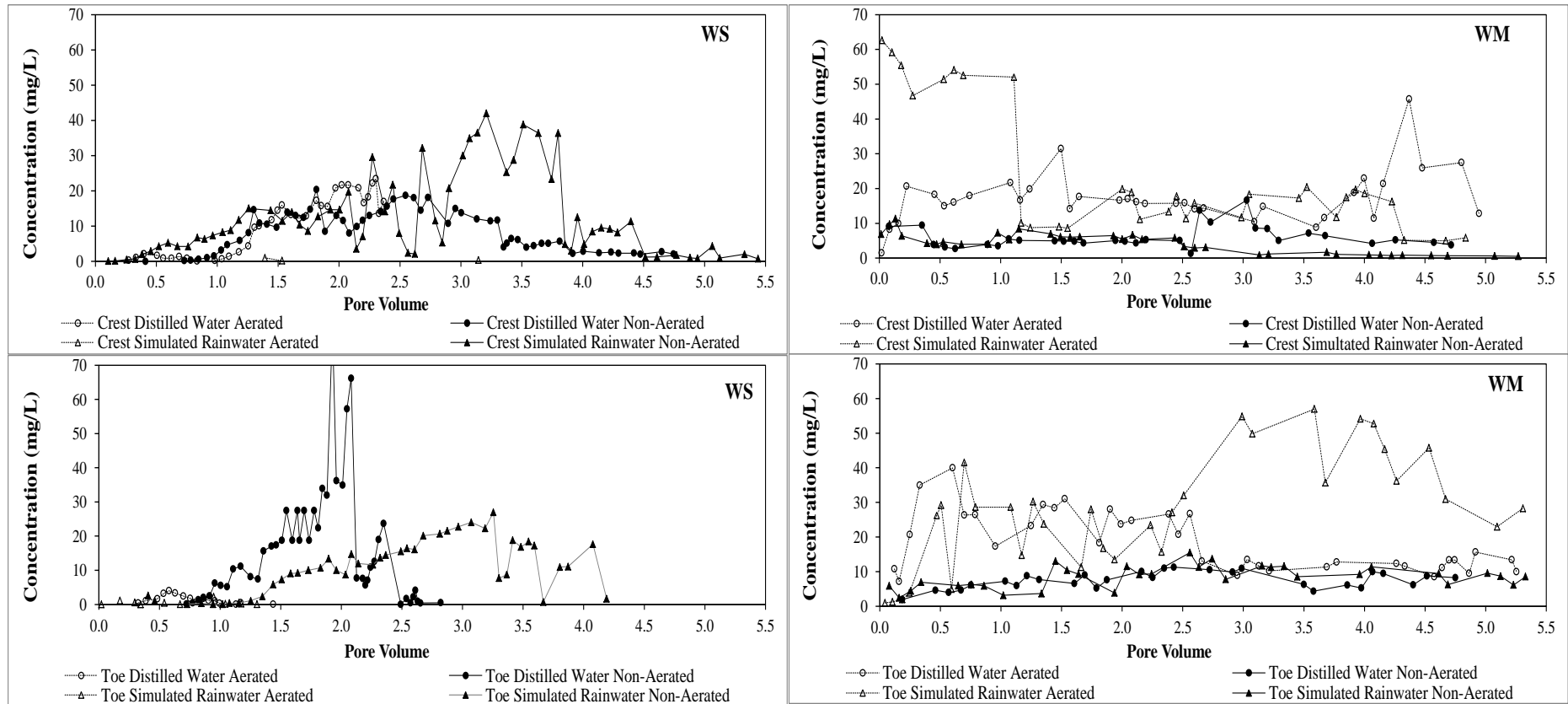


Figure 4.13 Iron breakthrough curves for WS (left: crest above, toe below) and WM (right: crest above, toe below) soil columns

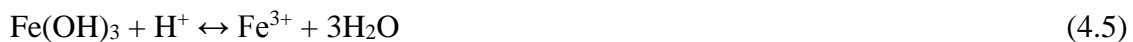
Table 4.12 Iron BTC shape, BTC, maximum and tail (after 2.5 pore volumes) concentration for WS and WM soil columns

Site	Slope position	Leaching solution	Level of aeration	Iron			
				BTC shape	Breakthrough concentration (mg/L)	Maximum concentration (mg/L)	Tail concentration (2.5 pore volumes) (mg/L)
<b>Weather Station</b>	Crest	Distilled Water	Aerated	5	0.3	23.4	17.0
			Non-aerated	4	0.0	20.4	17.7
		Simulated Rainwater	Aerated	*	*	*	*
			Non-aerated	5	0.1	29.6	8.0
	Toe	Distilled Water	Aerated	4	0.4	3.3	*
			Non-aerated	5	0.1	81.6	1.7
		Simulated Rainwater	Aerated	*	*	*	*
			Non-aerated	4	2.6	15.5	14.7
<b>Windmill</b>	Crest	Distilled Water	Aerated	5	1.5	31.5	15.9
			Non-aerated	5	9.1	9.5	5.0
		Simulated Rainwater	Aerated	5	62.6	75.6	11.4
			Non-aerated	5	6.9	11.3	3.3
	Toe	Distilled Water	Aerated	5	10.8	40.0	20.7
			Non-aerated	5	1.9	10.5	10.5
		Simulated Rainwater	Aerated	5	1.0	41.5	32.0
			Non-aerated	5	5.9	15.5	15.5

\*below detection level

The differences in leaching behaviour of WS and WM soils can also be explained by Mn and Fe chemistry. Manganese is commonly found in the +2 and +4 oxidation states and is soluble under acidic or low oxidation-reduction potentials (Lindsay, 1979). This explains the presence of Mn in the WS soil column leachate, as the redox potential values for the non-aerated columns are low (Figure 4.4: left). Although the WS toe distilled water column has high redox potential values compared to the other WS soil columns, Mn is available in solution due to the low leachate pH values (below 6.5) (Figure 4.3: left bottom). For the WM soils, the redox potential values are high (above 150 mV), resulting in little or no Mn in solution (Figure 4.4: right and Figure 4.12: right). Therefore, the leaching behaviour of WS soils is dependent on the redox conditions in the columns. For non-aerated columns, the redox conditions for WS soils are low and in the negative range, due to the absence of oxygen, as columns become saturated with water.

Iron is commonly found in either the +2 or +3 oxidation states. When in the +2 oxidation state, Fe behaves in a similar manner to Mn. The pH and redox potential diagram for Fe shows that at pH between 6.00 and 8.00 and redox potential values below 0.00 mV, Fe exists as Fe<sup>2+</sup> (Figure 2.3). The Fe<sup>2+</sup> ion is soluble in water, hence accounts for the Fe observed in leachate from WS non-aerated columns and shows the same breakthrough curve as Mn. On the other hand, the pH and redox potential diagram shows that at the same pH range, but with redox potential values greater than 0.00 mV, Fe exists as a hydroxide, Fe(OH)<sub>3</sub>. When conditions become acidic, the Fe(OH)<sub>3</sub> is released as Fe<sup>3+</sup>, as shown below (Lindsay, 1979):



The reaction is similar to Al(OH)<sub>3</sub> hydrolysis, mentioned above and explains the breakthrough curve observed for WM soils, were the Fe breakthrough curve has the same shape as that of Al (Figure 4.11: right).

#### 4.3.6 Sulphur

The Sulphur (S) leachate concentration for all WS soil columns starts by initially increasing from breakthrough to around 0.30 pore volumes and then gradually declines until constant concentrations are maintained (Figure 4.14: left). The S concentration in leachate from WS crest soils shows that a higher loss of S occurs from aerated columns than non-aerated

columns. The S BTCs shape is similar to that of Curve 3 for the WS soil columns, with the exception of the crest distilled water column, which is similar to Curve 2 (Table 4.13).

The S leachate concentration from all WM soil columns also starts by initially increasing and then declining to constant concentrations (Figure 4.14: right). For the WM crest soils, the decline occurs after 1.11 pore volumes for the simulated rainwater treatment and after 2.00 pore volumes for the rest of the crest treatments. On the other hand, the S concentration from WM toe soil columns declines from 0.50 pore volumes to similar and constant values. The highest S concentration for WM crest soils is achieved from the simulated rainwater treatment, whilst it is difficult to distinguish which column has the highest S concentration for toe soils. The S BTCs shape for WM soil columns is similar to Curve 2, with the exception of the crest aerated columns (Table 4.13).

The S leaching characteristics are explained by the chemical constituents of the leaching solutions. The simulated rainwater has more S ( $59.1 \mu\text{mol/L}$  or  $2.84 \text{ mg/L}$ ),  $\text{NO}_3^-$  ( $25.4 \mu\text{mol/L}$  or  $1.55 \text{ mg/L}$ ) and  $\text{NH}_4^+$  ( $22.3 \mu\text{mol/L}$  or  $0.40 \text{ mg/L}$ ), a higher ionic strength and a pH of 4.35, compared to distilled water with none of the mentioned components, a lower ionic strength and a neutral pH of 7.05. In the column leach experimental design, distilled water was used as a control, to determine the level of leaching in the absence of S and N deposition. Bohan *et al.* (1997) compared the differences between ion concentrations in leachate from simulated rainwater treatments and ion concentrations in leachate from distilled water for the same treatment and came up with the following conclusions:

- a) If the ion concentration is higher in distilled water, this means that the simulated rainwater resulted in the adsorption of the ion in question, and
- b) If the ion concentration is lower in distilled water, this means that simulated rainwater resulted in the release of the ion in excess of what was obtained with distilled water.

Applying the same logic to the WS and WM leachate concentrations of sulphur, nitrate and ammonia, illustrates differences in adsorption and the release characteristics of the soil. The S in crest aerated soils shows that, from breakthrough to 1.39 pore volumes, adsorption of S occurs with simulated rainwater, and thereafter, there is a release of S in excess of that shown by distilled water. The non-aerated columns show that adsorption of S occurs during the entire leaching process, whilst the WS toe aerated soils columns show the same initial adsorption and release that is shown by the crest aerated column. Adsorption in the non-

aerated columns observed throughout the leaching process is due to anaerobic conditions from the lack of oxygen, which result in the assimilation of S. This means that acid rainfall will not result in excess S being released into the soil system under reducing conditions, such as those observed during flood events and on toe slope positions with poor drainage. For the WM toe and crest soils, the columns show alternate adsorption and release of S in excess of that of distilled water. This cyclical adsorption and release is expected under field conditions at the crest slope positions, where alternating wetting and drying cycles are observed for these positions.

The S breakthrough curves show that an initial flush of S occurs and this is a result of soluble organic material releasing S. The other observation is that there seems to be no difference in S leaching between simulated rainwater and distilled water treatments. This is contrary to expectation, as the simulated rainwater has more S than distilled water. This difference is due to the different forms of S being released or the re-adsorption of sulphate onto Al oxides. The re-adsorption of S is a retention mechanism of S in the soil and reduces its concentration in soil solution, resulting in no impact on surface water. This makes the S retention for the WS and WM soils higher, compared to that obtained in the study conducted by Fey and Guy (1993), where the Vaal soils had low S retention. The shape of the S BTCs does not support the ion-pair theory that sulphate is the accompanying ion for the movement of cations. Sulphur could be acting as a catalyst, where other forms of S, aside from sulphate, are being released and could not be measured by the methods of analysis utilised, or that another anion is acting as the accompanying ion for cation leaching. The possible anion is bicarbonate, from the reaction of carbon dioxide with water, especially under anaerobic conditions (high carbon dioxide).

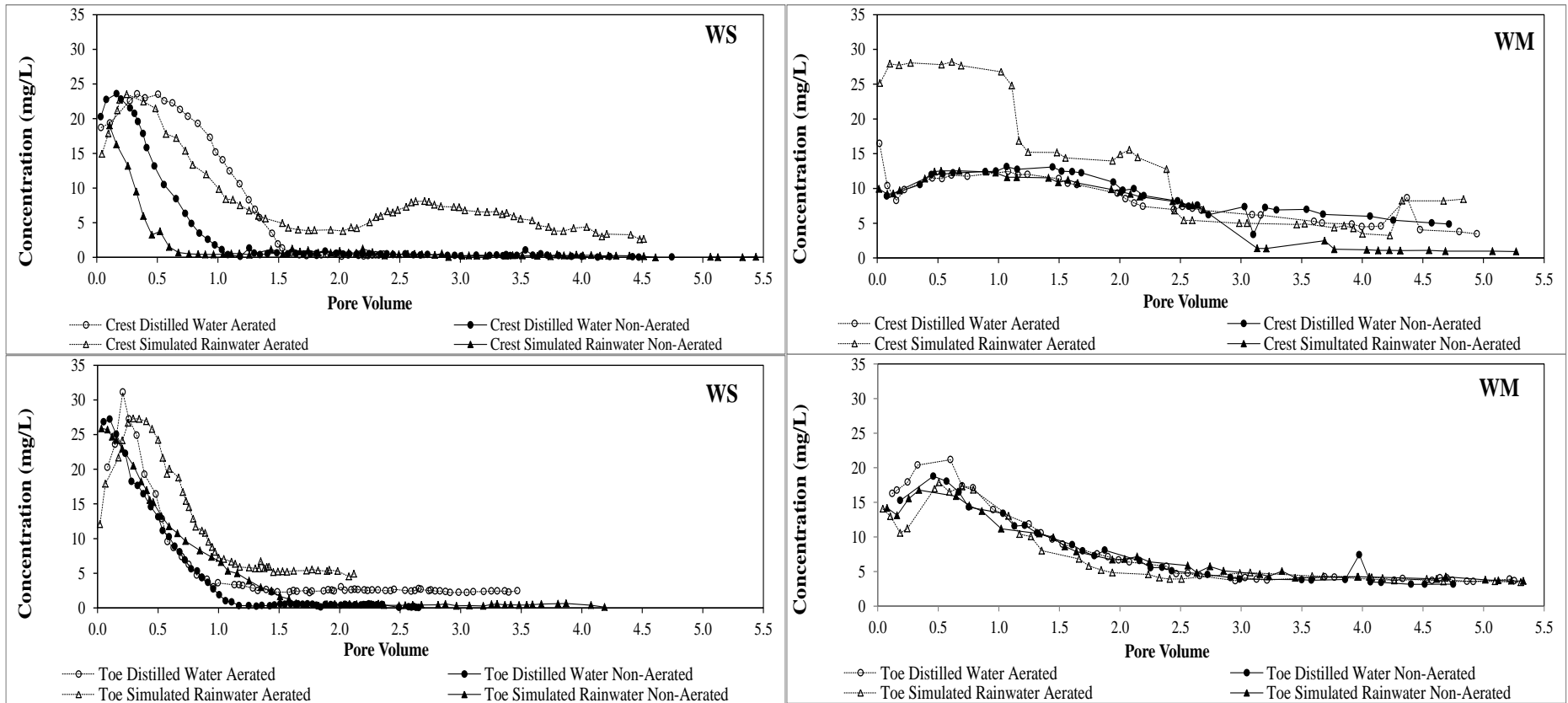


Figure 4.14 Sulphur breakthrough curves for WS (left: crest above, toe below) and WM (right: crest above, toe below) soil columns

Table 4.13 Sulphur BTC shape, BTC, maximum and tail (after 2.5 pore volumes) concentration for WS and WM soil columns

Site	Slope position	Leaching solution	Level of aeration	Sulphur			
				BTC shape	Breakthrough concentration (mg/L)	Maximum concentration (mg/L)	Tail concentration (2.5 pore volumes) (mg/L)
<b>Weather Station</b>	Crest	Distilled Water	Aerated	2	18.7	23.6	0.4
			Non-aerated	3	20.3	23.6	0.4
		Simulated Rainwater	Aerated	2	14.9	23.5	6.5
			Non-aerated	3	19.0	19.0	0.4
	Toe	Distilled Water	Aerated	3	20.3	31.1	2.7
			Non-aerated	3	26.8	27.2	0.1
		Simulated Rainwater	Aerated	3	12.1	27.3	4.5
			Non-aerated	3	25.9	25.9	0.4
<b>Windmill</b>	Crest	Distilled Water	Aerated	5	16.5	16.5	7.4
			Non-aerated	5	8.9	13.1	7.4
		Simulated Rainwater	Aerated	5	25.1	28.0	5.4
			Non-aerated	5	9.9	12.5	7.9
	Toe	Distilled Water	Aerated	2	16.3	21.2	4.7
			Non-aerated	2	15.3	18.8	4.6
		Simulated Rainwater	Aerated	2	14.1	17.9	3.9
			Non-aerated	2	14.2	16.8	5.9

#### 4.3.7 Nitrate and ammonium

The  $\text{NO}_3^-$  concentration in leachate from the WS soil columns is only present in leachate from aerated columns, with simulated rainwater resulting in higher  $\text{NO}_3^-$  concentration than in the distilled water columns for both crest and toe soils (Figure 4.15: left). The nitrate leaching behaviour to note is that the  $\text{NO}_3^-$  concentration BTC has the same bell-shape observed for EC and Ca, Mg and K (Table 4.14.), indicating that nitrate is the accompanying ion during the leaching of these bases. As for the WM soil columns, the leachate  $\text{NO}_3^-$  concentration from toe soils is higher than in the crest soils (Figure 4.15: right). The WM toe soil columns show a declining  $\text{NO}_3^-$  concentration (Curve 3) as leaching progresses, whereas for WM crest soils, the  $\text{NO}_3^-$  BTC shapes are undefined (Curve 5) (Table 4.14). Comparing the  $\text{NO}_3^-$  values between WS and WM, the WS aerated columns have the highest  $\text{NO}_3^-$  concentration, compared to the same treatments with WM. On the other hand, the WM soils have  $\text{NO}_3^-$  available from the non-aerated columns, whereas with the WS non-aerated treatment,  $\text{NO}_3^-$  is below detection limits (Figure 4.15: left). This is due to the reducing conditions found in the WS non-aerated conditions, resulting in the conversion of  $\text{NO}_3^-$  to  $\text{NH}_4^+$ .

The  $\text{NH}_4^+$  concentration in leachate from WS soils is higher in non-aerated columns than in aerated columns, and follows the same behaviour as that of EC, Ca, Mg and K (Figure 4.16: left and Table 4.15). The behaviours are related, as they are all cations, which are involved in the exchange reactions occurring on soil surfaces.

The  $\text{NH}_4^+$  concentration in leachate collected from the WM crest and toe soils displays a similar general decreasing concentration (Figure 4.16: right) The  $\text{NH}_4^+$  BTCs shape for WM soils are undefined (Curve 5) with the exception of crest aerated columns, which follow Curves 1 and 3, respectively (Table 4.15).

The impact of redox potential on the columns can also be seen in the  $\text{NO}_3^-$  and  $\text{NH}_4^+$  breakthrough curves. Under aerated conditions, the dominant form of N is  $\text{NO}_3^-$ , as can be seen by the availability of  $\text{NO}_3^-$  in WS aerated columns. Under reducing conditions such as WS non-aerated columns,  $\text{NO}_3^-$  is reduced to  $\text{NH}_4^+$ , giving rise to higher  $\text{NH}_4^+$  ions in leachate. However, for WM soil columns, under oxidising conditions such as the aerated columns due to the presence of oxygen, both  $\text{NO}_3^-$  and  $\text{NH}_4^+$  ions are leached out of the columns. The concentration of  $\text{NO}_3^-$  is higher than  $\text{NH}_4^+$ , due to its higher mobility and



leaching potential, whilst  $\text{NH}_4^+$  can be adsorbed onto soil exchange surfaces reducing its concentration in solution.

Nitrogen deposition in the leach column design was assumed to be in the form of  $\text{NO}_3^-$  and  $\text{NH}_4^+$ . For the WS soils,  $\text{NO}_3^-$  was only available in the aerated columns, with the crest column showing the excess release of nitrate with simulated rain, whilst the toe soil showed initial adsorption and then release after 1.11 pore volumes. On the other hand, the WM  $\text{NO}_3^-$  leaching profiles show initial adsorption for crest and toe aerated soil columns and initial excess release with non-aerated crest and toe soils for crest soils and thereafter the values become similar. This indicates that acid deposition on the WM hillslope does not have a significant impact on  $\text{NO}_3^-$  leaching, showing that  $\text{NO}_3^-$  will leach at the same rate with normal (non-acidic) and acid rainfall. The same behaviour is also observed with  $\text{NH}_4^+$  from the WM soils. On the other hand,  $\text{NH}_4^+$  from the WS fluctuates between adsorption and release and is a reflection of the effect of redox on the WS soils. Overall, under oxidising conditions with good soil drainage, such as crest slope,  $\text{NO}_3^-$  leaching is not dependent on acid deposition, but is a factor determined by plant uptake, and the excess of plant uptake is leached out of the soil. Under reducing conditions, such as toe slopes and poor drainage,  $\text{NO}_3^-$  is converted into  $\text{NH}_4^+$ , which, if there is excess of plant uptake, leaching as  $\text{NH}_4^+$  can be observed.

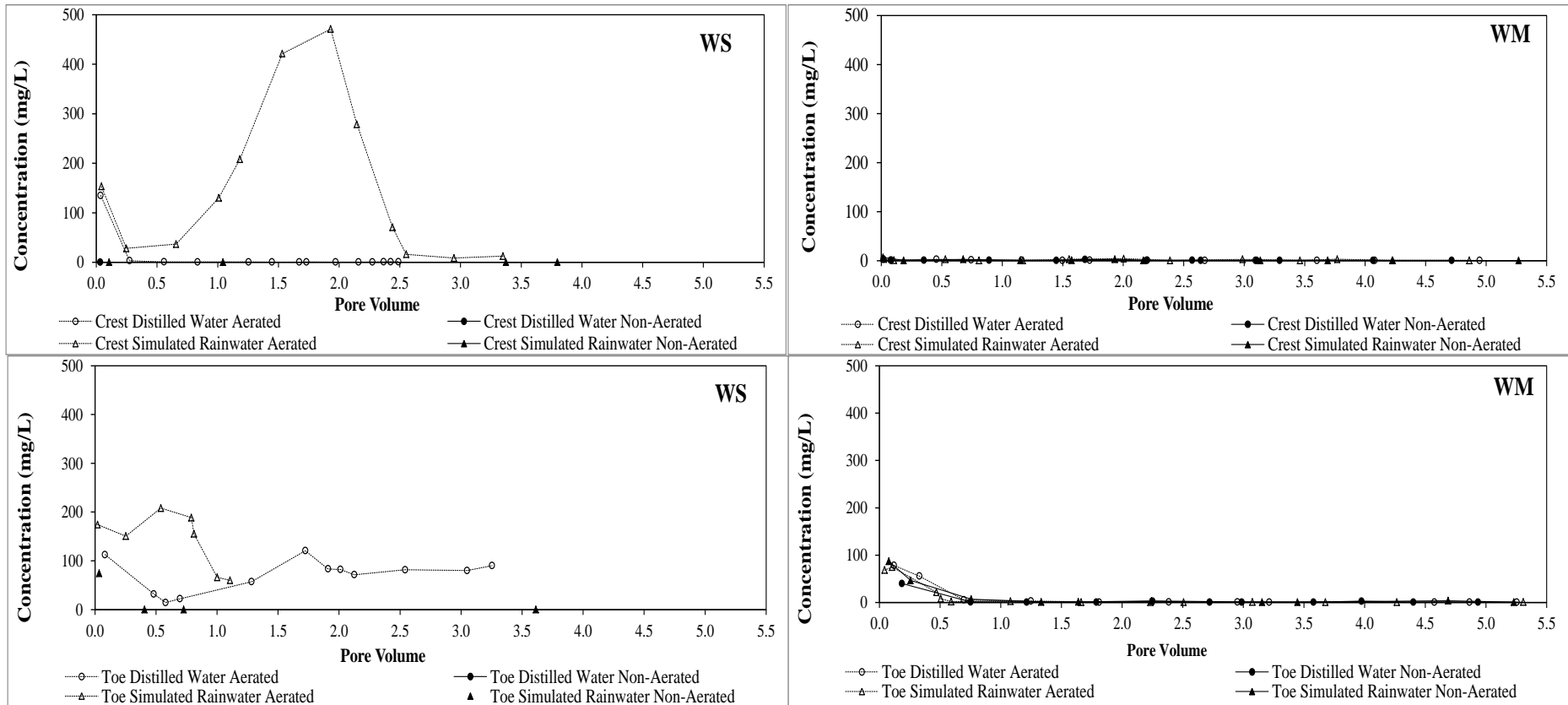


Figure 4.15 Nitrate breakthrough curves for WS (left: crest above, toe below) and WM (right: crest above, toe below) soil columns

Table 4.14 Nitrate BTC shape, BTC, maximum and tail (after 2.5 pore volumes) concentration for WS and WM soil columns

Site	Slope position	Leaching solution	Level of aeration	Nitrate			
				BTC shape	Breakthrough concentration (mg/L)	Maximum concentration (mg/L)	Tail concentration (2.5 pore volumes) (mg/L)
<b>Weather Station</b>	Crest	Distilled Water	Aerated	3	135.0	135.0	1.2
			Non-aerated	*	*	*	*
		Simulated Rainwater	Aerated	4	153.1	470.9	16.2
			Non-aerated	*	*	*	*
	Toe	Distilled Water	Aerated	5	112.6	120.8	81.6
			Non-aerated	*	*	*	*
		Simulated Rainwater	Aerated	5	174.3	208.1	*
			Non-aerated	3	74.4	74.4	*
<b>Windmill</b>	Crest	Distilled Water	Aerated	5	3.1	3.1	0.8
			Non-aerated	5	1.1	2.8	1.1
		Simulated Rainwater	Aerated	5	3.6	4.4	0.8
			Non-aerated	5	6.8	6.8	0.8
	Toe	Distilled Water	Aerated	3	78.5	78.5	1.0
			Non-aerated	3	40.2	40.2	0.8
		Simulated Rainwater	Aerated	3	68.6	75.0	0.9
			Non-aerated	3	86.9	86.9	0.9

\*below detection limit

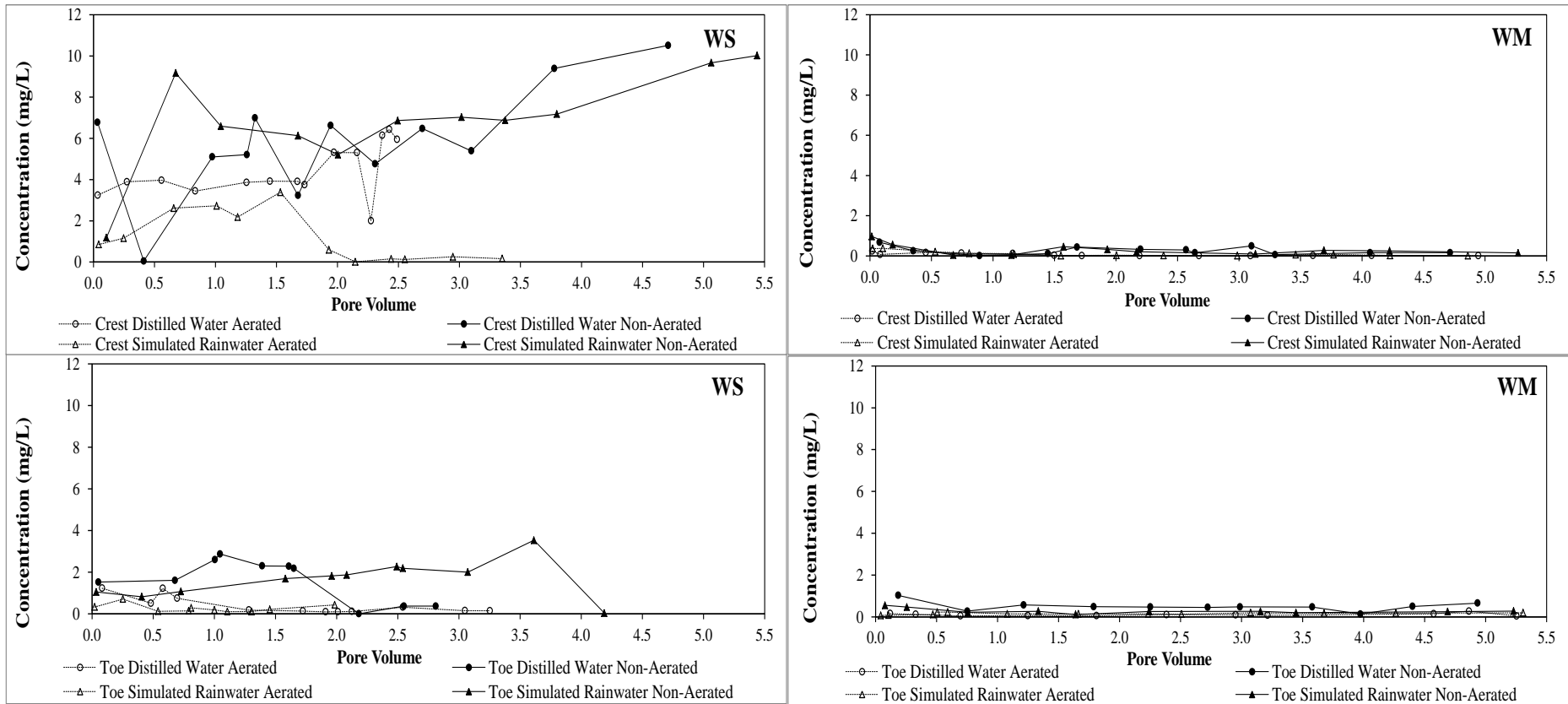


Figure 4.16 Ammonium breakthrough curves for WS (left: crest above, toe below) and WM (right: crest above, toe below) soil columns

Table 4.15 Ammonium BTC shape, BTC, maximum and tail (after 2.5 pore volumes) concentration for WS and WM soil columns

Site	Slope position	Leaching solution	Level of aeration	Ammonium			
				BTC shape	Breakthrough concentration (mg/L)	Maximum concentration (mg/L)	Tail concentration (2.5 pore volumes) (mg/L)
<b>Weather Station</b>	Crest	Distilled Water	Aerated	5	3.2	6.4	5.9
			Non-aerated	5	6.8	7.0	4.8
	Toe	Simulated Rainwater	Aerated	4	0.9	3.4	0.1
			Non-aerated	5	1.2	9.2	6.9
		Distilled Water	Aerated	3	1.2	1.2	0.3
			Non-aerated	4	1.5	2.9	0.4
		Simulated Rainwater	Aerated	5	0.3	0.7	*
			Non-aerated	5	1.1	2.3	2.3
<b>Windmill</b>	Crest	Distilled Water	Aerated	1	0.2	0.2	0.0
			Non-aerated	5	0.7	0.7	0.3
		Simulated Rainwater	Aerated	3	0.4	0.4	0.0
			Non-aerated	5	1.0	1.0	0.1
	Toe	Distilled Water	Aerated	5	0.2	0.2	0.1
			Non-aerated	5	1.0	1.0	0.5
		Simulated Rainwater	Aerated	5	0.1	0.3	0.1
			Non-aerated	5	0.6	0.6	0.3

\*below detection limit

#### **4.4 Leach Column Results Expressed as Cumulative Mass**

The results of the leach columns are expressed as cumulative mass (mg/kg soil) to show the actual amounts of base cations, Al and Mn, as well as anions leached from the soil columns. The cumulative mass for all elements are shown up to 2.00 pore volumes, for comparison purposes, as some columns were not leached beyond 5.00 pore volumes.

##### **4.4.1 Base cations cumulative mass**

The cumulative leaching amounts of Ca, Mg, K and Na are shown in Tables 4.16 and 4.17. The results show that, under field conditions, an increase in rainfall leads to a gradual increase in loss of base cations. During a single event the mass leached from the soil gradually decreases, but may start at the same level of availability for the next event. The results show the highest amount of Ca, Mg and K lost from the soil columns is realised in the crest soil column, with the simulated rainwater non-aerated set-up from WS soils and toe distilled water aerated set-up from WM soils. The highest loss of Na occurred with toe simulated rainwater aerated for WS soils and crest simulated rainwater aerated for WM soils.

##### **4.4.2 Sulphur and nitrate cumulative mass**

Sulphur and  $\text{NO}_3^-$ , as anions, accompany positively charged base cation when moving through the soil. The cumulative amounts of S and  $\text{NO}_3^-$  are shown in Table 4.18. The S and  $\text{NO}_3^-$  gradually increase with pore volume, indicating more loss with increased rainfall. The highest S cumulative mass after 2.00 pore volumes is from toe distilled water non-aerated for WS soil columns and crest simulated rainwater aerated for WM soil columns. The highest  $\text{NO}_3^-$  loss is with the crest simulated rainwater aerated treatment for WS soil columns and with crest simulated rainwater aerated and non-aerated soil treatments for WM soil columns.

Computing the values as the amount lost per hectare of land from the subsurface (0-100 mm depth), can give an indication of the amounts of elements that end being loaded into surface water. The streams and rivers in the Sandspruit Experimental Catchment derive most of their water directly from rainfall and from near surface water flows. Hence, the soil response to acid deposition, which has been described in this chapter, influences the surface water quality parameters in the Catchment. However, the challenge is that calculated cumulative masses

from the column leach tests cannot be used directly to determine the actual loading into surface waters. Other factors, such as plant uptake and direct water surface deposition, come into play. The next chapter will therefore look at the catchment water quality responses to acid deposition.

Table 4.16 Mass leached (mg/kg soil) of Mg and Ca up to 2.00 pore volumes

Site	Slope position	Leaching solution	Level of aeration	Mg mass leached (mg/kg soil) after given pore volumes				Ca mass leached (mg/kg soil) after given pore volumes			
				Breakthrough	0.5	1.0	2.0	Breakthrough	0.5	1.0	2.0
<b>Weather Station</b>	Crest	Distilled Water	Aerated	0.32	4.03	8.89	22.23	1.10	10.98	21.85	50.11
			Non-aerated	0.24	5.08	13.26	41.69	0.56	10.74	27.05	88.96
		Simulated Rainwater	Aerated	0.39	2.86	5.19	16.00	1.08	7.50	13.18	37.23
			Non-aerated	2.39	11.35	20.46	44.27	5.69	26.00	44.87	97.11
	Toe	Distilled Water	Aerated	0.66	2.85	4.01	7.41	1.41	7.05	9.80	16.93
			Non-aerated	0.48	2.70	5.34	19.97	0.93	5.46	10.91	40.32
		Simulated Rainwater	Aerated	0.11	4.35	7.73	13.65	0.42	10.64	17.83	31.33
			Non-aerated	0.30	2.96	5.42	14.74	0.60	5.98	10.93	29.39
<b>Windmill</b>	Crest	Distilled Water	Aerated	0.15	1.50	1.81	2.19	0.43	4.89	5.48	6.15
			Non-aerated	0.49	2.86	4.51	7.44	2.29	12.53	14.80	20.71
		Simulated Rainwater	Aerated	0.33	5.74	9.41	10.96	0.24	3.32	4.45	5.01
			Non-aerated	0.15	2.37	4.45	6.77	0.23	2.99	4.93	6.26
	Toe	Distilled Water	Aerated	1.90	7.86	9.44	13.30	4.09	16.21	19.48	26.22
			Non-aerated	0.85	1.84	3.17	4.01	2.64	5.79	9.66	12.36
		Simulated Rainwater	Aerated	0.12	1.38	2.30	2.81	0.42	6.48	8.90	10.12
			Non-aerated	0.56	2.24	2.54	3.12	1.86	6.69	7.38	8.74



Table 4.17 Mass leached (mg/kg soil) of Na and K up to 2.00 pore volumes

Site	Slope position	Leaching solution	Level of aeration	Na mass leached (mg/kg soil) after given pore volumes				K mass leached (mg/kg soil) after given pore volumes			
				Breakthrough	0.5	1.0	2.0	Breakthrough	0.5	1.0	2.0
<b>Weather Station</b>	Crest	Distilled Water	Aerated	0.56	3.64	5.13	6.95	0.02	0.66	1.59	4.33
			Non-aerated	0.06	0.64	1.36	2.87	0.06	0.97	2.24	5.92
		Simulated Rainwater	Aerated	0.37	2.27	3.26	5.17	0.07	0.77	1.49	4.30
			Non-aerated	0.28	1.23	2.07	3.46	0.38	1.88	3.41	6.60
	Toe	Distilled Water	Aerated	0.97	3.51	4.95	7.43	0.03	0.34	0.84	2.13
			Non-aerated	0.16	1.12	2.12	4.60	0.10	0.75	1.44	3.10
		Simulated Rainwater	Aerated	0.29	4.39	6.64	10.64	0.01	0.53	1.21	2.83
			Non-aerated	0.10	1.16	2.09	4.31	0.06	0.81	1.48	3.11
<b>Windmill</b>	Crest	Distilled Water	Aerated	0.91	4.85	5.30	5.88	0.01	0.17	0.26	0.50
			Non-aerated	1.03	6.52	7.97	10.14	0.05	0.36	0.61	1.21
		Simulated Rainwater	Aerated	1.57	18.83	26.21	28.82	0.02	0.58	1.03	1.33
			Non-aerated	0.22	1.72	2.58	2.90	0.01	0.22	0.44	0.87
	Toe	Distilled Water	Aerated	3.69	11.51	12.95	15.65	0.28	1.28	1.76	3.37
			Non-aerated	0.72	1.65	2.90	3.83	0.28	0.69	1.37	2.06
		Simulated Rainwater	Aerated	0.91	5.83	7.53	8.29	0.03	0.45	0.96	1.42
			Non-aerated	0.68	2.91	3.49	4.20	0.18	0.78	1.01	1.62

Table 4.18 Mass leached (mg/kg soil) of S and Nitrate after 2.00 pore volumes

Site	Slope position	Leaching solution	Level of aeration	S mass leached (mg/kg soil) after given pore volumes				Nitrate mass leached (mg/kg soil) after given pore volumes			
				Breakthrough	0.5	1.0	2.0	Breakthrough	0.5	1.0	2.0
<b>Weather Station</b>	Crest	Distilled Water	Aerated	0.20	3.42	6.49	7.55	1.46	1.63	1.66	1.71
			Non-aerated	0.20	2.90	3.80	3.97	0.001	0.001	0.001	0.001
		Simulated Rainwater	Aerated	0.19	3.09	5.33	6.95	1.99	3.44	7.59	48.41
			Non-aerated	0.61	1.72	1.82	2.06	0.00	0.00	0.00	0.00
	Toe	Distilled Water	Aerated	0.52	3.43	4.49	5.35	2.91	3.85	6.04	10.47
			Non-aerated	0.43	3.16	4.15	4.30	*	*	*	*
		Simulated Rainwater	Aerated	0.08	3.77	6.03	7.78	*	2.61	3.54	13.96
			Non-aerated	0.27	3.34	4.71	5.34	0.79	0.79	0.79	0.79
<b>Windmill</b>	Crest	Distilled Water	Aerated	0.12	2.37	3.78	7.38	0.03	0.34	0.48	0.63
			Non-aerated	0.28	2.39	4.61	9.77	0.03	0.15	0.26	0.47
		Simulated Rainwater	Aerated	0.23	6.01	10.19	15.69	0.03	0.39	0.46	0.67
			Non-aerated	0.06	2.09	4.64	9.17	0.04	0.25	0.28	0.67
	Toe	Distilled Water	Aerated	0.63	3.76	5.55	8.66	3.05	4.72	5.03	5.11
			Non-aerated	0.92	2.58	5.37	7.90	2.42	2.46	2.48	2.58
		Simulated Rainwater	Aerated	0.19	2.40	5.18	7.17	0.94	4.14	4.46	4.62
			Non-aerated	0.36	3.23	4.78	7.60	2.19	3.90	4.04	4.19

## 4.5 Conclusion

The results of the column leach tests show that leaching is a complex process, which is influenced by both the leaching solution used and the soil chemical and physical characteristics, as well as the column leach set up. Comparing the leaching characteristics of the two hillslope soils, both WS crest and toe soils result in leachate with higher EC values, indicating that there are more base cations and anions in WS soil column leachates than WM soil column leachates. This shows that the WS soils are more prone to leaching, compared to WM soils. The WS soils have a high CECe and therefore, a high buffering capacity, hence there is more release of Ca, Mg and K into soil solution. This release of base cations, buffers changes in acidity even under a simulated rainwater solution at pH 4.35. The WM soils have lower initial base cation and CECe, hence more base cations are depleted.

The pH for WS soil column leachates remained in the alkaline to slightly acidic range, whilst that for WM soil columns was mostly in the slightly acidic range. This indicates that even after the addition of an acidic solution, the soil has the capacity to neutralise some of the acidity through CECe and exchangeable bases. The soil oxidation and reduction conditions also determine the leaching characteristics of soil, as indicated by Mn and Fe behaviour. Anaerobic and aerobic cycles result in adsorption and release cycles that assist the soil in neutralising the effects of acidity, as observed from the results from WS soils. Under field conditions, this would be prevalent mostly in soils that experience short-term wetting and dry cycles. On the other hand, the WM soil column results indicate the type of leaching, where oxidation and reduction conditions are not the main driver of leaching. Under field conditions, this would be mostly prevalent in well-drained soils with no short-term wetting and drying cycles.

Under field conditions, the leaching behaviour is dependent on the amount of rainfall that an area receives. The Sandspruit Catchment area has a seasonally contrasting climate, characterised by summer rain and dry winters. This results in soil wetting and drying cycles that affect responses to atmospheric deposition, a phenomenon not covered under this leaching experiment. For this column leach set-up, one pore volume equals the average rainfall amount in a year in the Sandspruit Catchment. Hence, the results of the column leach test, up to one pore volume can be extrapolated to leaching under field conditions, taking into consideration differences in hydraulic characteristics between repacked soil columns and

undisturbed soils in the field. After the wet cycle, the organic matter in the soil increases, due to increased vegetation cover. The cations and anions in the soil will start at the same level of availability and repeat the same leaching characteristics observed up to one pore volume.

Hillslope position also affects the leaching characteristics of soils. Comparing leaching with the different hillslope positions (crest vs. toe), based on the EC results, it was found that the leaching of cations and anions for both WS and WM sites is higher from the crest slope position than at the toe slope position. This is attributed to the different soil textures from the crest and toe slope positions. The crests soil is characterised as sandy clay loam (24.70% clay), whilst the toe soil is classified as clay for WS soils and sandy loam for WM soils. Under field conditions, it is expected that crest soils have less clay than toe soils, making toe soils less prone to acidification. This phenomenon is evident in the WS soils, where more loss of bases occurred with crest soils than toe soils. However, for the WM soils, this phenomenon did not apply, as the WM crest soils were classified as sandy clay loam and had more clay (24%), whilst the toe soils were classified as sandy loam and had less clay (20%). However, there was not much difference in their leaching profiles, as indicated by EC and base cation results.

Soil texture also contributed to the leaching characteristics by influencing the column redox potentials during the leaching process. Although markedly different pH of the leaching liquids, the effect of redox potential due to saturated conditions, was far more influential in the mass release of cations and metals. The WS soils had higher clay content, resulting in low column pore velocity and major differences in redox potential values between aerated and non-aerated columns. On the other hand, the WM soils had lower clay content, resulting in higher column pore velocity (15 times more) and no major differences in redox potential values between aerated and non-aerated columns. The WS columns transitioned from oxidised to reduced, whilst the WM columns remained oxidised throughout the leaching process, resulting in the different leaching characteristics observed for the two hillslope transects.

The response of soils to acidic inputs signified by leaching with simulated rainwater did not result in the expected acidification of the soil, mainly because soil responses to acidification are a cumulative impact of factors, such as CECe, the amount of exchangeable bases, redox conditions and soil texture. The leaching behaviour observed under simulated rainfall in the laboratory will, therefore, require translation to leaching under field conditions, to determine

the impact on surface water chemistry. This requires the use of models to show how the soils will respond under field conditions.

## **5. THE IMPACT OF SO<sub>x</sub> AND NO<sub>x</sub> DEPOSITION ON SURFACE WATER QUALITY IN THE SANDSPRUIT CATCHMENT**

### **5.1 Introduction**

Soils receive, transport and process atmospheric emissions and ultimately determine the composition of drainage water. Impacts of atmospheric deposition on surface water are through direct wet and dry deposition unto rivers and lakes and run-off from overland and throughflow in soil. This poses a challenge in determining the extent to which the various catchment processes affect surface water quality. However, the purpose of this discussion is to link the leaching behaviour of soils observed in Chapter 4 to surface water quality parameters, such as pH, redox potential, electrical conductivity (EC), base cations, sulphate and nitrate.

### **5.2 Surface Water Quality Monitoring**

Water samples taken from the research catchment and the quaternary scale from tributaries close to the research site were analysed for pH, redox potential, EC, base cations, sulphate and nitrate. The results of these analyses are presented in graphical format, to show changes in the chemical parameters with seasons, from March 2011 to March 2012. The sampling points were chosen to show the water quality upstream of the research catchment, in the research catchment and downstream of the research catchment.

#### **5.2.1 pH and redox potential**

The pH of the samples from all the 12 sampling positions is between 7.14 and 9.44, that is, in the neutral to alkaline range (Figures 5.1, 5.2, 5.3 and 5.4). The highest pH from all the sampling sites is in June 2011 and declines over the next sampling dates. This decline in pH does not go beyond values less than 7, indicating that surface water acidification has not occurred within the Catchment. The data therefore suggests that, atmospheric deposition has not resulted in acidification of the Sandspruit Catchment surface waters. This surface water response to atmospheric deposition in the Sandspruit Catchment is controlled by the soil

processes, as evidenced by the leach column test results, where simulated acid rain with pH 4.3 was buffered to pH above 7 or more.

The response by the Sandspruit catchment is similar to that observed in Southern Europe by Neal, *et al.* (1995), where atmospheric deposition did not result in detrimental impacts on surface water. The response of surface waters in the Sandspruit catchment show that atmospheric deposition in the region has not yet reached critical levels to results in surface water pH below 5.4, as observed in the Hubbard Brook Experimental Catchment, in the United States (Likens, 2004) and also in Central Europe (Novak, *et al.*, 2000), showing that semi-arid grasslands respond differently to atmospheric deposition compared to temperate forests.

The redox potential values for all the sampling sites range from 69 to 166 mV (Figures 5.1, 5.2, 5.3 and 5.4). The redox potential increases with time, with the exception of samples taken in June 2011, which have the lowest redox potential values across all the sampling points. These low redox potential values coincide with the highest pH values obtained in June 2011. The reciprocal relationship is also observed in the initial pore volumes of non-aerated columns, again an indication that soil processes influence the response to atmospheric deposition by surface water. The low redox potential values in surface water are caused by low flows, resulting in maximum anaerobic conditions, characteristic of conditions in June. The low flows in June result in similar leach column conditions observed under low pore velocity, which resulted in anaerobic column conditions. The redox potential increases with the onset of the wet season, as flows increase, similar to column conditions under high pore velocity.

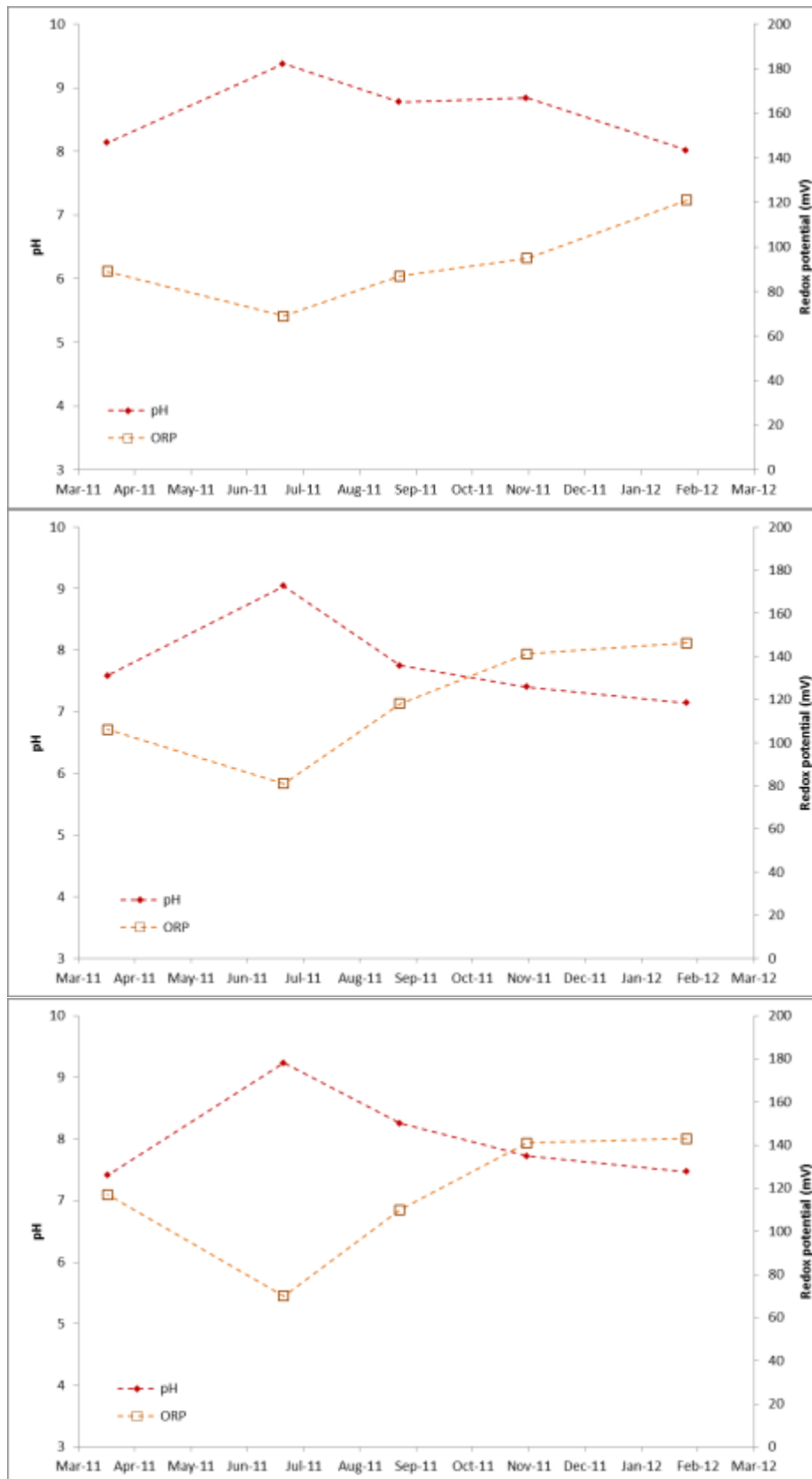


Figure 5.1 pH and redox potential variation at Sites, 1: Wessel borehole (top), 2: Wessel Spring (middle) and 3: Wessel Catchment Outlet at the Research Catchment



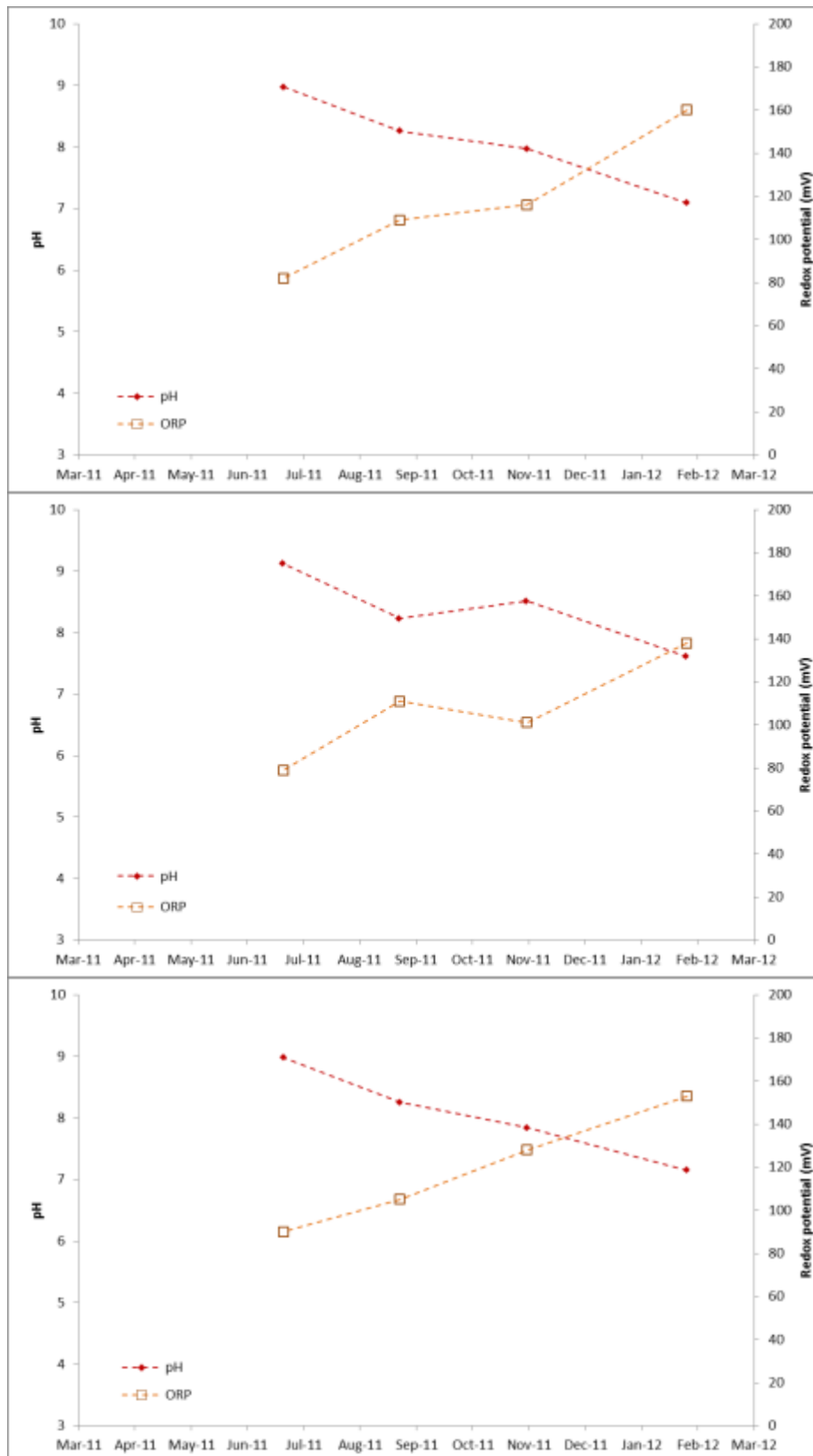


Figure 5.2 pH and redox potential variation at Sites 4: Sandspruit Kloof u/s of Junction (top), 5: Sandspruit Drift (middle) and 6: Sandspruit Bridge near Wessel Farm (bottom) in the Sandspruit Catchment

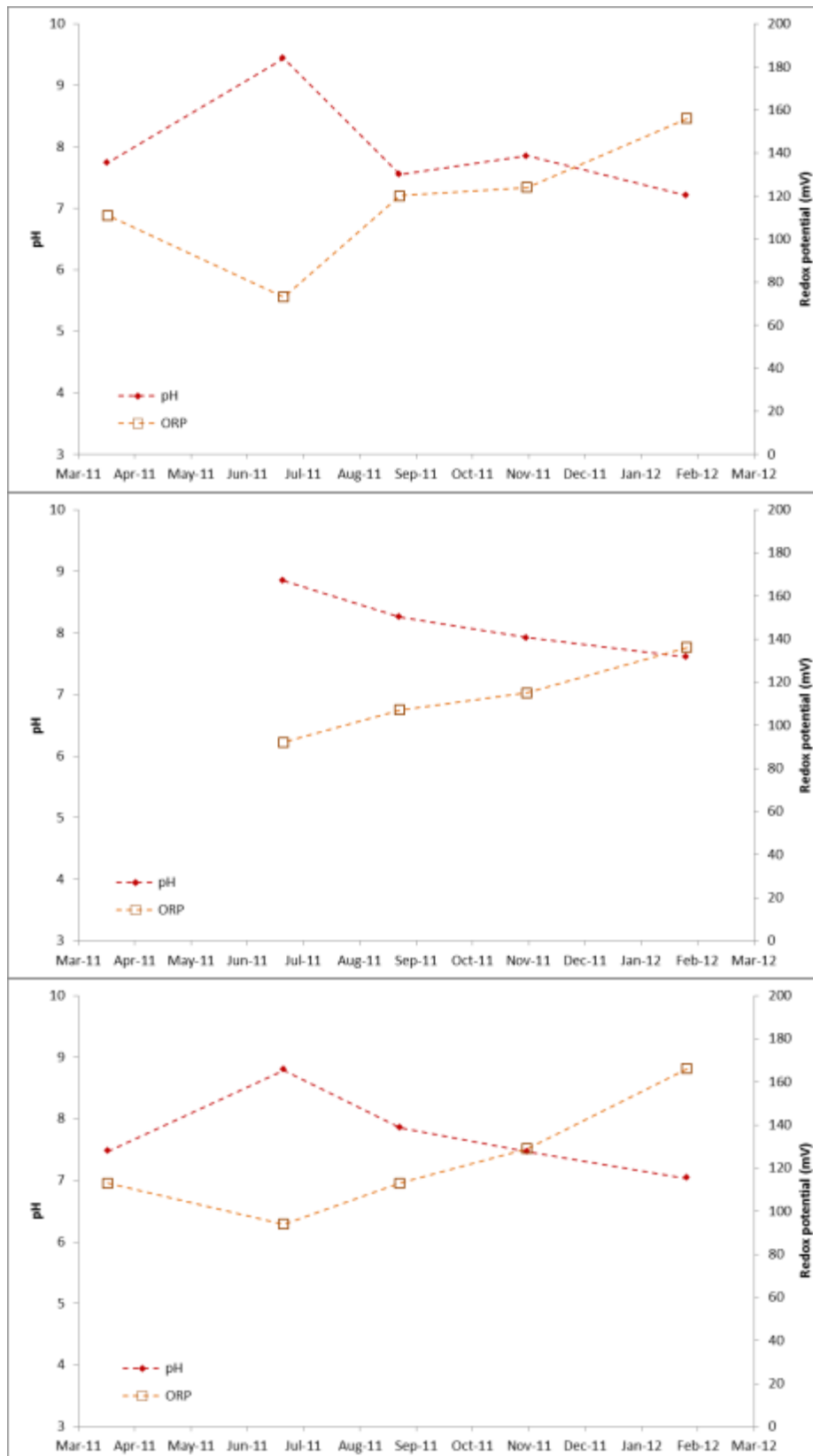


Figure 5.3 pH and redox potential variation at Sites 7: Sandspruit Bridge on N11 (top), 8: Steel Bridge on N23 (middle) and 9: Bridge near Perdokop (bottom) in the Sandspruit Catchment

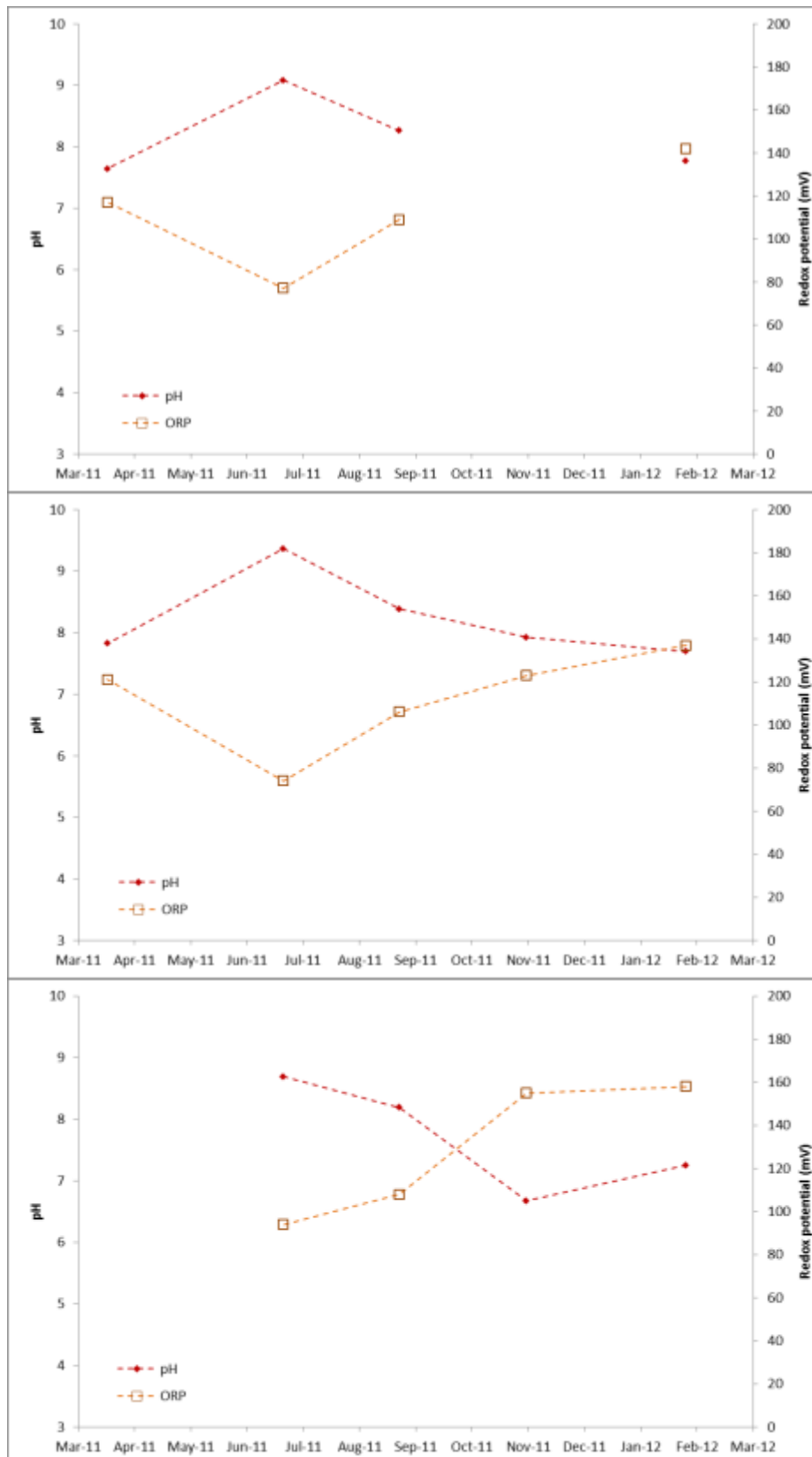


Figure 5.4 pH and redox potential variation at Sites 10: Sandspruit Junction off S446 Bridge (top), 11: Klip u/s of Junction (middle) and 12: Klip d/s of Junction (bottom) of the Sandspruit River

### 5.2.2 Electrical conductivity, sulphate and nitrate

The EC values of the water samples, across all sampling sites generally fall in the non-saline range, between 0.1 to 2.0 mS/cm (Appendix 11 to 15). The EC values for the Wessel Farm borehole (Site 1) are the same throughout the winter (June 2011) and summer (Nov 2011) sampling period, whilst the EC values for the rest of the sites are fluctuating with the seasons (Figure 5.5). The highest in EC values are obtained from Wessel Farm borehole located on the windmill (WM) catena. This is attributed to accumulation of salts from groundwater, which is the borehole's source and can be linked to high Na concentration observed from leach columns results from this site. Soil column leachates from the WM site had the highest amount of Na concentration (Figure 4.9: right) compared to the WS column.

The sulphate results for Site 1 (Wessel Spring) are constant and the lowest throughout the year (Figure 5.5). This indicates that the water source is not affected by direct deposition, which changes with seasons. However, the sulphate results for the rest of the sampling sites show the same trends of seasonal variation, with peaks in November (Figure 5.5). The sulphate concentration increases in a downstream direction and exceeds the atmospheric input of 2.84 mg/L, indicating sulphate loading in surface water. This trend is also observed in all the column breakthrough curves for WS and WM soils, where the sulphur concentration is also greater than 2.84 mg/L in the leachates from soil columns leached with simulated rainwater solution (Figure 4.14).

The nitrate concentration across the entire catchment is below the atmospheric input of 1.55 mg/L. This shows that the system is nitrogen-limited and that the nitrogen from atmospheric deposition is acting as a fertiliser, with most of it being utilised by plants and microorganisms, and reduced to nitrogen gas.

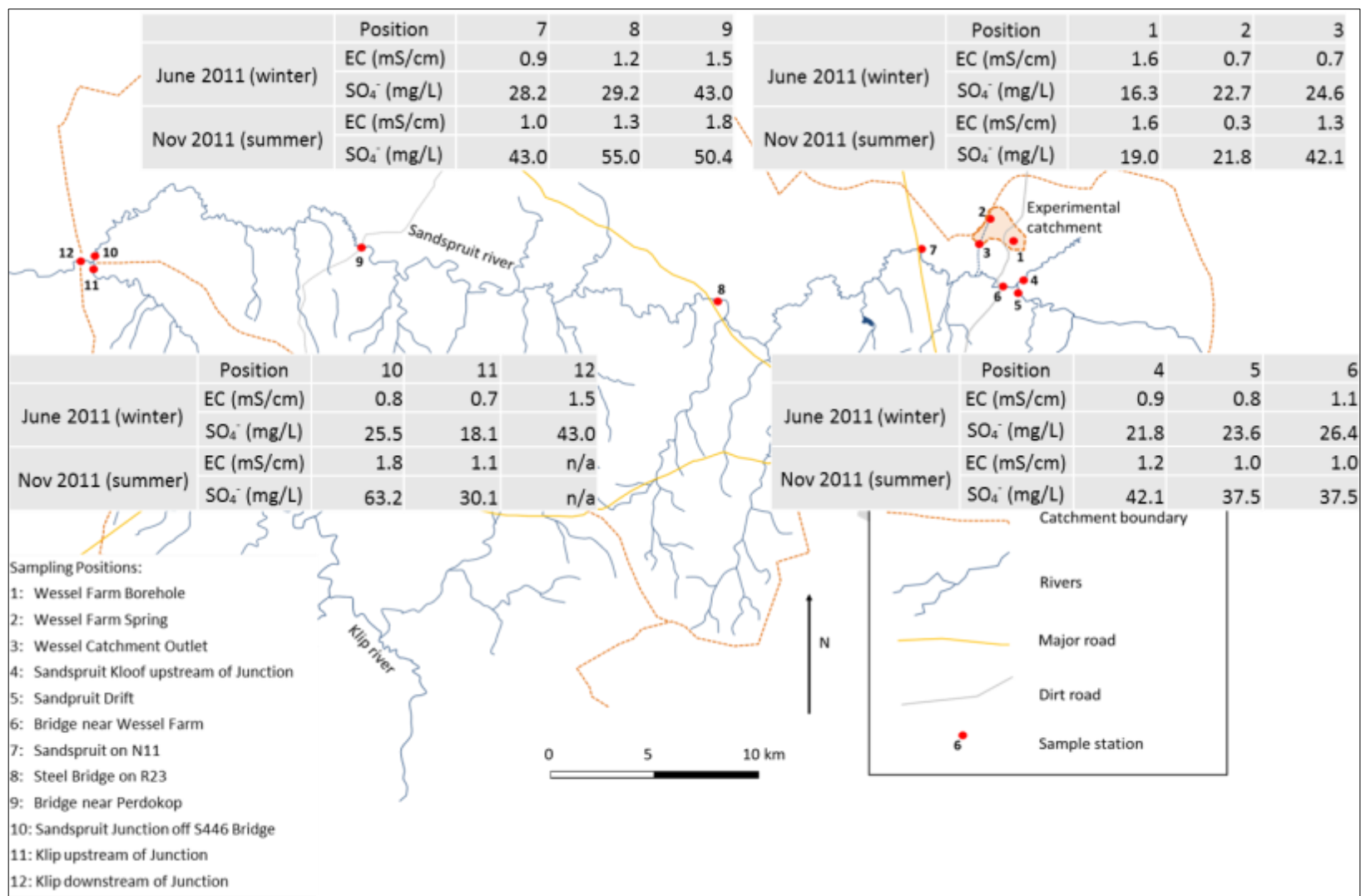


Figure 5.5 Map of the Sandspruit Catchment with the measured winter and summer EC and sulphate values for all the 12 sampling positions

### 5.2.3 Base Cations

The Ca, Mg and K concentration for the three research catchment sites, that is, Site 1, 2 and 3 show the same trends over time (Appendix 16 to 19). The lowest concentration of all three elements is derived from Wessel Farm borehole, with Mg concentration below detection limits (Figure 5.6). The concentrations of Ca, Mg and K for the three sites is highest during the summer period (November 2011) This trend is similar to that observed for sulphate, and could be attributed to lower flows during the dry months before the onset of the wet season. Lower flows result in less dilution of bases, resulting in an increase in their concentration. Similar seasonal trends were observed by Driscoll *et al.*, (2001) in the Hubbard Brook Catchment, whereby surface waters are more acidic in spring after precipitation events. The results of Ca, Mg and K for samples upstream of the research catchment (Sites 4, 5 and 6) and downstream of the research catchment (Sites 7, 8, 9, 10 and 11) also show similar trends to those observed for sulphate, of seasonal variation, with peaks in November and lower concentration during the winter months (Figure 5.6). This similar behaviour to sulphate is due to sulphate acting as an accompanying ion to the base cations.

The Na concentration is highest in samples derived from the borehole (Site 1) and has concentration greater than 50 mg/L (Figure 5.6). This is attributed to the leaching characteristics of soils from the WM catena, where the water from the borehole is abstracted. The leachate concentration from the WM soils has higher Na concentration compared to those from the WS soils (Figure 4.9: right). Hence, it can be assumed that the WM catena makes the higher contribution of Na to the research catchment.

The trends observed in the base cation concentration of surface water are due to the acid neutralisation processes that occur in soil. Base cation availability in surface water is because of the soil buffering mechanisms, which release bases into soil solution and ultimately drainage water (Kitchner and Lydersen, 1995). This base cation buffering mechanism is also similar to that observed in the WS and WM base cation column breakthrough curves, where the acidity from atmospheric deposition is neutralised by exchange of the  $H^+$  ion with base cations on soil surfaces. This enabled the soils to buffer acidic input of pH 4.35 to neutral pH values. There is no clear trend of either increase or reduction of base cations in surface water, indicating that atmospheric deposition has not resulted in surface water acidification in the Sandspruit Catchment. An increase in base cations in surface water would have indicated

surface water acidification, such as that observed in Norwegian catchments (Kitchner and Lydersen, 1995). The Sandspruit Catchment water quality results however, indicate that release of bases into water is a seasonal, with high release occurring during the summer months, where there is increased rainfall, resulting in more leaching of bases.

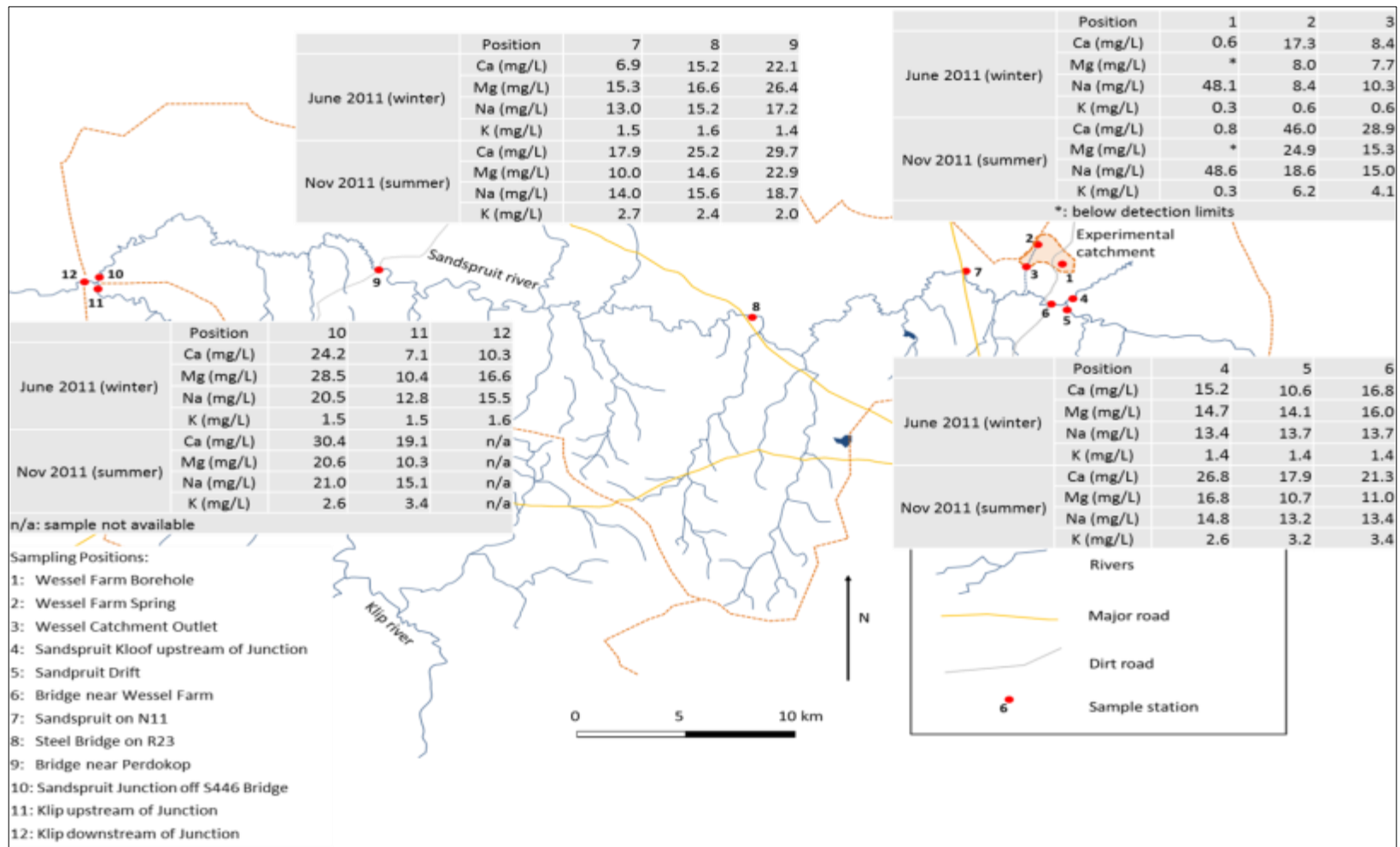


Figure 5.6 Map of the Sandspruit Catchment with the measured winter and summer Ca, Mg, Na and K values for all the 12 sampling positions



### 5.3 Conclusion

The surface water quality monitoring results show that, atmospheric deposition has not resulted in acidification of the water in the Sandspruit catchment. Furthermore, the acid buffering mechanisms in the soil, that were observed in both the WS and WM soil column results, ensure that most of the acidity is neutralised before the soil water drains into the surface water. The pH values from the column tests ranged from slightly acidic to neutral, hence under field conditions soil water within the same pH range would drain into surface water, without causing any acidification. The pH results contradict findings in the United States and Europe, whereby atmospheric deposition is correlated to surface water acidification (Kitchner and Lydersen, 1995; Jenkins, *et al.*, 1997; Novak, *et al.*, 2000; Likens, 2004).

The surface water quality monitoring results for sulphate also show the same trends observed in the sulphur leach column breakthrough curves. Both leach column and surface water results showed sulphate concentrations greater than those observed in atmospheric input, indicating that atmospheric deposition leads to loading of sulphate in soils and water.

Given the above results and discussion, we can conclude that there is a link between the leach column test results and measured stream water chemistry under field conditions.

## 6. GENERAL DISCUSSION, CONCLUSIONS AND RECOMENDATIONS

### 6.1 General Discussion

The leach column results show that the response of soils to atmospheric deposition is a function of the soil's chemical and physical parameters, such as CEC, redox conditions, organic matter content and texture. These parameters determine the extent to which soils are able to buffer incoming acidity from atmospheric deposition. The Sandspruit Research Catchment soils, with high CEC, organic matter content and a clayey soil texture have a high buffering capacity to acidification, as shown by the WS column leach test results. The pH of leachate from these soils did not decrease to acidic ranges. On the other hand, the WM soils, which have lower CEC, organic matter content and have a sandy soil classification, have a lower acid buffering capacity. This is shown by the leachate pH values which decreased to slightly acidic conditions and the high Al concentrations observed during the leaching process.

Another parameter which had a significant influence on the leach column test results was the column redox conditions. The WS soil columns, due to the high clay content of the soil and low saturated hydraulic conductivity, resulted in lower pore velocity being applied during the leaching process. This subsequently resulted in reducing conditions developing during the leaching process, leading to release of Fe and Mn, which becomes soluble under reducing conditions. On the other hand, the soil used for the WM columns had a higher saturated hydraulic conductivity, hence the columns remained oxidised throughout the leaching process. This resulted in no Mn being detected in the leachate.

The results of the column leach tests, such as neutralisation of acidity, reciprocal pH and redox potential values, non-saline EC values and sulphur concentrations greater than the atmospheric input, are similar to the processes that occur under field conditions, and ultimately determine surface water catchment parameters. Under field conditions, atmospherically deposited components are, first processed in the soil matrix, the resulting compounds released into soil water, and subsequently drains into surface and ground water. The atmospheric elements can also be deposited directly unto surface water, resulting in

short-term to long-term impacts. Therefore, when discussing the contribution of leaching characteristics of soils to surface water chemistry, discretion should be practiced. However, there is a relationship between the leach column results and the surface water chemical parameters measured in the Sandspruit Catchment.

The results of surface water quality monitoring show no evidence of acidification, as indicated by the WS soil columns which contribute directly to the Sandspruit Catchment. The results also show the presence of base cations, because of the soil buffering mechanisms which release bases into soil solution and ultimately drainage water. An interesting point to note are the results of water quality tests for the Wessel Farm borehole. The results are closely related to the leaching characteristics observed from the WM soil columns. For example, the Mg concentration from the column leach tests was lowest in the WM soils, whilst the Mg concentration at the borehole (Site 1) was below detection limits and the lowest across all sampling sites. The Na concentration from the column leach tests was highest in the WM soil columns, whilst the Na concentration was highest at the borehole (Site 1) across all sampling sites. This is because the soils for the WM soil columns were derived from close proximity to the source of the borehole. The source of the borehole is therefore, directly impacted by the soil leaching profile at this position. The results from the WS soil columns are closely related to those obtained from the spring (Site 2), which is located in close proximity to the WS hillslope transect. However, the spring water quality results do not differ from those obtained from the other sampling positions, like those from the borehole (Site 1).

## **6.2 Conclusions**

The purpose of this research was to determine the leaching characteristics of selected Sandspruit soils under atmospheric deposition. The results show that, the leaching characteristics are influenced by the soil characteristics themselves, rather than the components of atmospheric deposition. The various soil chemical characteristics buffer the soil against atmospheric deposition. Hence, atmospheric deposition over the Sandspruit Catchment is not sufficient to result in well observed acidification of soil and surface water.

Based on the surface water quality results for the Wessel Farm borehole, there is a link between the leaching characteristics and the water quality from the borehole. However, for

the other surface water sampling positions within the research and the quaternary catchment, it is difficult to say with certainty that there is a link between the leaching characteristics as soil water close to the sampling points were not extracted and analysed, and the sampling points were also exposed to direct atmospheric deposition. The contribution of direct surface water deposition on surface water quality was not included in the scope of this research.

### **6.3 Recommendations**

The following recommendations can be applied to future atmospheric deposition research.

- a) Soil chemical parameters are a function of the weathering processes of underlying rock formations. Weathering processes therefore determine the clay mineralogical composition of the soil and this influences the leaching parameters of the soil. Soil mineralogical analysis was not conducted during this research, as the equipment to conduct the analysis was not available. It is therefore recommended that future research should focus on the impact of clay mineralogy on leaching behaviour of soils.
- b) Organic matter in soils is a source of base cation and anions in soil and its breakdown in soil influences soil leachate composition. It is therefore recommended that, future research should consider organic matter solubilisation, by measuring the organic carbon content in the leachate and come up with breakthrough curves to show how organic carbon changes with leaching.
- c) This column leach study focused mainly on measuring leachate parameters. However, these types of investigations can also be extended to measure the same soil parameters such as pH, exchangeable bases, CEC and  $Al^{3+}$  concentration in soils from the column after the leaching process. This can assist in computing the percentage of reduction in pH and concentration of base cations and  $Al^{3+}$  after leaching.
- d) In order to determine the actual contribution of the soil leaching process to soil solution under field conditions, suction cup or pan lysimeters and/or piezometers can be installed in the field, soil water extracted and analysed for pH, bases and anions. This can assist quantification of losses from leaching under field conditions and provide direct links to the contribution of leaching to surface water quality.

- e) The results of the breakthrough curves can also be applied in acidification models that can assist in predicting the long term impacts of atmospheric deposition on soils and water.

## 7. REFERENCES

- Andreiadis, ES. 2005. *Breakthrough curves: determination of specific parameters*. Chemical Engineering Department, University of Bucharest, Bucharest, Romania.  
Available from [http://www.tankonyvtar.hu/hu/tartalom/tamop425/0032\\_vizkeszletgazdalkodas\\_es\\_vizminoseg/ch05s04.html](http://www.tankonyvtar.hu/hu/tartalom/tamop425/0032_vizkeszletgazdalkodas_es_vizminoseg/ch05s04.html). (Accessed 12 September 2013).
- Bernhard, A. 2010. The nitrogen cycle: processes, players and human impact. *Nature Education Knowledge* 2(2):12.
- Beukes, DJ. 1995. *Soil acidity in agriculture*. Agriculture Research Council, Pretoria, South Africa.
- Bohan, L, Seip, HM, and Larssen, T. 1995. Response of two Chinese forest soils to acidic inputs: leaching experiment. *Geoderma* 75(1-2):53-73.
- Carpenter, SR, Caraco, NF, Correll, DL, Howarth, RW, Sharpley, AN and Smith, VH. 1998. Nonpoint pollution of surface waters with phosphorous and nitrogen. *Ecological Applications* 8(3):559-568.
- Cho, JY, Han, KW, Nishiyama, M and Matsumoto, S. 2003. Leaching of Al, base cations and anions by simulated acid rain with varying NO<sub>3</sub><sup>-</sup>/SO<sub>4</sub><sup>2-</sup> ratios in reclaimed saline soils. *Agriculture, Chemistry and Biotechnology* 46(1):17-24.
- Chu, KH. 2004. Improved fixed bed models for bio-sorption. *Chemical Engineering Journal* 97(2-3):233-239.
- Clayton, JL, Kennedy, DA and Nagel, T. 1991. Soil responses to acid deposition, Wind River mountains, Wyoming:II. Column Leaching Studies. *Soil Science Society of America Journal* 55(5):1433-1439.
- Csaba, P and Csaba, J. 2011. *Water resources management and water quality protection*. [Internet]. Digitális Pedagógiai Osztály, European Union, Budapest, Hungary.
- Driscoll, CT, Lawrence, GB, Bulger, AJ, Butler, TJ, Cronan, CS, Eagar, C, Lambert, KF, Likens, GE, Stoddard, JL and Weathers, KC. 2001. Acidic deposition in the Northeastern United States: sources and inputs, ecosystem effects and management strategies. *BioScience* 51(3):180-198.
- Edwards, PJ. 1998. *Sulfur Cycling, Retention and Mobility in Soils. A Review*. General Technical Report, NE-250. USDA Forest Services, Radnor, PA. USA.

- Essington, ME. 2004. *Soil and Water Chemistry: An Integrative Approach*. CRC Press. Boca Raton, Florida, USA.
- Fallman, AM and Aurell, B. 1996. Leaching tests for environmental assessment of inorganic substances in wastes, Sweden. *The Science of the Total Environment* 178(1-3):71-84.
- Fernandez-Sanjurjo, MJ, Alvarez E, Vega, VF and Garcia-Rodeja E. 1997. Chemistry of soil solution under different kinds of vegetation in the vicinity of a thermal power station. *Environmental Pollution* 101(1):131-142.
- Fey, MV and Guy, SA. 1993. *The Capacity of Soils in the Vaal Dam Catchment to Retain Sulphate from Atmospheric Pollution*. Report No.414/1/93. Water Research Commission, Pretoria, South Africa.
- Goswami, RK and Mahanta, C. 2007. Leaching characteristics of residual lateritic soils stabilised with fly ash and lime for geotechnical applications. *Waste Management* 27(4):466-481.
- Gundersen, P and Bashkin, VN. 1994. Nitrogen Cycling. In: ed. Moldan, B and Cerny, J, *SCOPE 51 Biogeochemistry of Small Catchments: A Tool for Environmental Research*, Ch. 11, 256-283. John Wiley and Sons, New York, USA.
- Guyonnet, D. 2010. Comparison of percolation to batch and sequential leaching tests: theory and data. *Waste Management* 30(8-9):1746-1747.
- Hageman, PL. 2003. Leaching studies. In: ed. Authors, *USGS, Billings Symposium/ASMR Annual Meeting: Assessing the toxicity potential of mine waste piles Workshop, June 1 2003*. US Department of the Interior and US Geological Survey (USGS), Reston, Colorado, USA.
- Hazeth, PA and Murphy, B. 2007. *Interpreting soil test results. What do the numbers mean?* CSIRO Publishing, Collingwood, Australia.
- Hedl, R, Petrik P and Boulblik, K. 2011. Long-term patterns in soil acidification due to pollution in forests of eastern Sudetes Mountains. *Environmental Pollution* 159(10):2586-2593.
- Hendershot, WH And Duquette, M. 1986. A simple barium chloride method for determining cation exchange capacity and exchangeable cations. *Soil Science Society of America Journal* 50(3):605-608.
- Hultberg, H, Apsimon, H, Church, RM, Grennfelt, P, Mitchell, MJ, Moldan, F and Ross, HB. 1994. Sulphur. In: ed. Moldan, B and Cerny, J. *SCOPE 51 Biogeochemistry of Small Catchments: A Tool for Environmental Research*, Ch. 10, 229-254. John Wiley and Sons, New York, USA.

- Husson, O. 2013. Redox potential (Eh) and pH as drivers of soil/plant/microorganism systems: a transdisciplinary overview pointing to integrative opportunities for agronomy. *Plant and Soil* 362(1-2):389-417.
- Igbafe, AI. 2007. *Resolving the atmospheric sulphur budget over the Elandsfontein area of the Mpumalanga Highveld*. Unpublished PhD Thesis, Faculty of Engineering and the Built Environment, University of the Witwatersrand, Johannesburg, South Africa.
- Jeffrey, L. 2006. Challenges associated with further development of the Waterberg coalfield. *The Journal of the South African Institute of Mining and Metallurgy* 105(July):453-458.
- Jenkins, A, Ferrier, RC and Cosby, BJ. 1997. A dynamic model for assessing the impact of coupled sulphur and nitrogen deposition scenarios on surface water acidification. *Journal of Hydrology* 197(1-4):111-127.
- Johnson, DW. 1984. Sulphur cycling in forests. *Biogeochemistry* 1(1):29-43.
- Josipovic, M, Annegarn, HJ, Kneen, MA, Pienaar, JJ and Piketh, SJ. 2011. Atmospheric dry and wet deposition of sulphur and nitrogen species and assessment of critical loads of acidic deposition exceedance in South Africa. *South African Journal of Science* 107(3-4):1-10.
- Kennedy, IR. 1986. *Acid Soil and Acid Rain: The Impact on the Environment of Nitrogen and Sulphur Cycling*. Research Studies Press Ltd, England.
- Kitchner, JW and Lydersen, E. 1995. Base cation depletion and potential long-term acidification of Norwegian catchments. *Environmental Science and Technology* 29(8):1953-1960.
- Knox, RC, Sabatini, DA and Canter, LW. 1993. *Subsurface Transport and Fate Processes*. CRC Press Inc, Boca Raton, Florida, USA.
- Kuylenstierna, JCI, Rodhe, H, Cinderby, S and Hicks, K. 2001. Acidification in developing countries: ecosystem sensitivity and the critical load approach on a global scale. *AMBIO: A Journal of the Human Environment* 30(1):20-28.
- Larssen, T, Vogt, RD, Seip, HM, Furuberg, G, Liao, B, Xiao, J and Xiong, J. 1999. Mechanisms for aluminium release in Chinese acid forest soils. *Geoderma* 91(1-2):65-86.
- Lieb, AM, Darrouzet-Nardi, A and Bowman, WD. 2011. Nitrogen deposition decreases acid buffering capacity of alpine soils in the southern Rocky Mountains. *Geoderma* 164(3-4):220-224.



- Likens, GE and Bormann, FH. 1995. *Biogeochemistry of a Forested Ecosystem*, 2<sup>nd</sup> Ed. Springer-Verlag, New York, USA.
- Likens, GE, Buso, DC and Butler, TJ. 2005. Long-term relationships between SO<sub>2</sub> and NO<sub>x</sub> emissions and SO<sub>4</sub><sup>2-</sup> and NO<sub>3</sub><sup>-</sup> concentration in bulk deposition at the Hubbard Brook experimental forest, NH. *Journal of Environmental Monitoring* 7(10):964-968.
- Likens, GE, Driscoll, CT and Buso, DC. 1996. Long-term effects of acid rain: response and recovery of a forest ecosystem. *Science* 272(5259):244-246.
- Likens, GE. 2004. Some perspectives on long-term biogeochemical research from the Hubbard Brook Ecosystem Study. *Ecology* 85(9):2355-2362.
- Lindsay, WL. 1979. *Chemical equilibrium in soils*. John Wiley and Sons, New York, USA.
- Liu, KH, Fang, YT, Yu, FM, Liu, Q, Li, FR and Peng, SL. 2010. Soil acidification in response to acid deposition in three subtropical forests of subtropical China. *Pedosphere* 20(3):399-408.
- Lorentz, S, Blight, J and Snyman, N. 2010. *An Investigation into the Effects of Atmospheric Pollutants on the Soil-Water-Ecosystem Continuum in the Eastern Regions of South Africa: Focusing on Hydrogeochemical Catchment Dynamics*. Final Report, 2010. School of Bioresources Engineering and Environmental Hydrology, University of KwaZulu-Natal, Pietermaritzburg, South Africa.
- Macías, F and Arbestain MC. 2010. Soil carbon sequestration in a changing global environment. *Mitigation and Adaptation Strategies for Global Change* 15(6):511-529.
- Malmstrom, ME, Gleisner, M and Herbert, RB. 2006. Element discharge from pyretic mine tailings at limited oxygen availability in column experiments. *Applied Geochemistry* 21(1):184-202.
- Mast, AM, Turk, JT, Ingersoll, GP, Clow, DW and Kester, CL. 2001. Use of stable sulphur isotopes to identify sources of sulphate in Rocky mountain snowpacks. *Atmospheric Environment* 35(2001):3303-3313.
- Mayer, R. 1998. Soil acidification and cycling of metal elements: cause-effect relationships with regard to forestry practices and climatic changes. *Agriculture, Ecosystems and Environment* 67(2-3):145-152.
- McBride, MB. 1994. *Environmental Chemistry of Soils*. Oxford University Press, New York, USA.

- Moldan, B and Cerny, J. 1994. Small Catchment Research. In: ed. Moldan, B and Cerny, J, *SCOPE 51 Biogeochemistry of Small Catchments: A Tool for Environmental Research*, Ch. 1, 1-30. John Wiley and Sons, New York, USA.
- Mphepya, JN. 2002. Atmospheric deposition of sulphur over Mpumalanga. In: ed. Editors, *Proceedings of the 5<sup>th</sup> International Conference on Southern Hemisphere Meteorology and Oceanography*, Pretoria, South Africa.
- Mulder, J and Cresser, MS. 1994. Soil and Soil Solution Chemistry. In: ed. Moldan, B and Cerny, J, *SCOPE 51 Biogeochemistry of Small Catchments: A Tool for Environmental Research*, Ch. 5, 107-131. John Wiley and Sons, New York, USA.
- Nawaz, R, Parkpian, P, Garivait, H, Anurakpongsatorn, P, Delaune, RD and Jugsujinda, A. 2012. Impacts of acid rain on base cations, aluminium and acidity development in highly weathered soils of Thailand. *Communications in Soils Science and Plant Analysis* 43:1382-1400.
- Neal, C, Avila, A and Roda, F. 1995. Modelling the long-term impacts of atmospheric pollution deposition and repeated forestry cycles on stream water chemistry for a holm oak forest in north-eastern Spain. *Journal of Hydrology* 168(1-4):51-71.
- Nielsen, DR and Biggar, JW. 1962. Miscible displacement: III theoretical considerations. *Soil Science Society of America Proceedings*, 26(3): 216-221.
- Novak, M, Kitchener, JW, Groscheova, H, Havel, M, Cerny, J, Krejci, R and Buzek, F. 2000. Sulfur isotope dynamics in two central European watersheds affected by high atmospheric deposition of SO<sub>x</sub>. *Geochimica et Cosmochimica Acta* 64(3):367-383.
- OK, YS, Chang, SX and Feng, YS. 2007. Sensitivity to acidification of forest soils in two watersheds with contrasting hydrological regimes in the Oil Sands region of Alberta. *Pedosphere* 17(6):747-757.
- Rao, PSC. 1974. *Pore-geometry effects on solute dispersion in aggregated soils and evaluation of a predictive model*. Unpublished PhD Thesis. Agronomy and Soil Science, University of Hawaii, Hawaii.
- Reuss, JO and Johnson, DW. 1986. *Acid deposition and the acidification of soils and water*. Springer-Verlag, New York, USA.
- Reynolds, WD. 1993. Saturated Hydraulic Conductivity: Laboratory Measurement. In: ed. Carter, MR, *Soil Sampling and Methods of Analysis*, Ch. 55, 589-594. Canadian Society of Soil Science. Lewis Publishers, City, Canada.
- Rhoades, JC. 1996. Salinity: electrical conductivity and total dissolved solids. In: ed. Sparks, DL. *Methods of soil analysis. part 3: chemical methods*, Ch. 14, 417-436. Soil

- Science Society of America Book Series 5. Soil Science society of America Inc. and American Society of Agronomy. Madison Wisconsin, USA.
- Rhoades, JD, Chanduvi, F and Lesch, S. 1999. Soil salinity assessment-methods and interpretation of electrical conductivity measurements. FAO irrigation and drainage paper no. 57. FAO, Rome; Land and Water Development Division, Rome, Italy.
- Rogério, C. 2007. *Modelling sulphate dynamics in soils. The Effects of ion-pair adsorption*. Unpublished PhD Thesis in Soil Science. Massey University, Massey, Country.
- Ross, HB and Lindberg, SE.1994. Atmospheric chemical input to small catchments. In: ed. Moldan, B and Cerny, J, *SCOPE 51 Biogeochemistry of Small Catchments: A Tool for Environmental Research*, Ch. 3, 55-84. John Wiley and Sons, New York, USA.
- Scorgie, Y and Kornelius, G. 2009. *Investigation into the effects of atmospheric pollutants on the soil-water-ecosystem continuum atmospheric work- literature review and modelling of acid deposition over the Highveld*. Report No. APP/08/Rev O, ESKOM, Airshed Planning Professionals (Pty) Ltd, Johannesburg, South Africa.
- Söderlund, R and Svensson, BH. 1976. Nitrogen, Phosphorus and Sulphur: Global Cycles: Scope Report 7. *Ecological Bulletins* 22:23-73.
- Sumner, ME and Miller, PW. 1996. Cation exchange capacity and exchange co-efficients. In: ed. Sparks, DL, *Methods of Soil Analysis. Part 3: Chemical Methods*. Soil Science Society of America Book Series 5, Ch. 40, 1201-1230. Soil Science society of America Inc. and American Society of Agronomy. Madison Wisconsin, USA. Tan, KH. 2005. *Soil sampling, preparation and analysis*. Taylor and Francis Group, Boca Raton, Florida, USA.
- The Non-affiliated Soil Analysis Work Committee. 1990. *Handbook of standard soil testing methods for advisory purposes*. Soil Science Society of South Africa, Pretoria, South Africa.
- Thomas, GW. 1996. Soil pH and soil acidity. In: ed. Sparks, DL, *Methods of Soil Analysis. Part 3: Chemical Methods*. Soil Science Society of America Book Series 5, Ch. 16, 457-490. Soil Science society of America Inc. and American Society of Agronomy. Madison Wisconsin, USA.
- van der Sloot, HA. 1996. Developments in evaluating environmental impact from utilization of bulk inert wastes using laboratory leaching tests and field verification. *Waste Management* 16(1-3):65-81.
- van Reeuwijk, LP. 2002. *Procedures for Soil Analysis*. Technical Paper 9/ International Soil Reference and Information Centre, Wageningen, Netherlands.

- von Blottnitz, H, Fedorsky, C and Bray, W. 2009. Air quality. In: ed. Strydom, HA and King, ND, *Environmental Management in South Africa*, Ch 16, 579-629. Juta Law, Cape Town, South Africa.
- Wamukonya, N, Masambuko, B, Gowa, E and Asamoah, J. 2006. Atmosphere. In: ed. Editors, *Africa Environmental Outlook 2: Our Environment, Our Wealth*, Ch.2, 48-77. United Nations Environmental Programme (UNEP), Nairobi, Kenya.
- Warby, RAF. 2007. *The Chemical Response of Surface Waters and Organic Soils Across the North-eastern U.S.A., Following Reduced inputs of Acidic Deposition: 1984-2001*. Unpublished PhD Thesis, Syracuse University, Syracuse, USA.
- Water Research Commission (WRC). 2009. *Water Resources of South Africa, 2005*. Report No. K511491. Water Research Commission, Pretoria, South Africa.
- Zheng, S, Zheng, X and Chen C. 2012. Leaching behaviour of heavy metals and transformation of their speciation in polluted soil receiving simulated acid rain. *PLOS One* 7(11)1-7.

## 8. APPENDICES

### 8.1 Appendix 1

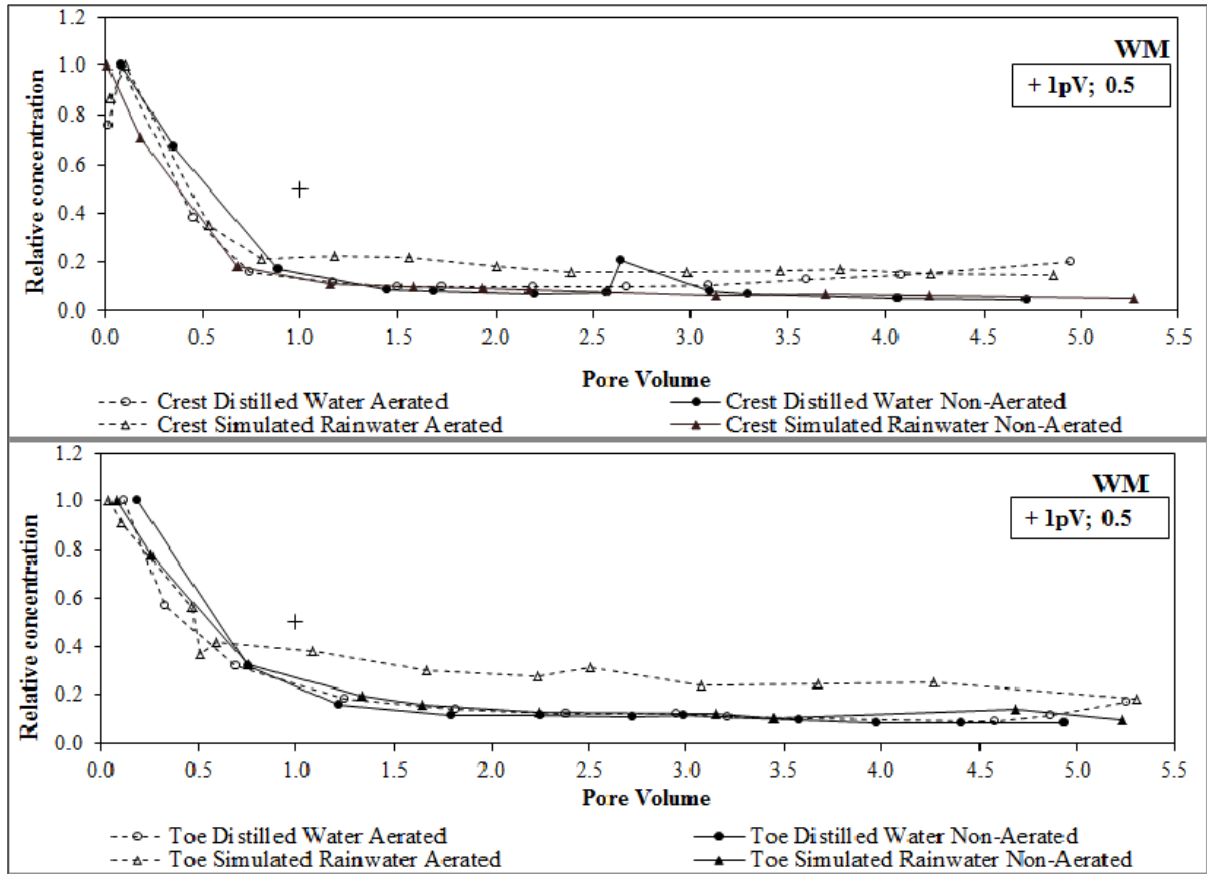


Figure 8.1 Chloride BTC curve as relative concentration for WM (crest: top and toe: bottom) soil columns

## 8.2 Appendix 2

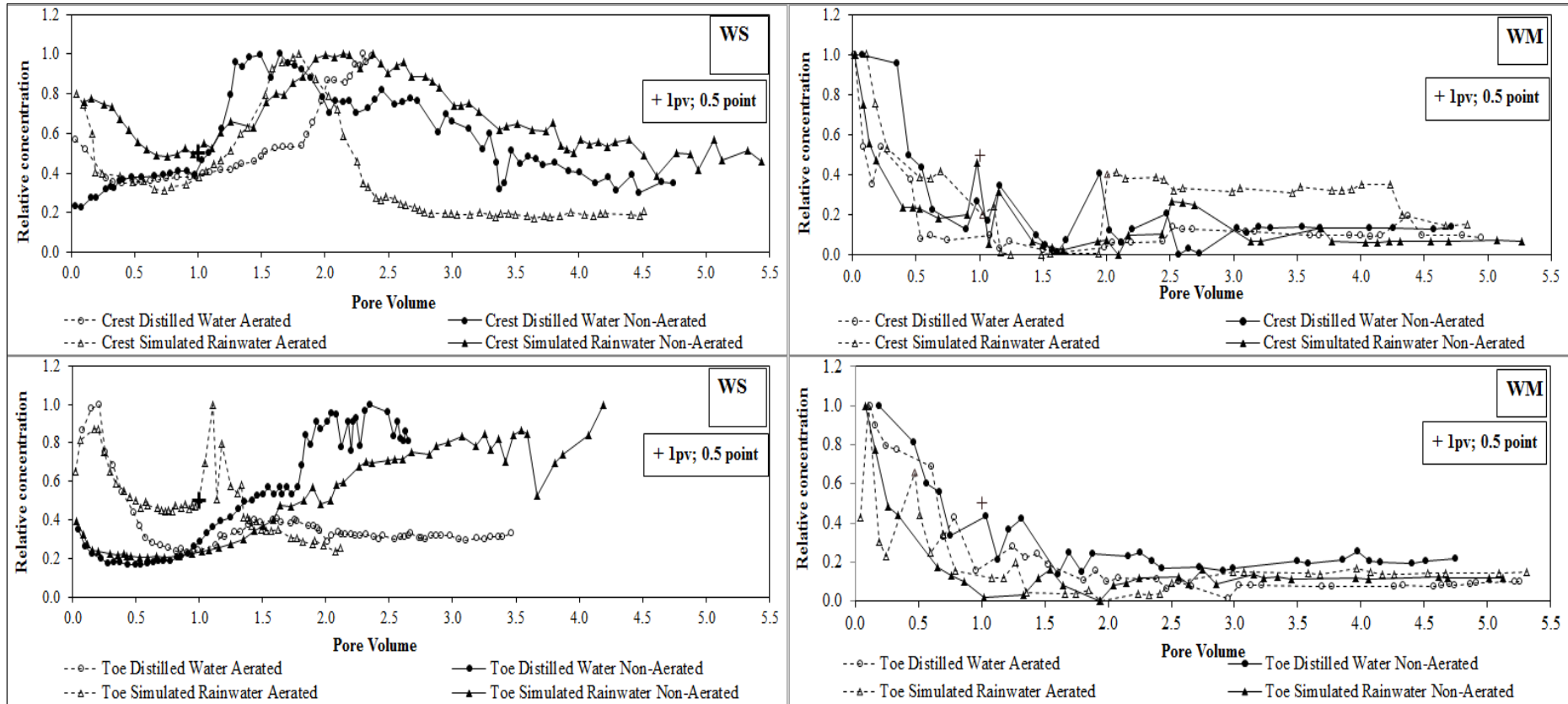


Figure 8.2 Calcium BTC curve as relative concentration for WS (left, crest: top and toe: bottom) and WM (right, crest: top and toe: bottom) soil columns

### 8.3 Appendix 3

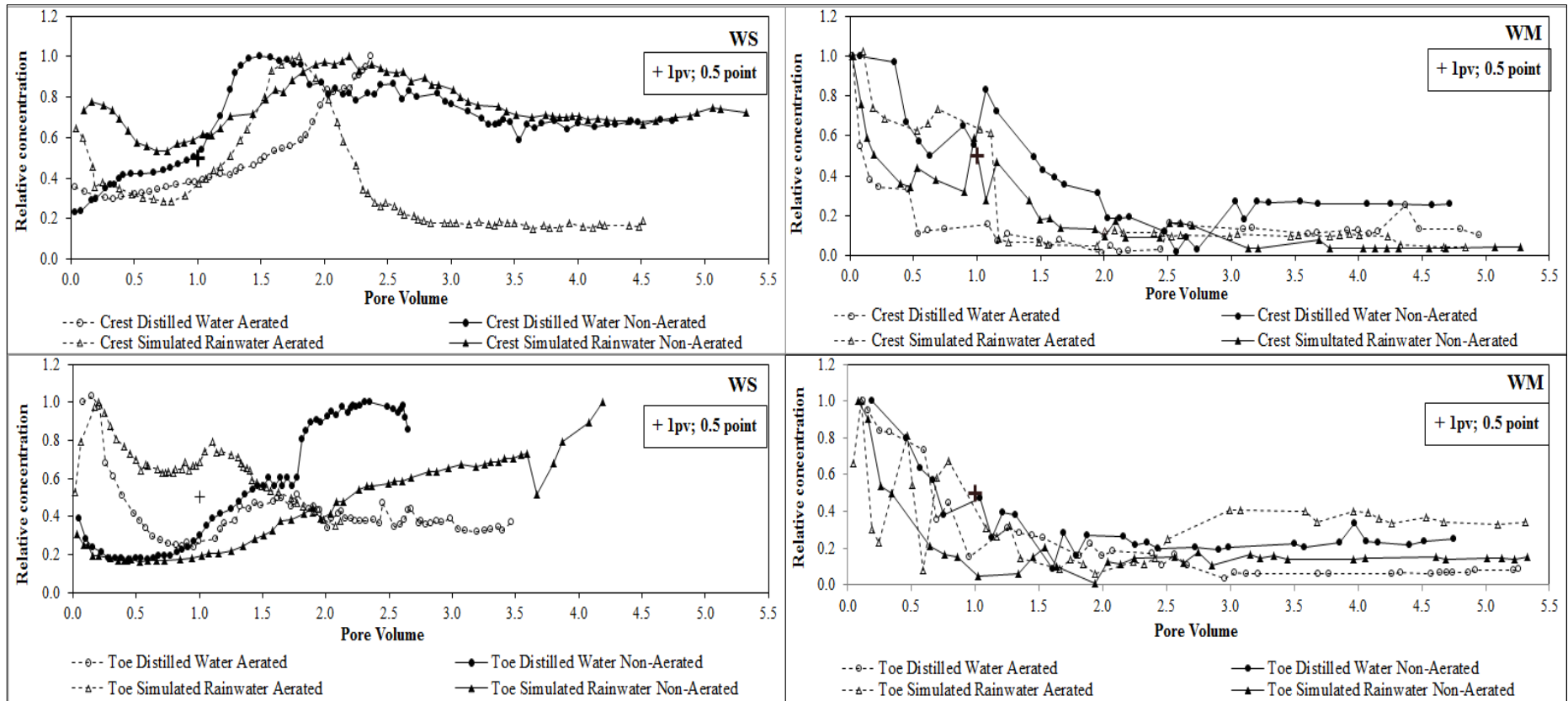


Figure 8.3 Magnesium BTC curve as relative concentration for WS (left, crest: top and toe: bottom) and WM (right, crest: top and toe: bottom) soil columns

## 8.4 Appendix 4

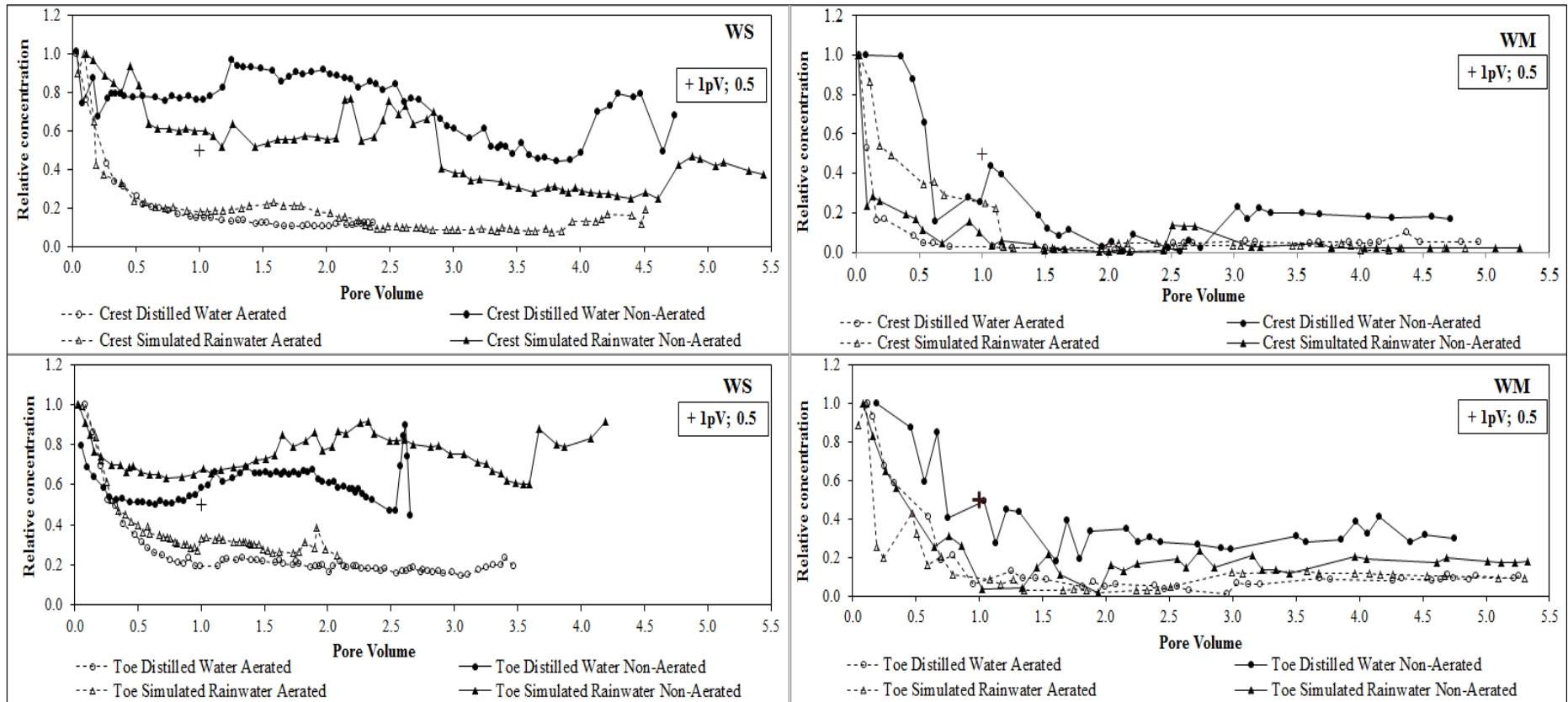


Figure 8.4 Sodium BTC curve as relative concentration for WS (left, crest: top and toe: bottom) and WM (right, crest: top and toe: bottom) soil columns



## 8.5 Appendix 5

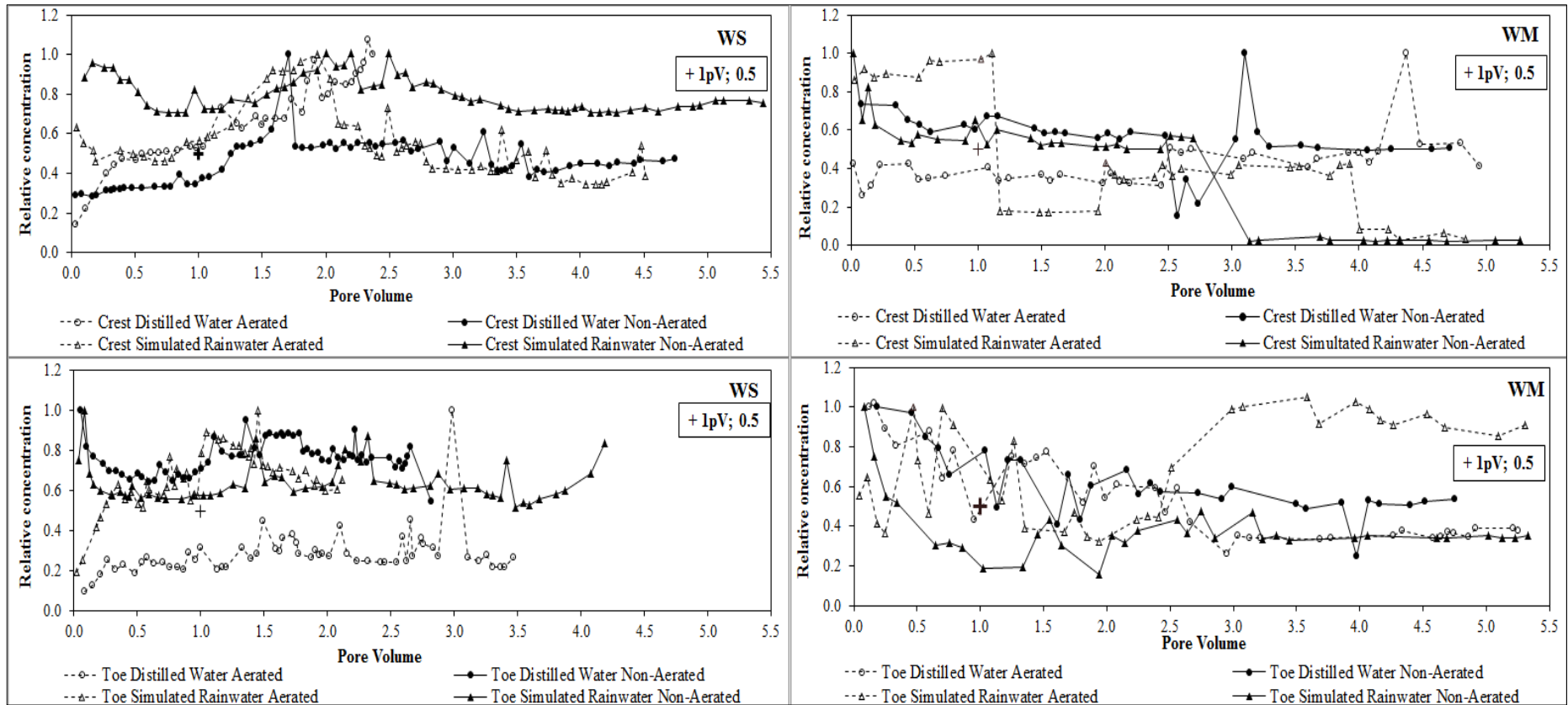


Figure 8.5 Potassium BTC curve as relative concentration for WS (left, crest: top and toe: bottom) and WM (right, crest: top and toe: bottom) soil columns

## 8.6 Appendix 6

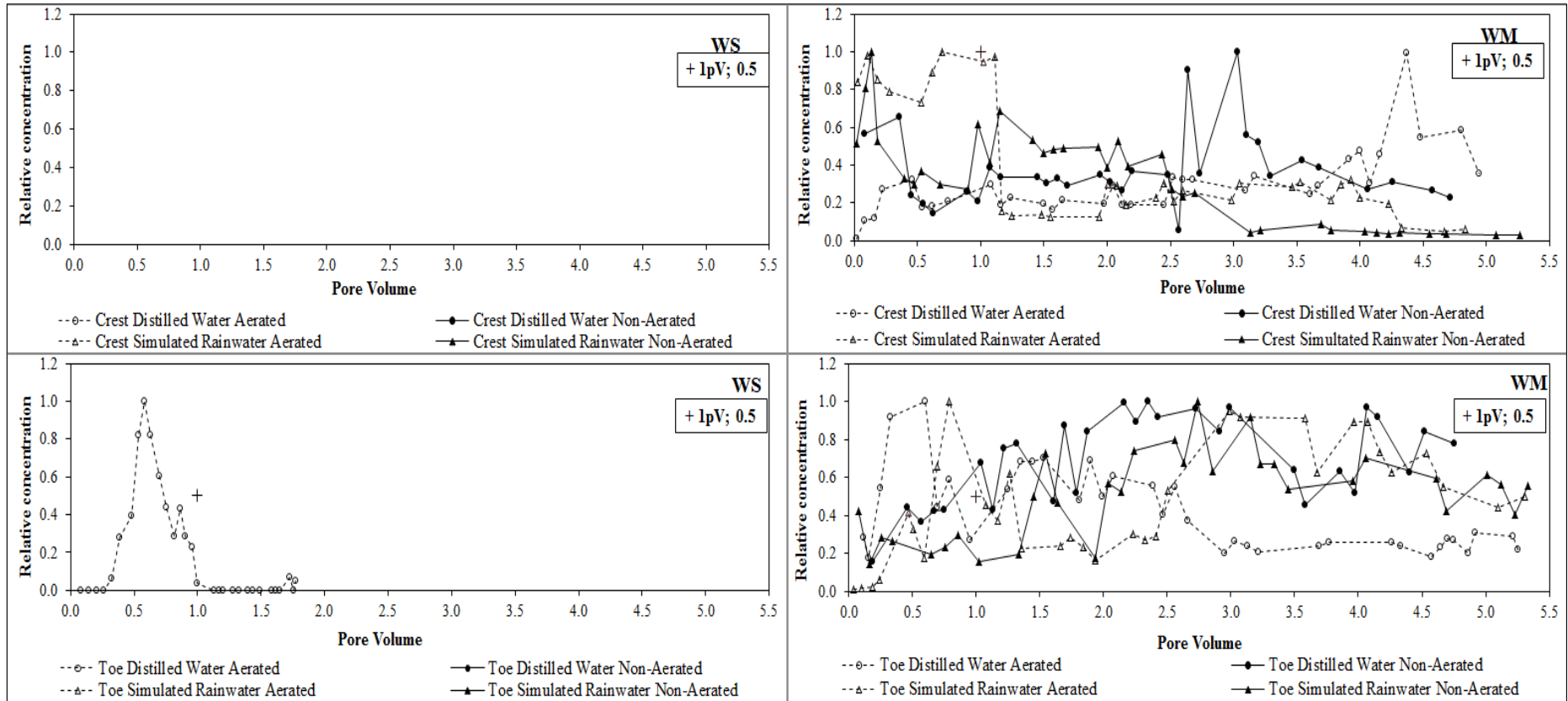


Figure 8.6 Aluminium BTC curve as relative concentration for WS (left, crest: top and toe: bottom) and WM (right, crest: top and toe: bottom) soil columns

## 8.7 Appendix 7

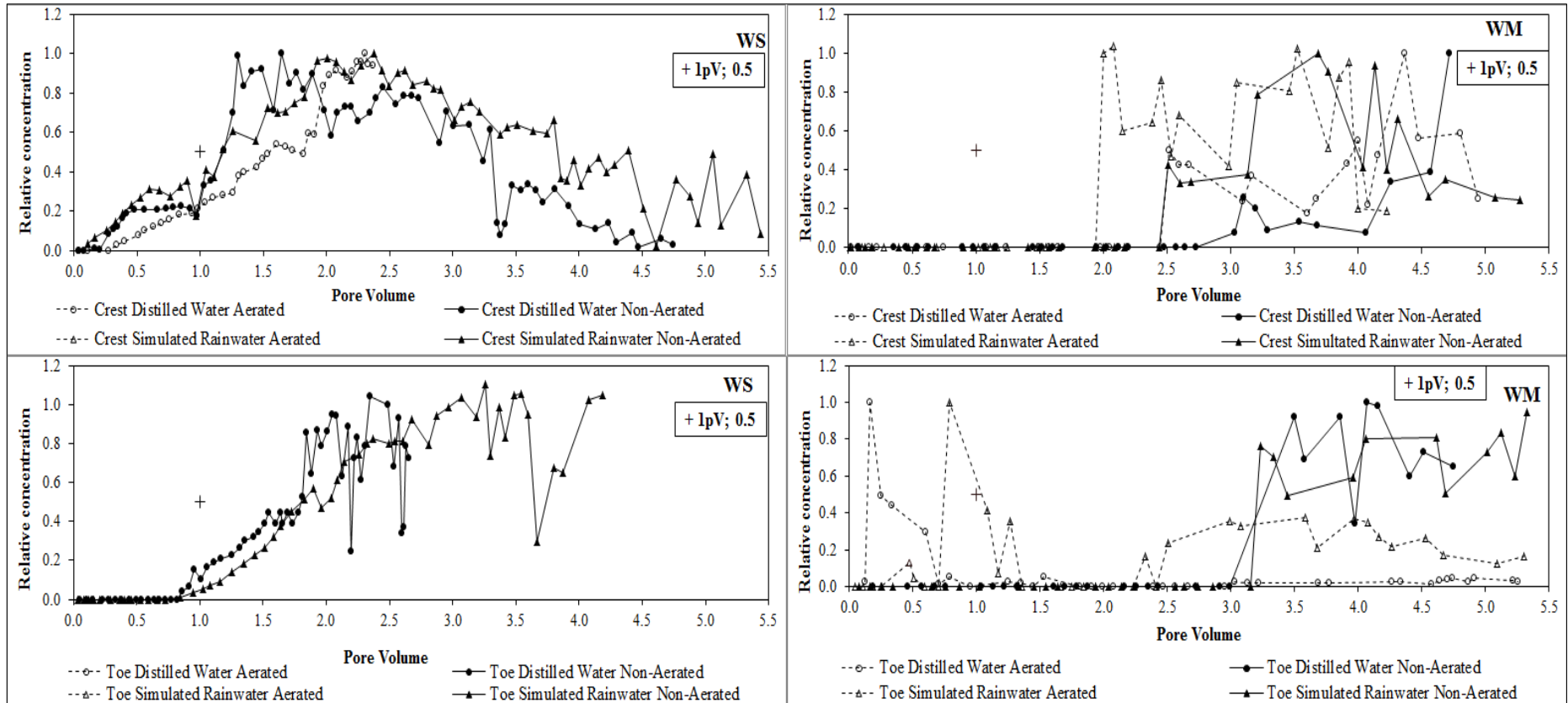


Figure 8.7 Manganese BTC curve as relative concentration for WS (left, crest: top and toe: bottom) and WM (right, crest: top and toe: bottom) soil columns

## 8.8 Appendix 8

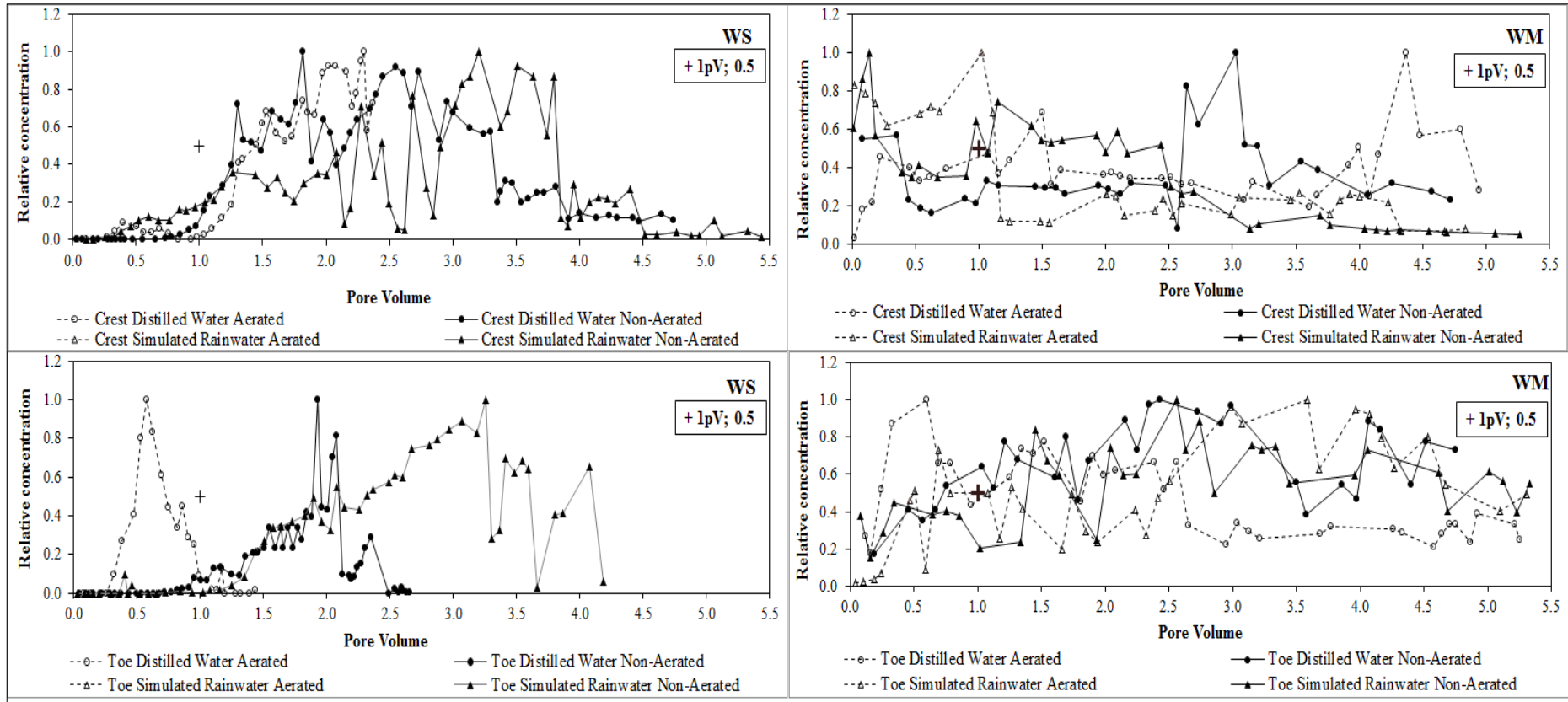


Figure 8.8 Iron BTC curve as relative concentration for WS (left, crest: top and toe: bottom) and WM (right, crest: top and toe: bottom) soil columns

## 8.9 Appendix 9

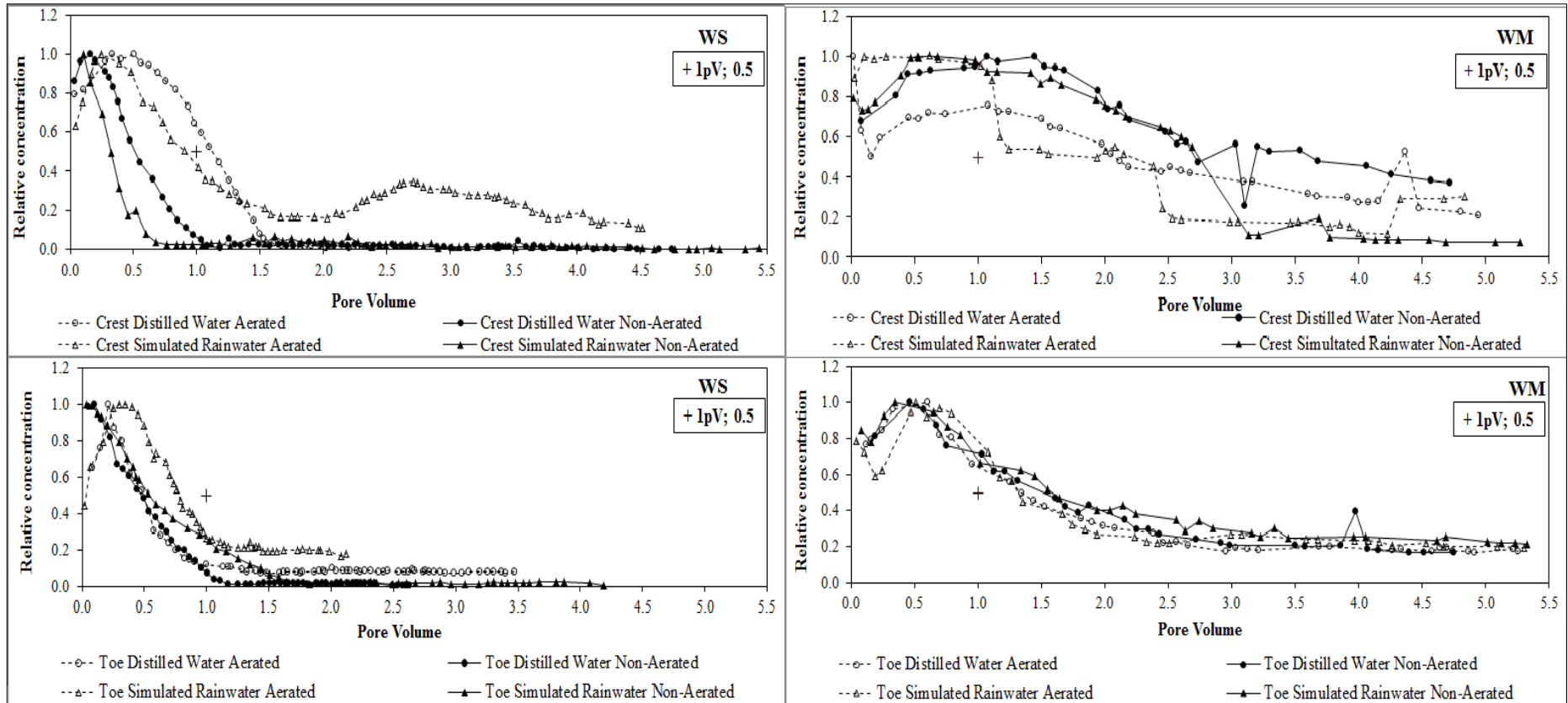


Figure 8.9 Sulphur BTC curve as relative concentration for WS (left, crest: top and toe: bottom) and WM (right, crest: top and toe: bottom) soil columns

## 8.10 Appendix 10

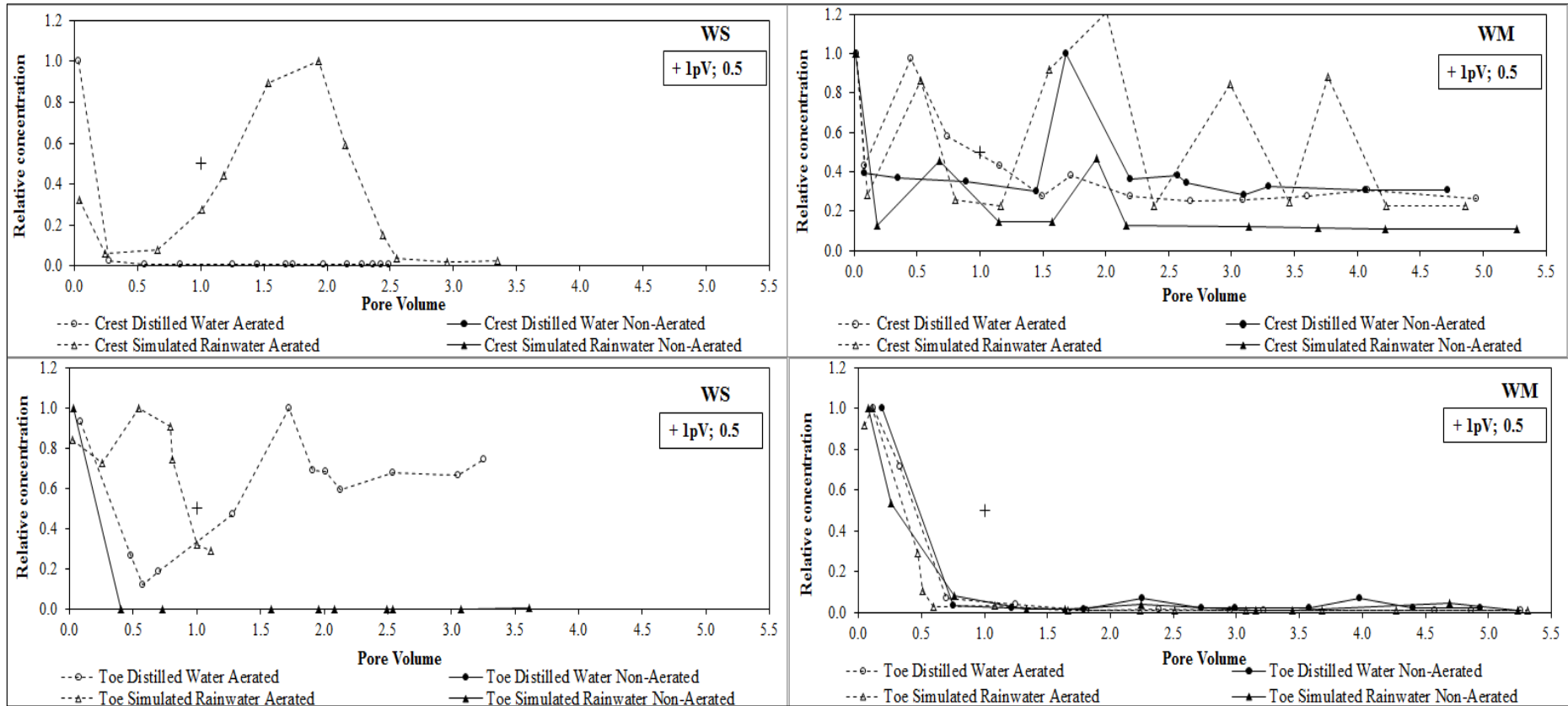


Figure 8.10 Nitrate BTC curve as relative concentration for WS (left, crest: top and toe: bottom) and WM (right, crest: top and toe: bottom) soil columns

## 8.11 Appendix 11

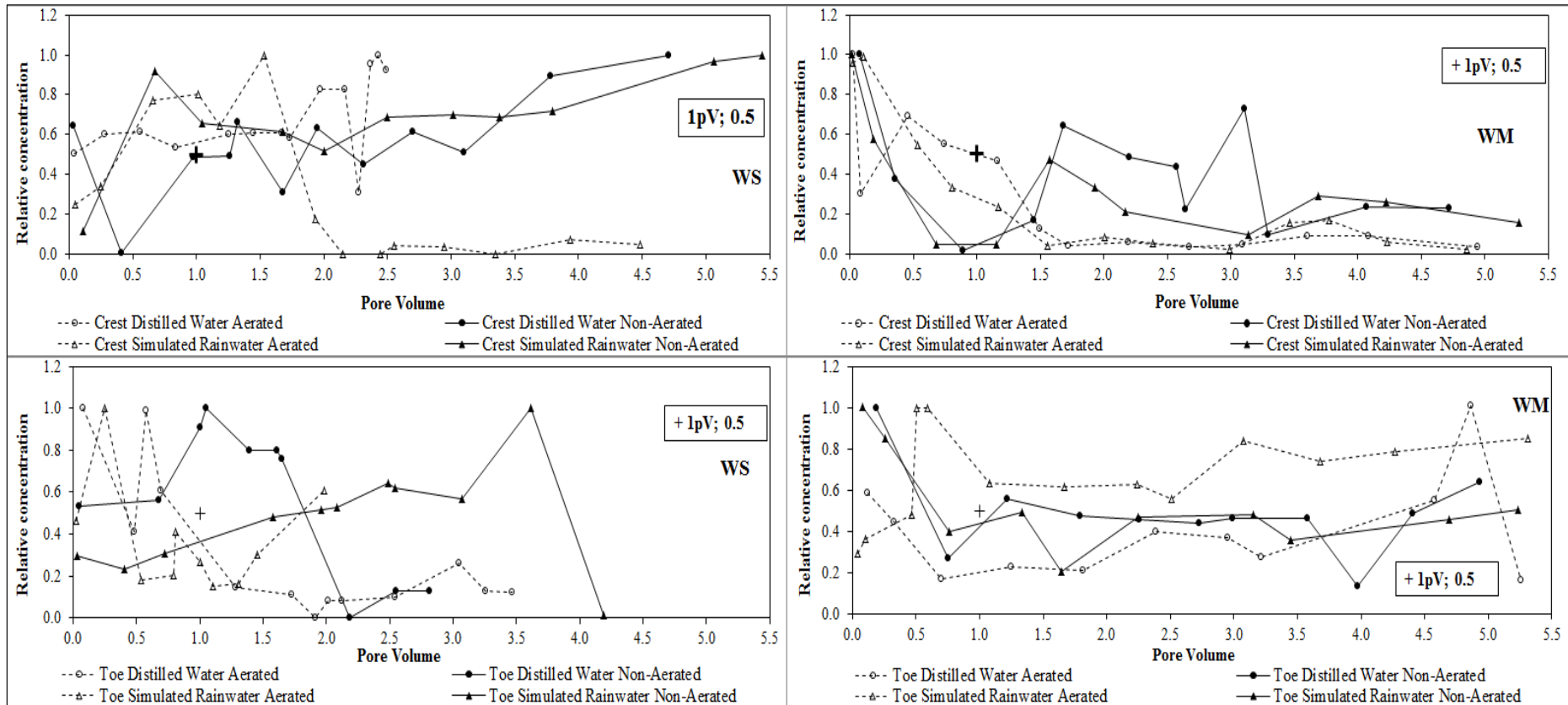


Figure 8.11 Ammonium BTC curve as relative concentration for WS (left, crest: top and toe: bottom) and WM (right, crest: top and toe: bottom) soil columns

## 8.12 Appendix 12

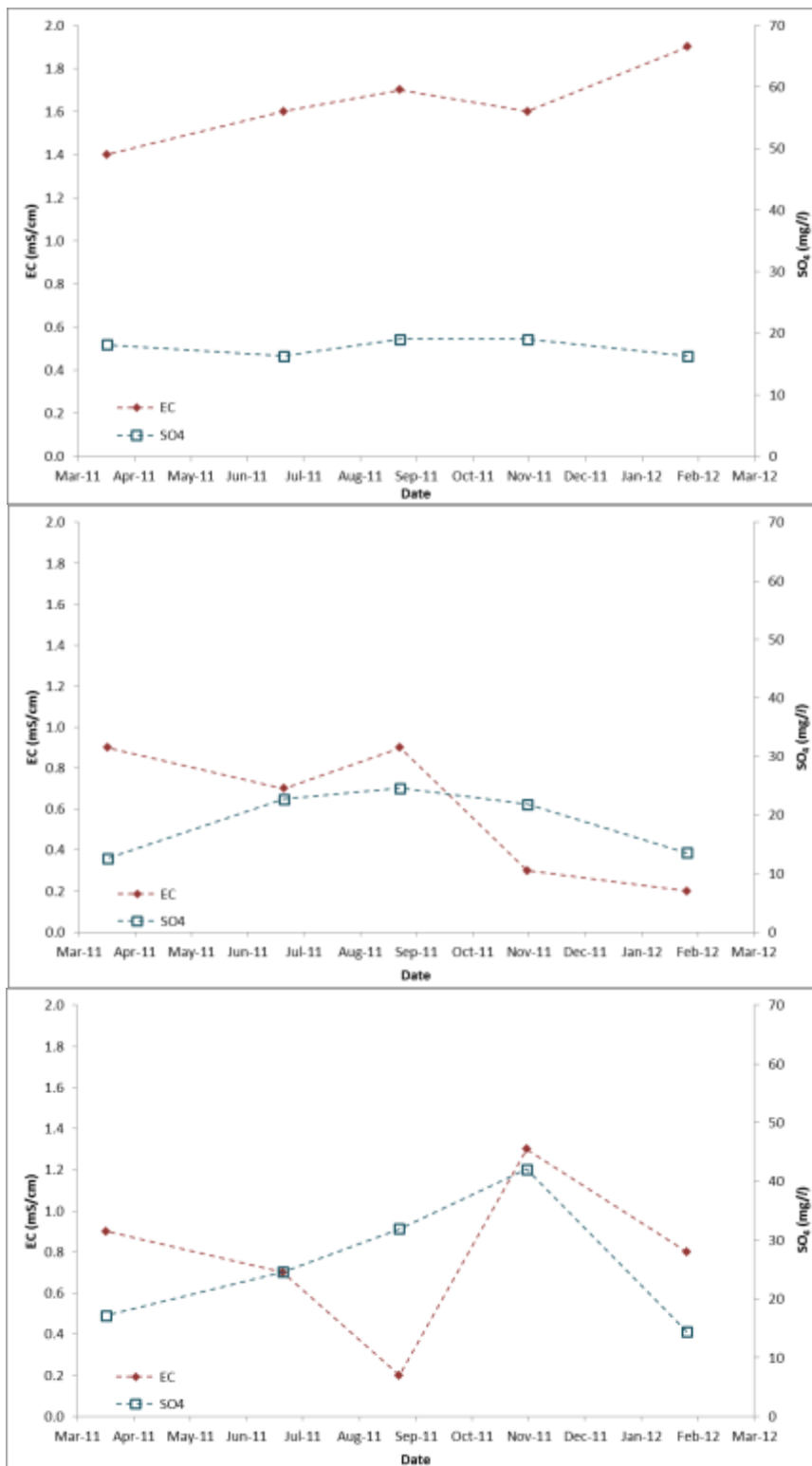


Figure 8.12 EC and sulphate variation at Sites, 1: Wessel borehole (top), 2: Wessel Spring (middle) and 3: Wessel Catchment Outlet (bottom) at the Research Catchment



### 8.13 Appendix 13

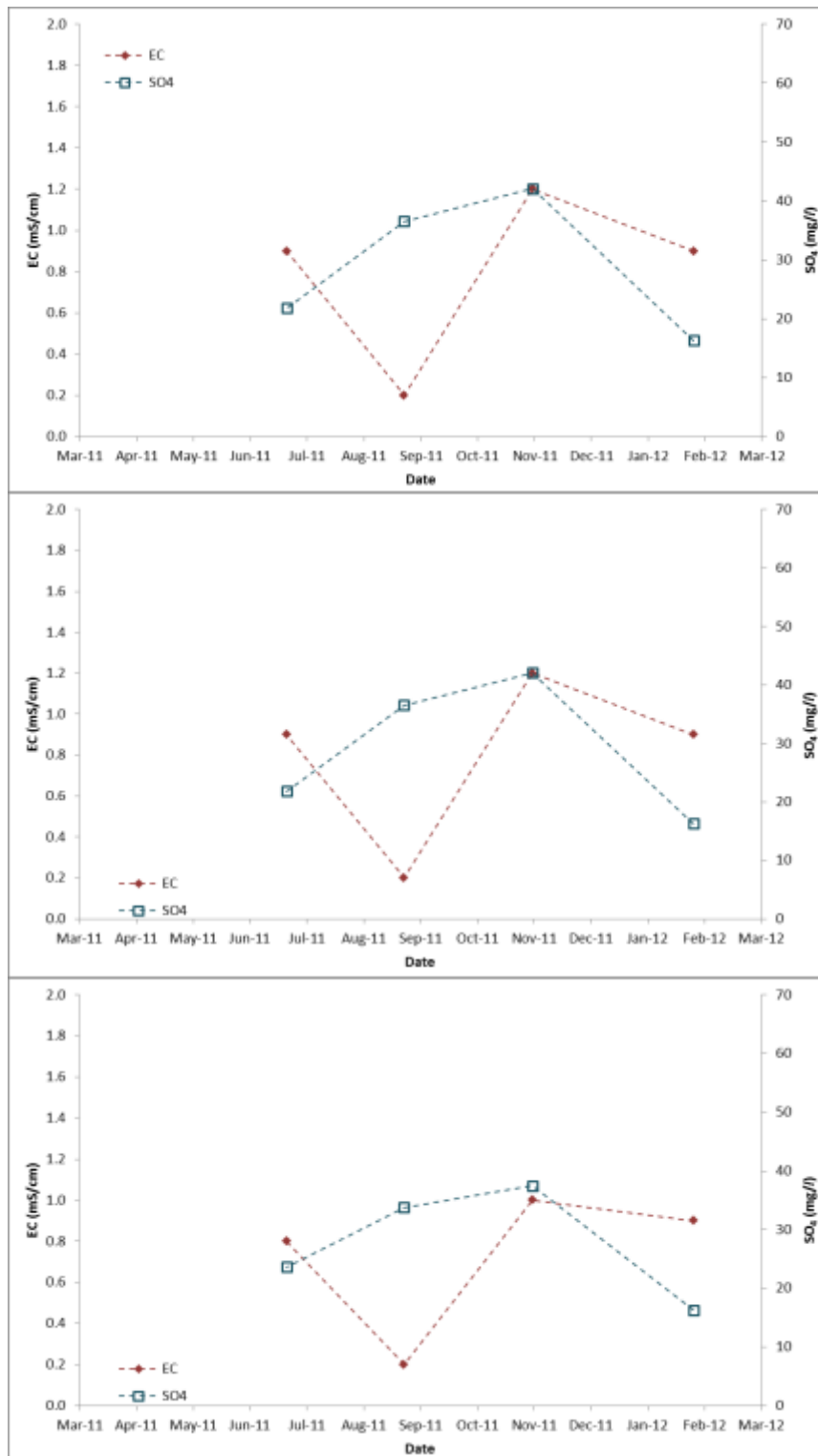


Figure 8.13 EC and sulphate variation at Sites 4: Sandspruit Kloof u/s of Junction (top), 5: Sandspruit Drift (middle) and 6: Sandspruit Bridge near Wessel Farm (bottom) in the Sandspruit Catchment

## 8.14 Appendix 14

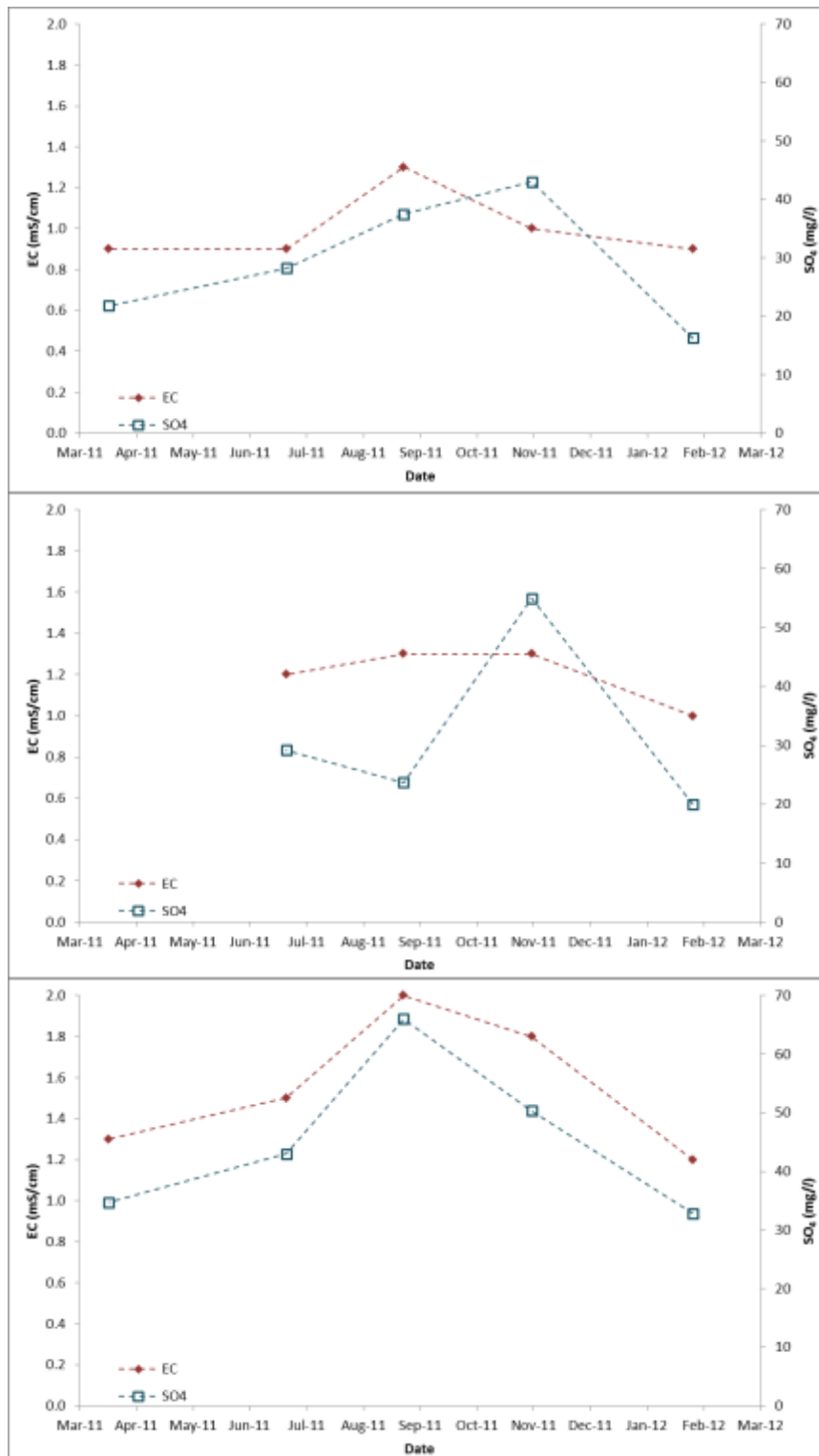


Figure 8.14 EC and sulphate variation at Sites 7: Sandspruit Bridge on N11 (top), 8: Steel Bridge on N23 (middle) and 9: Bridge near Perdokop (bottom) in the Sandspruit Catchment

## 8.15 Appendix 15

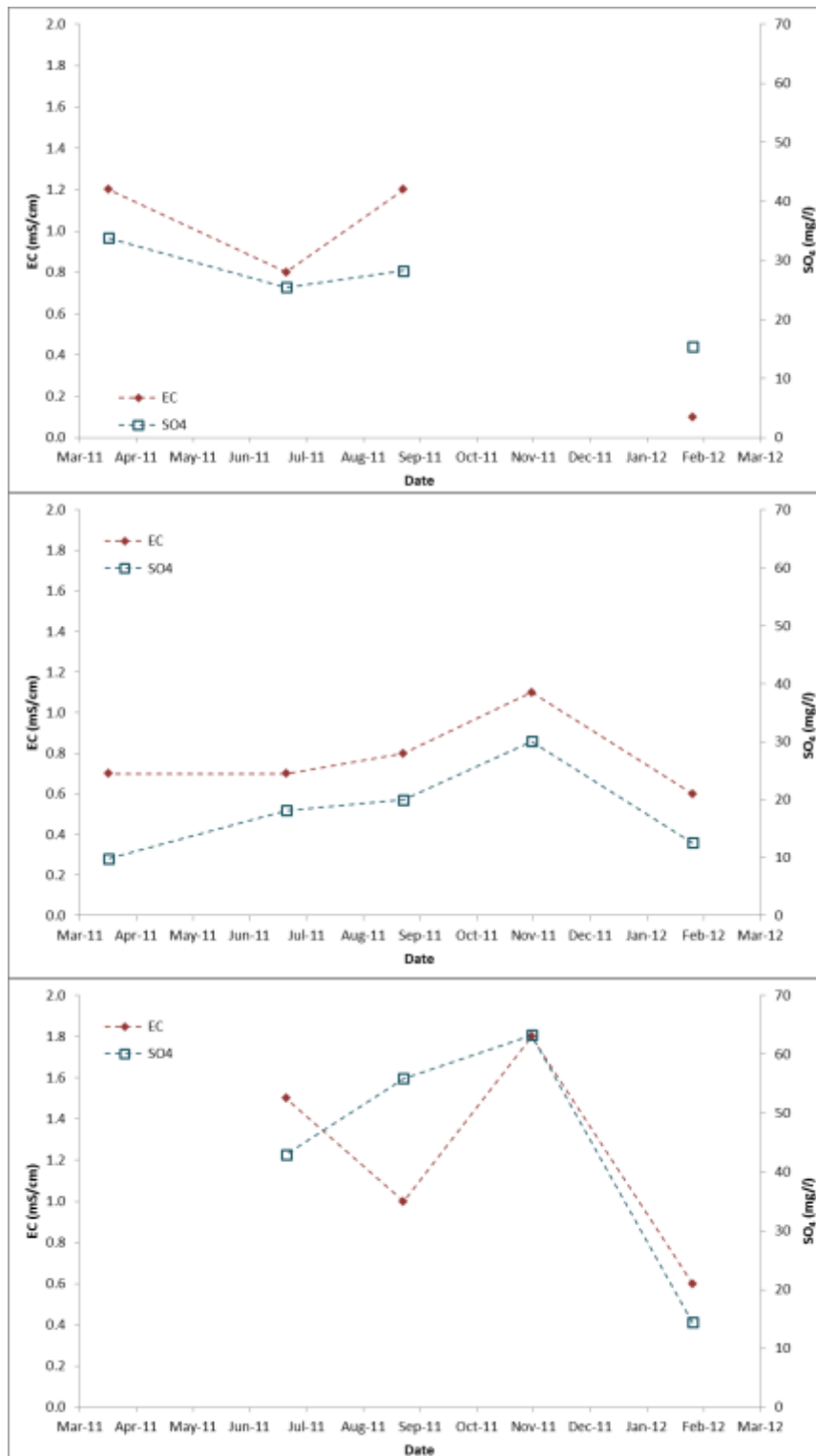


Figure 8.15 EC and sulphate variation at Sites 10: Sandspruit Junction off S446 Bridge (top), 11: Klip u/s of Junction (middle) and 12: Klip d/s of Junction (bottom) of the Sandspruit River

## 8.16 Appendix 16

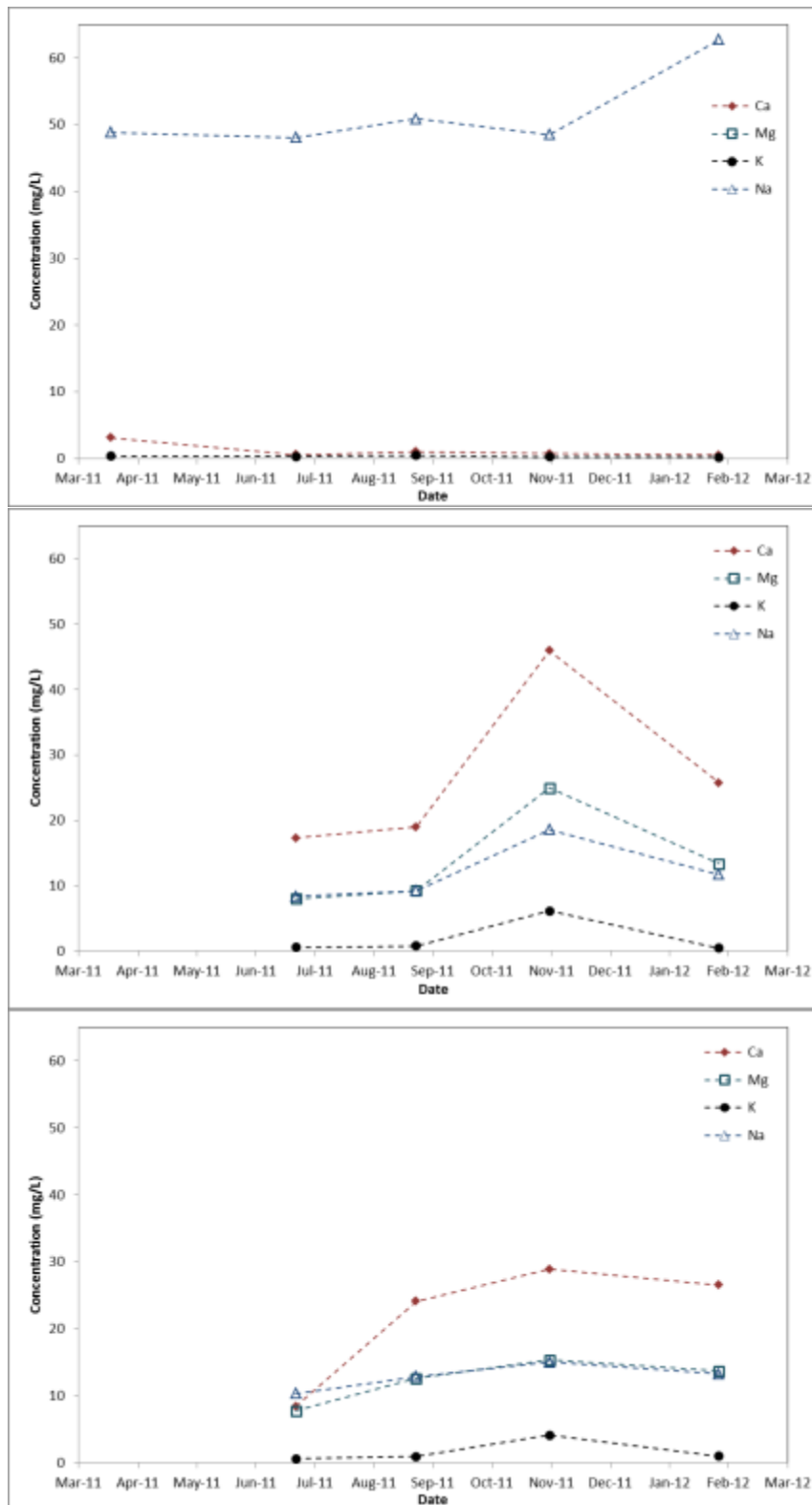


Figure 8.16 Ca, Mg, K and Na variation at Sites, 1: Wessel borehole (top), 2: Wessel Spring (middle) and 3: Wessel Catchment Outlet at the Research Catchment

## 8.17 Appendix 17

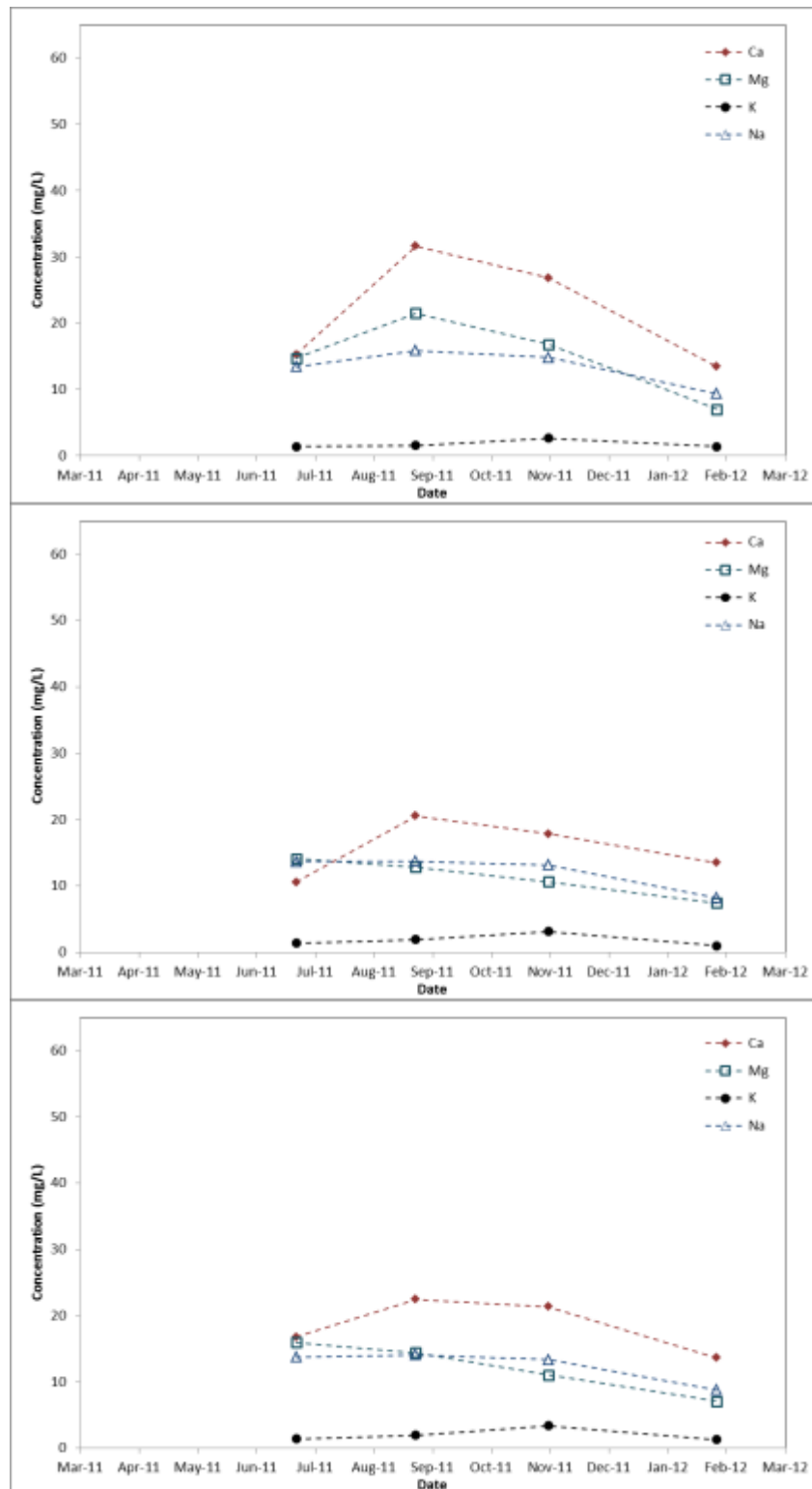


Figure 8.17 Ca, Mg, K and Na variation Sites 4: Sandspruit Kloof u/s of Junction (top), 5: Sandspruit Drift (middle) and 6: Sandspruit Bridge near Wessel Farm (bottom) in the Sandspruit Catchment

## 8.18 Appendix 18

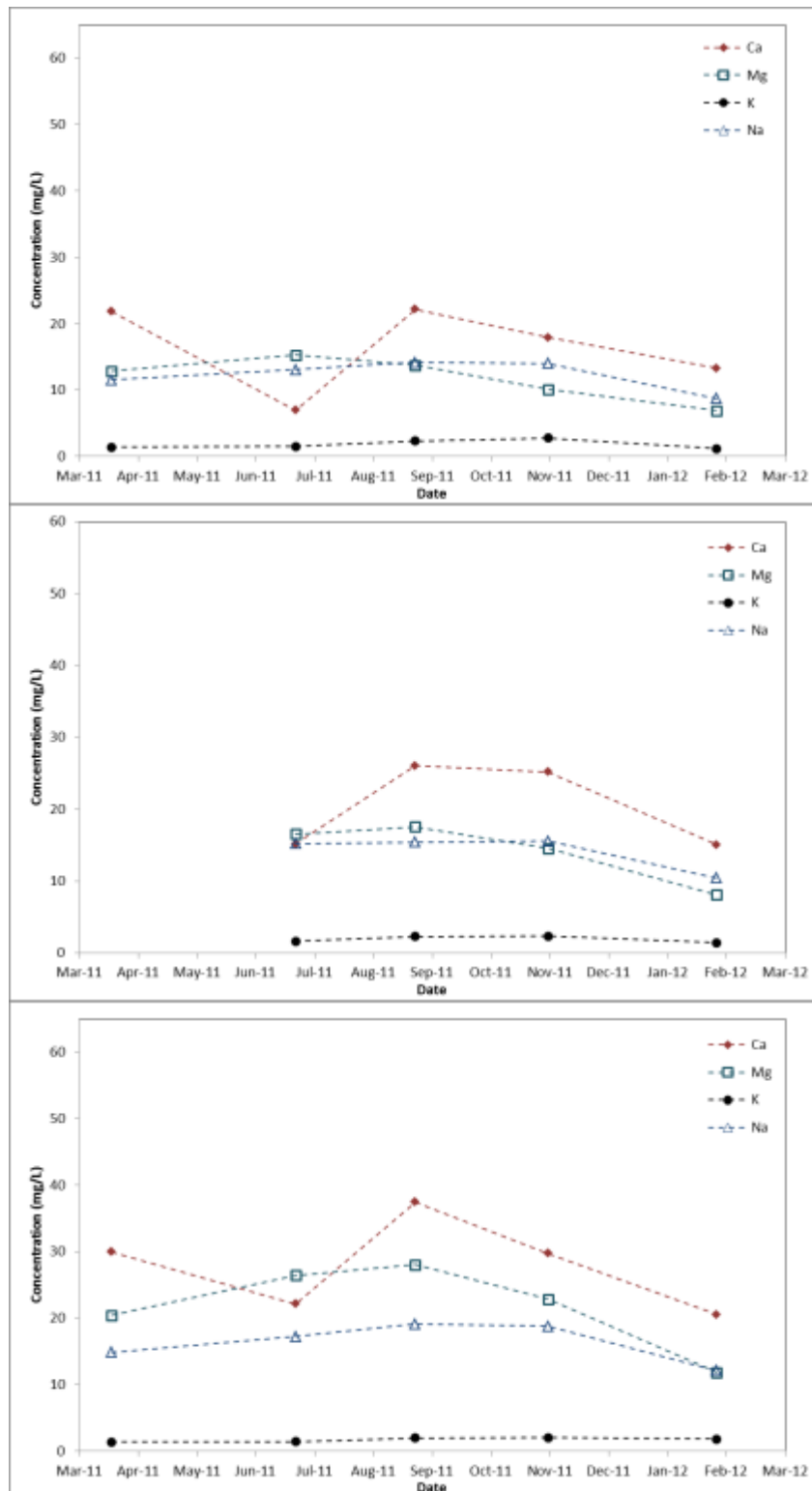


Figure 8.18 Ca, Mg, K and Na at Sites 7: Sandspruit Bridge on N11 (top), 8: Steel Bridge on N23 (middle) and 9: Bridge near Perdokop (bottom) in the Sandspruit Catchment

8.19 Appendix 19

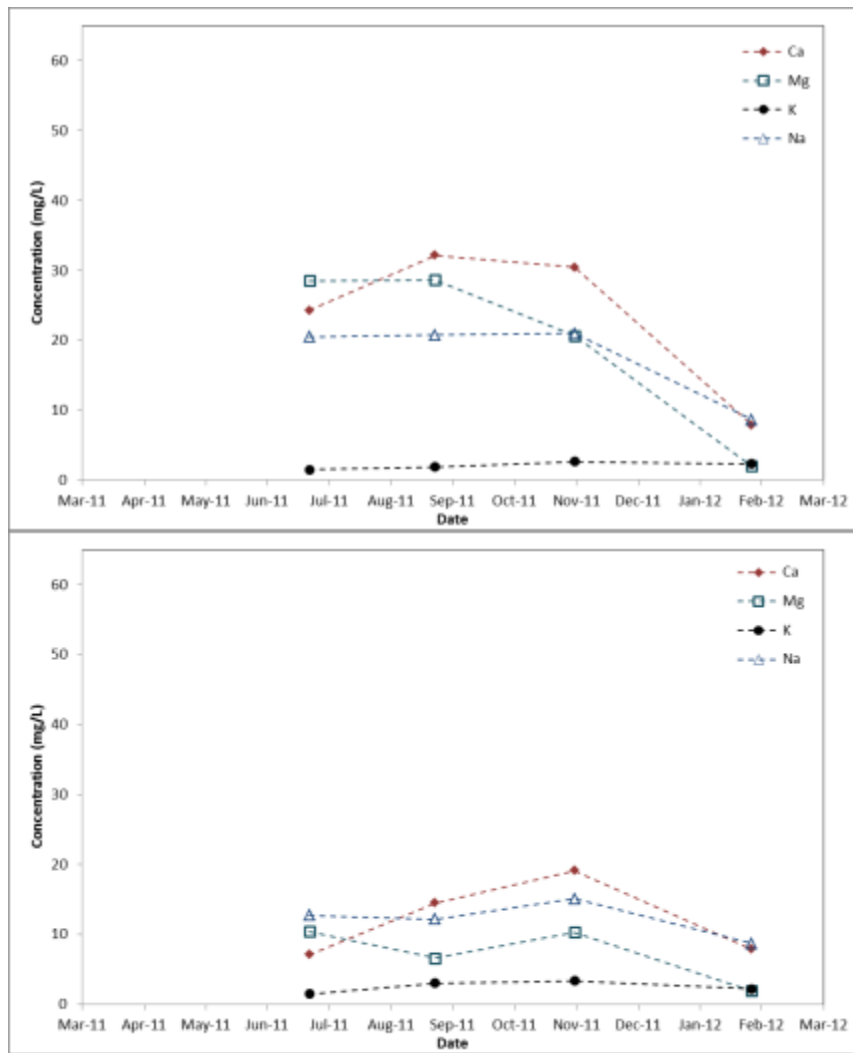


Figure 8.19 Ca, Mg, K and Na variation at Sites 10: Sandspruit Junction off S446 Bridge (top) and 11: Klip u/s of Junction (bottom) of the Sandspruit River